Problems

20.1 Spontaneous breaking of $SU(5)$. Consider a gauge theory with the gauge group $SU(5)$, coupled to a scalar field Φ in the adjoint representation. Assume that the potential for this scalar field forces it to acquire a nonzero vacuum expectation value. Two possible choices for this expectation value are

$$\langle\Phi\rangle = A\begin{pmatrix} 1 & & & & \\ & 1 & & & \\ & & 1 & & \\ & & & 1 & \\ & & & & -4 \end{pmatrix} \quad \text{and} \quad \langle\Phi\rangle = B\begin{pmatrix} 2 & & & & \\ & 2 & & & \\ & & 2 & & \\ & & & -3 & \\ & & & & -3 \end{pmatrix}.$$

For each case, work out the spectrum of gauge bosons and the unbroken symmetry group.

20.2 Decay modes of the W and Z bosons.

(a) Compute the partial decay widths of the W boson into pairs of quarks and leptons. Assume that the top quark mass m_t is larger than m_W, and ignore the other quark masses. The decay widths to quarks are enhanced by QCD corrections. Show that the correction is given, to order α_s, by Eq. (17.9). Using $\sin^2\theta_w = 0.23$, find a numerical value for the total width of the W^+.

(b) Compute the partial decay widths of the Z boson into pairs of quarks and leptons, treating the quarks in the same way as in part (a). Determine the total width of the Z boson and the fractions of the decays that give hadrons, charged leptons, and invisible modes $\nu\bar{\nu}$.

20.3 $e^+e^- \to$ hadrons with photon-Z^0 interference

(a) Consider a fermion species f with electric charge Q_f and weak isospin I_L^3 for its left-handed component. Ignore the mass of the f. Compute the differential cross section for the process $e^+e^- \to f\bar{f}$ in the standard electroweak model. Include the effect of the Z^0 width using the Breit-Wigner formula, Eq. (7.60). Plot the behavior of the total cross section as a function of CM energy through the Z^0 resonance, for u, d, and μ.

(b) Compute the forward-backward asymmetry for $e^+e^- \to f\bar{f}$, defined as

$$A_{FB}^f = \frac{\left(\int_0^1 - \int_{-1}^0\right) d\cos\theta (d\sigma/d\cos\theta)}{\left(\int_0^1 + \int_{-1}^0\right) d\cos\theta (d\sigma/d\cos\theta)},$$

as a function of center of mass energy.

(c) Show that, just on the Z^0 resonance, the forward-backward asymmetry is given by

$$A_{FB}^f = \frac{3}{4} A_{LR}^e A_{LR}^f.$$

(d) Show that the cross section at the peak of the Z^0 resonance is given by

$$\sigma_{\text{peak}} = \frac{12\pi}{m_Z^2} \frac{\Gamma(Z^0 \to e^+e^-)\Gamma(Z^0 \to f\bar{f})}{\Gamma_Z^2},$$

where Γ_Z is the total width of the Z^0. Notice that both the total width of the Z^0 and the peak height are affected by the presence of extra invisible decay modes. Compute the shifts in Γ_Z and σ_{peak} that would be produced by a hypothetical fourth neutrino species, and compare these shifts to the cross section measurements shown in Fig. 20.5.

20.4 Neutral-current deep inelastic scattering.

(a) In Eq. (17.35), we wrote formulae for neutrino and antineutrino deep inelastic scattering with $W^\pm$ exchange. Neutrinos and antineutrinos can also scatter by exchanging a Z^0. This process, which leads to a hadronic jet but no observable outgoing lepton, is called the *neutral current* reaction. Compute $d\sigma/dxdy$ for neutral current deep inelastic scattering of neutrinos and antineutrinos from protons, accounting for scattering from u and d quarks and antiquarks.

(b) Next, consider deep inelastic scattering from a nucleus A with equal numbers of protons and neutrons. For such a target, $f_u(x) = f_d(x)$, and similarly for antiquarks. Show that the formulae in part (a) simplify in such a situation. In particular, let R^ν, $R^{\bar\nu}$ be defined as

$$R^\nu = \frac{d\sigma/dxdy(\nu A \to \nu X)}{d\sigma/dxdy(\nu A \to \mu^- X)}, \qquad R^{\bar\nu} = \frac{d\sigma/dxdy(\bar\nu A \to \bar\nu X)}{d\sigma/dxdy(\bar\nu A \to \mu^+ X)}.$$

Show that R^ν and $R^{\bar\nu}$ are given by the following simple formulae:

$$\begin{aligned} R^\nu &= \frac{1}{2} - \sin^2\theta_w + \frac{5}{9}\sin^4\theta_w(1+r), \\ R^{\bar\nu} &= \frac{1}{2} - \sin^2\theta_w + \frac{5}{9}\sin^4\theta_w(1+\frac{1}{r}), \end{aligned}$$

where

$$r = \frac{d\sigma/dxdy(\bar\nu A \to \mu^+ X)}{d\sigma/dxdy(\nu A \to \mu^- X)}.$$

These formulae remain true when R^ν and $R^{\bar\nu}$ are redefined to be the ratios of neutral- to charged-current cross sections integrated over the region of x and y that is observed in a given experiment.

(c) By setting r equal to the observed value—say, $r = 0.4$—and varying $\sin^2\theta_w$, the relations of part (b) generate a curve in the plane of R^ν versus $R^{\bar\nu}$ that is known as *Weinberg's nose.* Sketch this curve. The observed values of R^ν, $R^{\bar\nu}$ lie close to this curve, near the point corresponding to $\sin^2\theta_w = 0.23$.

20.5 A model with two Higgs fields.

(a) Consider a model with two scalar fields ϕ_1 and ϕ_2, which transform as $SU(2)$ doublets with $Y = 1/2$. Assume that the two fields acquire parallel vacuum expectation values of the form (20.23) with vacuum expectation values v_1, v_2. Show that these vacuum expectation values produce the same gauge boson mass matrix that we found in Section 20.2, with the replacement

$$v^2 \to (v_1^2 + v_2^2).$$

(b) The most general potential function for a model with two Higgs doublets is quite complex. However, if we impose the discrete symmetry $\phi_1 \to -\phi_1$, $\phi_2 \to \phi_2$, the most general potential is

$$V(\phi_1,\phi_2) = -\mu_1^2\phi_1^\dagger\phi_1 - \mu_2^2\phi_2^\dagger\phi_2 + \lambda_1(\phi_1^\dagger\phi_1)^2 + \lambda_2(\phi_2^\dagger\phi_2)^2$$
$$+ \lambda_3(\phi_1^\dagger\phi_1)(\phi_2^\dagger\phi_2) + \lambda_4(\phi_1^\dagger\phi_2)(\phi_2^\dagger\phi_1) + \lambda_5((\phi_1^\dagger\phi_2)^2 + \text{h.c.}).$$

Find conditions on the parameters μ_i and λ_i so that the configuration of vacuum expectation values required in part (a) is a locally stable minimum of this potential.

(c) In the unitarity gauge, one linear combination of the upper components of ϕ_1 and ϕ_2 is eliminated, while the other remains as a physical field. Show that the physical charged Higgs field has the form

$$\phi^+ = \sin\beta\,\phi_1^+ - \cos\beta\,\phi_2^+,$$

where β is defined by the relation

$$\tan\beta = \frac{v_2}{v_1}.$$

(d) Assume that the two Higgs fields couple to quarks by the set of fundamental couplings

$$\mathcal{L}_m = -\lambda_d^{ij}\overline{Q}_L^i\cdot\phi_1 d_R^j - \lambda_u^{ij}\epsilon^{ab}\overline{Q}_{La}^i\phi_{2b}^\dagger u_R^j + \text{h.c.}$$

Find the couplings of the physical charged Higgs boson of part (c) to the mass eigenstates of quarks. These couplings depend only on the values of the quark masses and $\tan\beta$ and on the elements of the CKM matrix.

Chapter 21

Quantization of Spontaneously Broken Gauge Theories

In Chapter 20 we saw that when a gauge symmetry is spontaneously broken, the gauge bosons acquire mass. This phenomenon allowed us to construct a realistic theory of the weak interactions. Up to this point, however, we have discussed spontaneously broken gauge theories only in a simplistic way. To isolate the physical degrees of freedom, we have used the device of going to the unitarity gauge. However, it is not at all clear what the rules of perturbation theory are in this gauge, or how the unitarity gauge constraint is maintained when we compute Feynman diagrams. We have also seen that the Goldstone bosons that are absorbed into the massive gauge bosons play an important role in formal arguments about these theories, so we would like to quantize these theories in a gauge that does not eliminate these particles from the beginning.

In this chapter we will address these problems, by carrying out the formal gauge-fixing of theories with spontaneously broken gauge symmetry using the Faddeev-Popov method. We will define a class of gauges, called the R_ξ gauges, almost all of which contain the Goldstone bosons of the original spontaneous symmetry breaking. These particles cancel the effects of other unphysical particles in the formalism to maintain the unitarity of the theory. These cancellations are a more intricate version of the cancellations between gauge and ghost degrees of freedom that we saw in Chapter 16. However, we will see in Section 21.2 that a theory does not forget that it contains Goldstone bosons and that, under some circumstances, the properties of the Goldstone bosons in the theory without gauge couplings can carry over to the theory with massive gauge bosons.

Finally, having defined the perturbation theory and clarified the role of the Goldstone bosons in spontaneously broken gauge theories, we will carry out some explicit loop calculations of interest in the theory of weak interactions. Here we will see applications of the ideas of Chapter 11, that a theory with spontaneously broken symmetry can be renormalized with the counterterms of the symmetric Lagrangian. In Section 21.3 we will show through some examples that this result applies with equal force to gauge theories, and that it endows the weak-interaction gauge theory with substantial predictive power.

21.1 The R_ξ Gauges

In our discussion of the low-energy effective Lagrangian for weak interactions, we proposed in Eq. (20.89) the following expression for the propagator of a massive gauge boson:

$$\langle A^\mu(p)A^\nu(-p)\rangle \stackrel{?}{=} \frac{-ig^{\mu\nu}}{p^2-m^2}. \tag{21.1}$$

This expression is a natural first guess, generalizing the Feynman-'t Hooft gauge. However, it is unsatisfactory in a number of ways.

The most important of these defects concerns the treatment of gauge boson polarization states. The propagator (21.1) contains four components, corresponding to the transverse, longitudinal, and timelike polarizations. We saw in Chapters 5 and 16 that, for massless gauge bosons, the unphysical longitudinal and timelike components cancel in computations. For a massive gauge boson, however, the longitudinal polarization state corresponds to a real physical particle; we do not want it to cancel. Expression (21.1) does not take this change into account.

An Abelian Example

To understand this and other formal problems that arise for gauge theories with spontaneously broken symmetry, we need to carefully redo the Faddeev-Popov quantization of these theories. To begin, we will quantize the spontaneously broken Abelian gauge theory introduced in Eq. (20.1):

$$\mathcal{L} = -\tfrac{1}{4}(F_{\mu\nu})^2 + \left|D_\mu\phi\right|^2 - V(\phi), \tag{21.2}$$

with $D_\mu = \partial_\mu + ieA_\mu$. Here $\phi(x)$ is a complex scalar field. However, it will be most convenient to analyze the model by writing ϕ in terms of its real components,

$$\phi = \frac{1}{\sqrt{2}}\left(\phi^1 + i\phi^2\right). \tag{21.3}$$

Then the infinitesimal local symmetry transformation is

$$\delta\phi^1 = -\alpha(x)\phi^2, \qquad \delta\phi^2 = \alpha(x)\phi^1, \qquad \delta A_\mu = -\frac{1}{e}\partial_\mu\alpha. \tag{21.4}$$

Let us assume that $V(\phi)$ forces the scalar field to acquire a vacuum expectation value: $\langle\phi^1\rangle = v$. Then we should change variables by a shift:

$$\phi^1(x) = v + h(x); \qquad \phi^2 = \varphi. \tag{21.5}$$

The field ϕ^2 or φ is the Goldstone boson. The Lagrangian (21.2) now takes the form

$$\mathcal{L} = -\tfrac{1}{4}(F_{\mu\nu})^2 + \tfrac{1}{2}\left(\partial_\mu h - eA_\mu\varphi\right)^2 + \tfrac{1}{2}\left(\partial_\mu\varphi + eA_\mu(v+h)\right)^2 - V(\phi). \tag{21.6}$$

This Lagrangian is still invariant under an exact local symmetry,

$$\delta h = -\alpha(x)\varphi, \qquad \delta\varphi = \alpha(x)(v+h), \qquad \delta A_\mu = -\frac{1}{e}\partial_\mu\alpha. \tag{21.7}$$

Thus, in order to define the functional integral over the variables (h, φ, A_μ). we must introduce Faddeev-Popov gauge fixing.

Starting from the functional integral

$$Z = \int \mathcal{D}A\mathcal{D}h\mathcal{D}\varphi\; e^{i\int \mathcal{L}[A,h,\varphi]}, \tag{21.8}$$

we can introduce a gauge-fixing constraint as we did in Section 9.4. Following the steps leading from Eq. (9.50) to Eq. (9.54), we find

$$Z = C\cdot\int \mathcal{D}A\mathcal{D}h\mathcal{D}\varphi\; e^{i\int \mathcal{L}[A,h,\varphi]}\,\delta\big(G(A,h,\varphi)\big)\det\Big(\frac{\delta G}{\delta\alpha}\Big), \tag{21.9}$$

where C is a constant proportional to the volume of the gauge group and $G(A,h,\varphi)$ is a gauge-fixing condition. Alternatively, we can introduce the gauge-fixing constraint as $\delta(G(x)-\omega(x))$ and integrate over $\omega(x)$ with a Gaussian weight, as in the derivation of Eq. (9.56). This gives

$$Z = C'\cdot\int \mathcal{D}A\mathcal{D}h\mathcal{D}\varphi\;\exp\Big[i\int d^4x\big(\mathcal{L}[A,h,\varphi]-\tfrac{1}{2}(G)^2\big)\Big]\det\Big(\frac{\delta G}{\delta\alpha}\Big). \tag{21.10}$$

The gauge-fixing function G is arbitrary, but we can simplify our formalism by choosing it appropriately.

An especially convenient choice of the gauge-fixing function is

$$G = \frac{1}{\sqrt{\xi}}\big(\partial_\mu A^\mu - \xi ev\varphi\big). \tag{21.11}$$

When we form G^2, the term quadratic in A_μ will provide the same gauge-dependent addition to the gauge field action that we saw in the derivation of Eqs. (9.58) and (16.29). In addition, the cross term between A_μ and φ is engineered to cancel the quadratic term of the form $\partial_\mu\varphi A^\mu$ coming from the third term of (21.6). With this choice, the quadratic terms of the gauge-fixed Lagrangian $(\mathcal{L}-\frac{1}{2}G^2)$ are

$$\begin{aligned}\mathcal{L}_2 = &-\frac{1}{2}A_\mu\Big(-g^{\mu\nu}\partial^2 + \big(1-\frac{1}{\xi}\big)\partial^\mu\partial^\nu - (ev)^2 g^{\mu\nu}\Big)A_\nu \\ &+\frac{1}{2}(\partial_\mu h)^2 - \frac{1}{2}m_h^2 h^2 + \frac{1}{2}(\partial_\mu\varphi)^2 - \frac{\xi}{2}(ev)^2\varphi^2.\end{aligned} \tag{21.12}$$

The mass term for the h field comes from the expansion of $V(\phi)$, as in (20.6). The mass term for the gauge field comes from the Higgs mechanism, that is, from the third term of (21.6). Notice that the formalism also produces a mass for the Goldstone boson φ:

$$m_\varphi^2 = \xi(ev)^2 = \xi m_A^2. \tag{21.13}$$

The fact that this mass is gauge-dependent is a signal that the Goldstone boson is a fictitious field, which will not be produced in physical processes.

To complete the Faddeev-Popov quantization procedure, we must derive the Lagrangian of the ghosts. This Lagrangian depends on the gauge variation of G, which can be computed by inserting (21.7) into (21.11). We find

$$\frac{\delta G}{\delta \alpha} = \frac{1}{\sqrt{\xi}}\Big(-\frac{1}{e}\partial^2 - \xi e v(v+h)\Big). \tag{21.14}$$

The determinant of this operator can be accounted for by including a set of Faddeev-Popov ghosts with the Lagrangian,

$$\mathcal{L}_{\text{ghost}} = \bar{c}\Big[-\partial^2 - \xi m_A^2\big(1+\frac{h}{v}\big)\Big]c, \tag{21.15}$$

where $m_A = ev$ as in Eq. (21.13). Since this is an Abelian gauge theory, the ghost field does not couple directly to the gauge field. It does, however, couple to the physical Higgs field, so it cannot be completely ignored as in QED.

From the quadratic terms in the Lagrangians for A_μ, h, φ, and the ghosts, we can readily find the propagators for these fields. All four propagators are shown in Fig. 21.1. The only complicated case is that of the gauge field. The term in (21.12) involving A_μ involves an operator whose Fourier transform is

$$\begin{aligned} g^{\mu\nu}k^2 - \big(1-\frac{1}{\xi}\big)k^\mu k^\nu - m_A^2 g^{\mu\nu} \\ = \Big(g^{\mu\nu} - \frac{k^\mu k^\nu}{k^2}\Big)(k^2 - m_A^2) + \Big(\frac{k^\mu k^\nu}{k^2}\Big)\frac{1}{\xi}(k^2 - \xi m_A^2). \end{aligned} \tag{21.16}$$

The inverse of this matrix gives the A_μ field propagator:

$$\begin{aligned} \langle A^\mu(k)A^\nu(-k)\rangle &= \frac{-i}{k^2-m_A^2}\Big(g^{\mu\nu} - \frac{k^\mu k^\nu}{k^2}\Big) + \frac{-i\xi}{k^2-\xi m_A^2}\Big(\frac{k^\mu k^\nu}{k^2}\Big) \\ &= \frac{-i}{k^2-m_A^2}\Big(g^{\mu\nu} - \frac{k^\mu k^\nu}{k^2-\xi m_A^2}(1-\xi)\Big). \end{aligned} \tag{21.17}$$

Notice that the transverse components of the A field and the component h of the Higgs field acquire the masses m_A, m_h that we found in Section 20.1. The unphysical components of A, the Goldstone bosons, and the ghosts all acquire the same gauge-dependent mass $\sqrt{\xi}m_A$.

ξ Dependence in Perturbation Theory

Because the parameter ξ was introduced only in the gauge fixing, we expect it to cancel out of all computations of expectation values of gauge-invariant operators and of S-matrix elements. This cancellation can be proved to all orders in perturbation theory by using the BRST symmetry of the gauge-fixed Lagrangian.* Here, however, we will simply illustrate the cancellation of ξ in a simple example.

*See, for example, Taylor (1976).

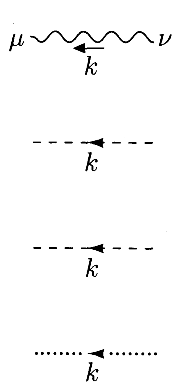

$$A_\mu: \quad = \frac{-i}{k^2 - m_A^2}\left(g^{\mu\nu} - \frac{k^\mu k^\nu}{k^2 - \xi m_A^2}(1-\xi)\right)$$

$$h: \quad = \frac{i}{k^2 - m_h^2}$$

$$\varphi: \quad = \frac{i}{k^2 - \xi m_A^2}$$

$$c: \quad = \frac{i}{k^2 - \xi m_A^2}$$

Figure 21.1. Propagators of the gauge field, Higgs fields, and ghosts in the Abelian model with spontaneously broken symmetry.

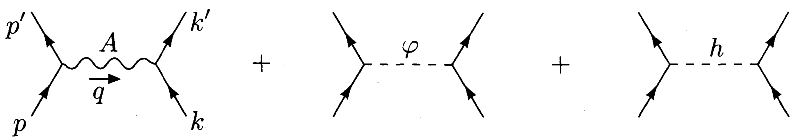

Figure 21.2. Diagrams contributing to fermion-fermion scattering at leading order in the Abelian model with spontaneous symmetry breaking.

Consider coupling a fermion to the spontaneously broken gauge theory through a chiral interaction:

$$\mathcal{L}_f = \bar{\psi}_L(i\not{D})\psi_L + \bar{\psi}_R(i\not{\partial})\psi_R - \lambda_f\left(\bar{\psi}_L\phi\psi_R + \bar{\psi}_R\phi^*\psi_L\right), \tag{21.18}$$

with $D_\mu = \partial_\mu + ieA_\mu$ as before. This is a stripped-down, Abelian version of the coupling of fermions to the weak interaction gauge theory. The fermion ψ receives a mass

$$m_f = \lambda_f \frac{v}{\sqrt{2}} \tag{21.19}$$

from the spontaneous symmetry breaking. (This theory has an axial vector anomaly that would render loop calculations inconsistent, but we will analyze it only at the level of tree diagrams.)

In this theory, the leading-order diagrams contributing to fermion-fermion scattering are those shown in Fig. 21.2. Notice that the contribution from the exchange of the unphysical particle φ must be included, since this particle appears in the Feynman rules. The ghosts do not appear in this process until the one-loop level. Since the propagator of the physical Higgs particle h is independent of ξ, the cancellation of the ξ dependence must take place between the transverse and longitudinal components of A_μ and the Goldstone boson φ.

The graph with exchange of the Goldstone boson has the value

$$i\mathcal{M}_\varphi = \left(\frac{\lambda_f}{\sqrt{2}}\right)^2 \bar{u}(p')\gamma^5 u(p) \frac{i}{q^2 - \xi m_A^2} \bar{u}(k')\gamma^5 u(k). \tag{21.20}$$

The ξ dependence of this expression must be canceled by that of the gauge boson exchange diagram,

$$\begin{aligned} i\mathcal{M}_A &= (-ie)^2 \bar{u}(p')\gamma_\mu \left(\frac{1-\gamma^5}{2}\right) u(p) \\ &\times \frac{-i}{q^2 - m_A^2}\left(g^{\mu\nu} - \frac{q^\mu q^\nu}{q^2 - \xi m_A^2}(1-\xi)\right) \bar{u}(k')\gamma_\nu \left(\frac{1-\gamma^5}{2}\right) u(k). \end{aligned} \tag{21.21}$$

The ξ dependence of this term looks quite intricate. However, we can make some simplifications by rewriting the gauge boson propagator as

$$\begin{aligned} &\frac{-i}{q^2 - m_A^2}\left(g^{\mu\nu} - \frac{q^\mu q^\nu}{m_A^2} + q^\mu q^\nu \left[\frac{1}{m_A^2} - \frac{1}{q^2 - \xi m_A^2}(1-\xi)\right]\right) \\ &\quad = \frac{-i}{q^2 - m_A^2}\left(g^{\mu\nu} - \frac{q^\mu q^\nu}{m_A^2}\right) + \frac{-i}{q^2 - \xi m_A^2}\left(\frac{q^\mu q^\nu}{m_A^2}\right). \end{aligned} \tag{21.22}$$

The first term of (21.22) is ξ-independent. The second term can be simplified in (21.21) by using the identity

$$\begin{aligned} q^\mu \bar{u}(p')\gamma_\mu \left(\frac{1-\gamma^5}{2}\right) u(p) &= \frac{1}{2}\bar{u}(p')\left[(\not{p} - \not{p}') - (\not{p} - \not{p}')\gamma^5\right] u(p) \\ &= \frac{1}{2}\bar{u}(p')\left[\not{p}'\gamma^5 + \gamma^5 \not{p}\right] u(p) \\ &= m_f \bar{u}(p')\gamma^5 u(p), \end{aligned} \tag{21.23}$$

and the analogous identity on the other fermion line. After making these rearrangements and inserting the explicit values $m_f = \lambda_f v/\sqrt{2}$ and $m_A = ev$, the gauge boson exchange amplitude (21.21) takes the form

$$\begin{aligned} i\mathcal{M}_A =& (-ie)^2 \bar{u}(p')\gamma_\mu \left(\frac{1-\gamma^5}{2}\right) u(p) \frac{i}{q^2 - m_A^2}\left(g^{\mu\nu} - \frac{q^\mu q^\nu}{m_A^2}\right) \bar{u}(k')\gamma_\nu \left(\frac{1-\gamma^5}{2}\right) u(k) \\ &+ \left(\frac{\lambda_f}{\sqrt{2}}\right)^2 \bar{u}(p')\gamma^5 u(p) \frac{-i}{q^2 - \xi m_A^2} \bar{u}(k')\gamma^5 u(k). \end{aligned} \tag{21.24}$$

The second term of (21.24) precisely cancels the Goldstone boson exchange diagram (21.20). The terms that remain in the fermion-fermion scattering amplitude are independent of ξ.

This demonstration merits two additional comments. First, throughout this book, we have become accustomed to dotting the gauge boson momentum into a gauge boson vertex and finding zero or contact terms. However, in spontaneously broken gauge theories, we typically find a different result. The fermionic current $\bar{\psi}\gamma^\mu(1-\gamma^5)\psi$ is not conserved, with the nonconservation being proportional to the fermion mass. This allows the manipulation (21.23) to contribute terms proportional to the Higgs boson vacuum expectation value, which interplay with the Goldstone boson contributions. We will discuss this point further, and find a physical application of it, in Section 21.2.

The second point concerns the final form of the gauge-invariant sum of the gauge boson and Goldstone boson exchange diagrams. These give just the result we would have found by neglecting the Goldstone boson and computing the gauge boson exchange using the first term of (21.22) as the propagator:

$$\langle A_\mu(q)A_\nu(-q)\rangle = \frac{-i}{q^2-m_A^2}\left(g^{\mu\nu}-\frac{q^\mu q^\nu}{m_A^2}\right). \tag{21.25}$$

The tensor structure represents a gauge boson polarization sum. To identify what vectors are summed over, notice that, if the vector boson is on-shell, and if we boost to its rest frame, this structure becomes precisely the projection onto the three purely spatial directions. These are the three polarization states of an on-shell massive vector particle. In a general frame, still for q^μ on-shell, the tensor in (21.25) remains the projection onto physical polarization states:

$$\sum_{\epsilon^\mu q_\mu=0} \epsilon^\mu\epsilon^{\nu *} = -\left(g^{\mu\nu}-\frac{q^\mu q^\nu}{m_A^2}\right). \tag{21.26}$$

Thus, in the cancellation of the ξ-dependent parts of the gauge boson propagator, we also find that the Goldstone boson diagram cancels the contribution of the unphysical timelike polarization state of the gauge boson, leaving over the required three physical polarizations.

The perturbation theory rules that we have developed have a very different character for different values of ξ. Thus, it is even more true in the case of spontaneously broken symmetry that we can find different special simplifications by choosing different values of this gauge parameter. For $\xi = 0$, Lorentz gauge, the Goldstone boson is massless and has exactly the couplings it has in the ungauged model of symmetry breaking, while the gauge boson propagator is purely transverse:

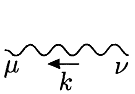

$$= \frac{-i}{k^2-m_A^2}\left(g^{\mu\nu}-\frac{k^\mu k^\nu}{k^2}\right);$$
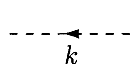

$$= \frac{i}{k^2}. \tag{21.27}$$

This gauge is especially useful for analyzing models of symmetry breaking. Both propagators have poles at $k^2 = 0$. However, we know that there are no corresponding physical particles, because these poles move away from $k^2 = 0$ as we change ξ, while the S-matrix must be ξ-independent.

For $\xi = 1$, we recover the simple form of the gauge boson propagator given in (21.1). This choice of the gauge boson propagator is not consistent, however, unless we also include Goldstone boson exchanges in which the Goldstone boson is also assigned the mass m_A:

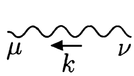

$$= \frac{-ig^{\mu\nu}}{k^2-m_A^2};$$
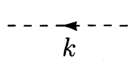

$$= \frac{i}{k^2-m_A^2}. \tag{21.28}$$

This gauge, still called the Feynman-'t Hooft gauge, is the most convenient one for general higher-order computations.

For any finite value of ξ, the gauge boson and Goldstone boson propagators fall off as $1/k^2$ and thus obey the general power-counting analysis of Section 10.1. It follows that, in any one of these gauges, the perturbation theory will be renormalizable, in the sense that the divergences are removed by a finite set of counterterms. Furthermore, the analysis of Section 11.6 tells us that the only counterterms required are those that are symmetric under the original global symmetry of the theory. However, we should require one further condition of our renormalization procedure: We should insist that the counterterms preserve local gauge invariance, and, in particular, preserve the property that S-matrix elements and the matrix elements of gauge-invariant operators are independent of ξ. This result was proved to all orders in perturbation theory by 't Hooft and Veltman and by Lee and Zinn-Justin.[†] Thus, in the gauge defined by any finite value of ξ, we can, in principle, straightforwardly compute a physical quantity to any order. The gauges defined by the possible values of ξ are known as the *renormalizability*, or R_ξ, gauges.

By taking the limit $\xi \to \infty$ of the R_ξ gauges, we find a gauge with very different simplifying features. In this limit, the unphysical degrees of freedom, which have masses proportional to $\sqrt{\xi}$, disappear from the theory. The gauge boson and Goldstone boson propagators become:

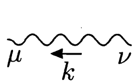
$$= \frac{-i}{k^2 - m_A^2}\left(g^{\mu\nu} - \frac{k^\mu k^\nu}{m_A^2}\right); \qquad$$
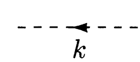
$$= 0. \tag{21.29}$$

The gauge boson propagator contains exactly the three spacelike polarization states. In this gauge, the only singularities of Feynman diagrams correspond to the propagation of physical intermediate states. Thus, the unitarity of the S-matrix follows from the Cutkosky rules, as in the globally symmetric theories considered in Section 7.3, without the need to worry about the cancellation of unphysical states.[‡] The $\xi \to \infty$ limit of the R_ξ gauges thus gives the quantum-mechanical realization of the *unitarity* (or U) gauge, introduced in Eq. (20.12).

It is not straightforward to prove renormalizability directly in the U gauge. In this gauge, the gauge boson propagator falls off more slowly than $1/k^2$ at large k. This signals trouble for the evaluation of loop diagrams. Typically, in fact, individual loop diagrams will diverge as $\log \xi$ or worse as $\xi \to \infty$. Still, the gauge invariance of the S-matrix implies that these divergences must cancel in the sum of all diagrams contributing to a given process, so that this sum has a smooth limit as $\xi \to \infty$. There is no difficulty of principle with the fact that we use one gauge to prove the renormalizability of spontaneously

[†]G. 't Hooft and M. J. G. Veltman, *Nucl. Phys.* **B50**, 318 (1972), B. W. Lee and J. Zinn-Justin, *Phys. Rev.* **D5**, 3121, 3137, 3155 (1972), **D7**, 1049 (1973).

[‡]In the more sophisticated language of Section 16.4, the crucial identity (16.54), which is required for the unitarity of the S-matrix, is true manifestly.

broken gauge theories and another gauge to prove their unitarity. In fact, this method of argumentation makes natural use of the underlying symmetries of the theory.

Non-Abelian Analysis

Now that we have thoroughly examined the R_ξ gauges for an Abelian gauge theory, we are ready to generalize to the non-Abelian case. There is no difficulty in being completely general, so let us consider a Yang-Mills gauge theory with gauge group G, spontaneously broken by the vacuum expectation value of a scalar field.

We will build on our classical analysis of this system following Eq. (20.13). As in that analysis, it will be most convenient to write the scalars as a multiplet ϕ_i of real-valued fields. Then the gauge transformation of the ϕ_i takes the form

$$\delta\phi_i = -\alpha^a(x)T^a_{ij}\phi_j, \tag{21.30}$$

where the T^a_{ij} are real, antisymmetric representation matrices of G. Similarly, the transformation of the gauge fields is

$$\delta A^a_\mu = \frac{1}{g}\partial_\mu\alpha^a - f^{abc}\alpha^b A^c_\mu = \frac{1}{g}(D_\mu\alpha)^a. \tag{21.31}$$

(If the gauge group is not simple, the coupling g need not be the same for every a.) The Lagrangian invariant under these gauge transformations is

$$\mathcal{L} = -\tfrac{1}{4}(F^a_{\mu\nu})^2 + \tfrac{1}{2}(D_\mu\phi)^2 - V(\phi), \tag{21.32}$$

with

$$D_\mu\phi_i = \partial_\mu\phi_i + gA^a_\mu T^a_{ij}\phi_j. \tag{21.33}$$

Assume that the potential $V(\phi)$ is minimized at a point where some of the components of ϕ acquire vacuum expectation values. As in (20.16), define

$$\langle\phi_i\rangle = (\phi_0)_i. \tag{21.34}$$

We will expand ϕ_i about this value:

$$\phi_i(x) = \phi_{0i} + \chi_i(x). \tag{21.35}$$

It will be convenient to divide the space of values χ_i into two subspaces. The vectors $T^a\phi_0$ correspond to symmetry transformations of the vacuum expectation value of ϕ. The field fluctuations along these directions are the Goldstone bosons. Let $\{n_i\}$ be an orthonormal basis for this subspace; then the unit vectors n_i are in 1-to-1 correspondence with the Goldstone bosons. The field fluctuations orthogonal to all of the vectors $T^a\phi_0$ correspond to the (massive) physical scalar fields of the spontaneously broken gauge theory.

In the discussion to follow, the vectors $T^a\phi_0$ will play an important role. We should then recall the notation for these vectors that we introduced in Eq. (20.51):

$$F^a{}_i = T^a_{ij}\phi_{0j}. \tag{21.36}$$

The matrix $F^a{}_i$ is not generally square; it has one row for each gauge generator, and one column for each component of ϕ. However, many of its elements are zero. Its nonzero elements connect the spontaneously broken gauge generators and the Goldstone bosons. In Eq. (20.56), we showed that the gauge boson masses generated through the Higgs mechanism can be written

$$m^2_{ab} = g^2 F^a{}_j F^b{}_j. \tag{21.37}$$

To give a concrete example of a matrix $F^a{}_j$, let us compute it in the GWS electroweak theory. Following the conventions introduced in Eq. (20.14), we should rewrite the Higgs field of the GWS model in terms of four real scalar fields. A convenient parametrization is

$$\phi = \frac{1}{\sqrt{2}} \begin{pmatrix} -i(\phi^1 - i\phi^2) \\ v + (h + i\phi^3) \end{pmatrix}. \tag{21.38}$$

The fields ϕ^i are the Goldstone bosons, and h is the massive Higgs boson. The vacuum state is simply

$$\phi_0 = \frac{1}{\sqrt{2}} \begin{pmatrix} 0 \\ v \end{pmatrix}.$$

The real representation matrices are

$$T^a = -i\tau^a = -i\frac{\sigma^a}{2}, \qquad T^Y = -iY = -i\frac{1}{2}.$$

A simple computation then shows, for instance, that $T^1\phi_0$ equals $v/2$ times a unit vector in the ϕ^1 direction. Filling in the remaining components of $F^a{}_i$, with $a = 1, 2, 3, Y$ and $i = 1, 2, 3$, we find

$$gF^a{}_i = \frac{v}{2} \begin{pmatrix} g & 0 & 0 \\ 0 & g & 0 \\ 0 & 0 & g \\ 0 & 0 & -g' \end{pmatrix}. \tag{21.39}$$

We do not need to include the components of $F^a{}_i$ along the direction of the physical Higgs field h; the vectors $T^a\phi_0$ are all orthogonal to this direction.

If we insert (21.35) into (21.32) as a change of variables, we find, for the quadratic terms in the Lagrangian,

$$\begin{aligned} \mathcal{L}_2 = &-\tfrac{1}{2} A^a_\mu(-g^{\mu\nu}\partial^2 + \partial^\mu\partial^\nu)A^a_\nu + \tfrac{1}{2}(\partial_\mu\chi)^2 \\ &+ g\partial^\mu\chi_i A^a_\mu F^a{}_i + \tfrac{1}{2}(m^2_A)^{ab} A^a_\mu A^{\mu b} - \tfrac{1}{2} M_{ij}\chi_i\chi_j, \end{aligned} \tag{21.40}$$

where $(m^2_A)^{ab}$ is the gauge boson mass matrix (21.37) and

$$M_{ij} = \frac{\partial^2}{\partial\phi_i\partial\phi_j} V(\phi)\Big|_{\phi_0}. \tag{21.41}$$

We proved in Eq. (11.13) that

$$n_i M_{ij} = 0 \tag{21.42}$$

for all possible directions n_i in the subspace spanned by the $T^a\phi_0$, so the Goldstone bosons are massless.

To study the quantum theory of this system we start with the functional integral

$$Z = \int \mathcal{D}A\mathcal{D}\chi \, e^{i\int \mathcal{L}[A,\chi]}. \tag{21.43}$$

Using the Faddeev-Popov gauge-fixing procedure, we define this integral, analogously to (21.10), as

$$Z = C' \cdot \int \mathcal{D}A\mathcal{D}\chi \, \exp\Big[i\int d^4x \big(\mathcal{L}[A,\chi] - \tfrac{1}{2}(G)^2\big)\Big] \det\Big(\frac{\delta G}{\delta\alpha}\Big), \tag{21.44}$$

for an arbitrary gauge-fixing function $G(A,\chi)$. The R_ξ gauges are defined by the choice

$$G^a = \frac{1}{\sqrt{\xi}}\big(\partial_\mu A^{a\mu} - \xi g F^a{}_i \chi_i\big). \tag{21.45}$$

Note that G involves only the components of χ that lie in the subspace of the Goldstone bosons.

The gauge-fixing term adds to the Lagrangian the following set of quadratic terms:

$$(-\tfrac{1}{2}G^2)_2 = \tfrac{1}{2}A^a_\mu\big(\tfrac{1}{\xi}\partial^\mu\partial^\nu\big)A^a_\nu + g\partial_\mu A^{a\mu}F^a{}_i\chi_i - \tfrac{1}{2}\xi g^2\big[F^a{}_i\chi_i\big]^2. \tag{21.46}$$

The term that mixes A^a_μ and χ_i is arranged to cancel between (21.40) and (21.46). The final quadratic Lagrangian for the gauge and Goldstone boson fields is

$$\begin{aligned}\mathcal{L}_2 = -\frac{1}{2}A^a_\mu\Big(\Big[-g^{\mu\nu}\partial^2 + \big(1-\frac{1}{\xi}\big)\partial^\mu\partial^\nu\Big]\delta^{ab} - g^2F^a{}_iF^b{}_i g^{\mu\nu}\Big)A^b_\nu \\ + \frac{1}{2}(\partial_\mu\chi)^2 - \frac{1}{2}\xi g^2 F^a{}_iF^a{}_j\chi_i\chi_j.\end{aligned} \tag{21.47}$$

The mass matrices of gauge bosons and Goldstone bosons in this Lagrangian are closely related to one another. The gauge boson mass matrix is

$$(m_A^2)^{ab} = g^2F^a{}_iF^b{}_i = g^2(FF^T)^{ab}. \tag{21.48}$$

In an R_ξ gauge, the timelike components of the gauge bosons acquire the mass matrix

$$\xi m_A^2 = \xi g^2(FF^T)^{ab}. \tag{21.49}$$

At the same time, the Goldstone bosons acquire the mass matrix

$$(m_G^2)_{ij} = \xi g^2F^a{}_iF^a{}_j = \xi g^2(F^TF)_{ij}. \tag{21.50}$$

The two matrices (21.49) and (21.50) have different numbers of zero eigenvalues, but their nonzero eigenvalues are in 1-to-1 correspondence. This is precisely the correspondence induced by the Higgs mechanism between the massive gauge bosons and the Goldstone bosons that they absorbed to gain mass.

Finally, we must construct the ghost Lagrangian. This is found from the gauge variation of the gauge-fixing term G^a. Inserting (21.30) and (21.31) into (21.45), we find

$$\frac{\delta G^a}{\delta \alpha^b} = \frac{1}{\sqrt{\xi}}\Big(\frac{1}{g}(\partial_\mu D^\mu)^{ab} + \xi g (T^a\phi_0)\cdot T^b(\phi_0+\chi)\Big). \qquad (21.51)$$

Thus, the ghost Lagrangian is

$$\mathcal{L}_{\text{ghost}} = \bar{c}^a\big[-(\partial_\mu D^\mu)^{ab} - \xi g^2 (T^a\phi_0)\cdot T^b(\phi_0+\chi)\big]c^b. \qquad (21.52)$$

Notice that the ghosts have exactly the same mass matrix (21.49) as the unphysical components of the gauge bosons. This Lagrangian also contains both the familiar coupling of the ghosts to the gauge fields and the coupling to the physical Higgs fields that we found in the Abelian case (21.15).

We have now computed the kinetic energy terms for gauge fields, scalar fields, and ghosts in an R_ξ gauge. It is straightforward to convert these results to the calculation of propagators for these fields; the computations are exactly the same as in the Abelian case. We find for the three propagators

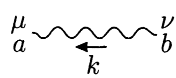

$$= \left(\frac{-i}{k^2 - g^2FF^T}\Big[g^{\mu\nu} - \frac{k^\mu k^\nu}{k^2-\xi g^2FF^T}(1-\xi)\Big]\right)^{ab},$$

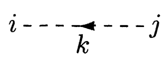

$$= \left(\frac{i}{k^2 - \xi g^2 F^TF - M^2}\right)_{ij},$$

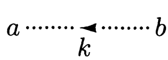

$$= \left(\frac{i}{k^2 - \xi g^2 FF^T}\right)^{ab}. \qquad (21.53)$$

All of these equations involve the matrix F defined in Eq. (21.36); the appearance of a matrix in the denominator should be interpreted as a matrix inverse. The scalar field propagator also includes the mass matrix (21.41) of the physical Higgs bosons. There is no conflict between this matrix and the mass matrix of the Goldstone bosons, since they project onto orthogonal subspaces.

Although the preceding discussion has been extremely abstract, it is not hard to specialize to a particular example. So consider, once again, the GWS electroweak theory, for which the matrix $F^a{}_i$ is given by Eq. (21.39).

The gauge boson mass matrix in the GWS theory is

$$g^2FF^T = \frac{v^2}{4}\begin{pmatrix} g^2 & 0 & 0 & 0\\ 0 & g^2 & 0 & 0\\ 0 & 0 & g^2 & -gg'\\ 0 & 0 & -gg' & g'^2\end{pmatrix},$$

in agreement with Eq. (20.124). (The g on the left-hand side should be interpreted as g' for the fourth component of F.) Diagonalizing this matrix gives the familiar relations (20.62). Thus, in the basis of mass eigenstates, the four gauge-boson propagators decouple to give simply

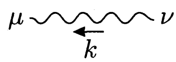

$$= \frac{-i}{k^2 - m^2}\left[g^{\mu\nu} - \frac{k^\mu k^\nu}{k^2 - \xi m^2}(1-\xi)\right], \tag{21.54}$$

where m^2 is m_W^2, m_Z^2, or, for the photon, zero. Notice that, for the photon, this expression precisely reproduces Eq. (9.58).

The mass matrix of the Goldstone bosons in the GWS theory is

$$\xi g^2 F^T F = \xi \frac{v^2}{4}\begin{pmatrix} g^2 & 0 & 0 \\ 0 & g^2 & 0 \\ 0 & 0 & g^2 + g'^2 \end{pmatrix}.$$

These fields therefore have the propagator

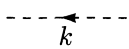

$$= \frac{i}{k^2 - \xi m^2}, \tag{21.55}$$

with $m^2 = m_W^2$ for ϕ^1 and ϕ^2 (the bosons eaten by the $W^\pm$) and $m^2 = m_Z^2$ for ϕ^3 (the boson eaten by the Z). The field $h(x)$, which is the physical Higgs field, propagates independently with a mass determined by the Higgs potential (and no factor of ξ in the propagator).

Finally, there are four ghost fields. According to Eq. (21.53), these have the propagator

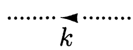

$$= \frac{i}{k^2 - \xi m^2}, \tag{21.56}$$

with the same values of m^2 as the four gauge bosons.

The Feynman rules for the interaction vertices of these particles are complicated to write out, due to the large number of possible combinations. However, it is quite straightforward to generate these rules by expanding the weak interaction Lagrangian and reading off the vertices term by term. We will work out a few examples in the following section.*

21.2 The Goldstone Boson Equivalence Theorem

From the results of the previous section, we see that perturbative calculations in the R_ξ gauges involve intricate cancellations among unphysical particles. Sometimes, however, these unphysical particles can still leave their footprints in physical observables. In this section we will see that, in the high-energy limit, the unphysical Goldstone boson that is eaten by a massive gauge boson still controls the amplitude for emission or absorption of the gauge boson in its longitudinal polarization state.

*The complete Feynman rules for the weak-interaction gauge theory are given in Appendix B of Cheng and Li (1984).

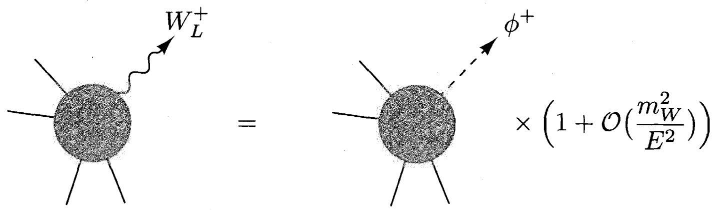

Figure 21.3. The Goldstone boson equivalence theorem. At high energy, the amplitude for emission or absorption of a longitudinally polarized massive gauge boson becomes equal to the amplitude for emission or absorption of the Goldstone boson that was eaten by the gauge boson.

When we introduced the Higgs mechanism for vector boson mass generation, we pointed out that it involves a certain conservation of degrees of freedom. A massless gauge boson, which has two transverse polarization states, combines with a scalar Goldstone boson to produce a massive vector particle, which has three polarization states. When the massive vector particle is at rest, its three polarization states are completely equivalent, but when it is moving relativistically, there is a clear distinction between the transverse and longitudinal polarization directions. This suggests that a rapidly moving, longitudinally polarized massive gauge boson might betray its origin as a Goldstone boson. The strongest version of this idea is expressed in Fig. 21.3: The amplitude for emission or absorption of a longitudinally polarized gauge boson becomes equal, at high energy, to the amplitude for emission or absorption of the Goldstone boson that was eaten. Remarkably, this statement is precisely correct, as a consequence of the underlying local gauge invariance. This *Goldstone boson equivalence theorem* was first proved by Cornwall, Levin, Tiktopoulos, and Vayonakis.†

Formal Aspects of Goldstone Boson Equivalence

The proof of the Goldstone boson equivalence theorem is based on the Ward identities of the spontaneously broken gauge theory. To give a complete proof of the theorem, we would have to construct and analyze these Ward identities in some detail. However, it is possible to understand the idea of the proof by examining the special case of the theorem in which a single massive vector boson is emitted or absorbed in a scattering process. The analysis of this special case requires only the relatively simple Ward identity satisfied by a current between on-shell states.‡

---

†J. M. Cornwall, D. N. Levin, and G. Tiktopoulos, *Phys. Rev.* **D10**, 1145 (1974); C. E. Vayonakis, *Lett. Nuov. Cim.* **17**, 383 (1976). For an illuminating discussion of the equivalence theorem, see B. W. Lee, C. Quigg, and H. Thacker, *Phys. Rev.* **D16**, 1519 (1977).

‡For a careful derivation of the equivalence theorem, including processes involving

To prepare for a discussion of longitudinal vector bosons, we need some simple kinematics. A vector boson at rest has momentum $k^\mu = (m, 0, 0, 0)$ and a polarization vector that is a linear combination of the three orthogonal unit vectors

$$(0,1,0,0), \qquad (0,0,1,0), \qquad (0,0,0,1). \tag{21.57}$$

If we boost this particle along the $\hat{3}$ axis, its momentum boosts to $k^\mu = (E_{\mathbf{k}}, 0, 0, k)$. The three possible polarization vectors are now the three unit vectors satisfying

$$\epsilon^\mu k_\mu = 0, \qquad \epsilon^2 = -1. \tag{21.58}$$

Two of these are the first two vectors in (21.57); these give the transverse polarizations. The third vector satisfying (21.58) is the longitudinal polarization vector

$$\epsilon_L^\mu(k) = \left(\frac{k}{m}, 0, 0, \frac{E_{\mathbf{k}}}{m}\right), \tag{21.59}$$

which is the boost of the third vector in (21.57). An important and somewhat counterintuitive feature of (21.59) is that it becomes increasingly parallel to k^μ as k becomes large. In fact, component by component,

$$\epsilon_L^\mu(k) = \frac{k^\mu}{m} + \mathcal{O}(m/E_{\mathbf{k}}) \tag{21.60}$$

as $k \to \infty$. Since the components of k^μ are growing as k, this statement is consistent with the requirement that $\epsilon_L \cdot k = 0$ while $k \cdot k = m^2$.

With this kinematic situation in mind, let us analyze the Ward identity satisfied by a gauge current matrix element between on-shell states. It is simplest to work in Lorentz gauge ($\xi = 0$), where the gauge-fixing term (21.45) does not involve the Goldstone boson fields. The Ward identity can then be written as follows:

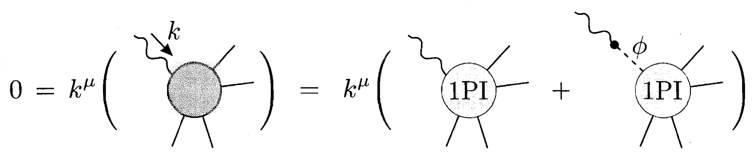

(21.61)

In the last expression we have written the matrix element as the sum of two pieces. First, the current can couple directly into a one-particle-irreducible vertex function $\Gamma^\mu(k)$. This gives the class of diagrams that contribute to the scattering of a gauge boson from the external states. However, for a spontaneously broken gauge theory, there is an additional term, which is not one-particle-irreducible, in which the current creates a Goldstone boson and it is this particle that couples to the external states through a 1PI vertex $\Gamma(k)$.

Let us write the relation linking the gauge current and the Goldstone boson state as

$$\langle 0 | J^\mu | \pi(k) \rangle = -iFk^\mu, \tag{21.62}$$

---

multiple absorptions and emissions of massive vector bosons, see M. S. Chanowitz and M. K. Gaillard, *Nucl. Phys.* **B261**, 379 (1985).

as in Eq. (20.46). Then the argument leading to Eq. (20.56) tells us that the gauge boson mass is given by

$$m = gF, \tag{21.63}$$

where g is the gauge boson coupling constant.

With these identifications, we can write the Ward identity that follows from the conservation of the gauge current:

$$k_\mu \langle J^\mu \rangle = 0, \tag{21.64}$$

between on-shell states. Writing each term shown in (21.61) in terms of the appropriate one-particle-irredicible vertex function, we find

$$k_\mu \Gamma^\mu(k) + k_\mu (igFk^\mu) \frac{i}{k^2} \Gamma(k) = 0. \tag{21.65}$$

Thus,

$$k_\mu \Gamma^\mu(k) = m\Gamma(k). \tag{21.66}$$

Now use this equation in the limit of large gauge boson momentum. Since the gauge boson vertex is one-particle-irreducible, the momenta of propagators inside the vertex are not, in general, collinear with k^μ. Then, according to (21.60), we may replace k^μ/m by the longitudinal polarization vector. Notice that this would not be permissible (but, also, is not necessary) in the second term of (21.65). Our final result is

$$\epsilon_{L\mu}(k)\Gamma^\mu(k) = \Gamma(k), \tag{21.67}$$

as $k \to \infty$, with an error of order m^2/k^2. That is, in the high-energy limit, the couplings of longitudinal gauge bosons become precisely those of their associated Goldstone bosons.

The equivalence theorem can be derived in another way, using the counting of physical states in spontaneously broken gauge theories, which we discussed below Eq. (21.26). In the previous section, we saw that, at least at the tree level, unitarity is maintained in spontaneously broken gauge theories by the cancellation of diagrams that produce timelike-polarized gauge bosons against diagrams that produce Goldstone bosons.

The situation is most clear in Feynman-'t Hooft gauge. There, the numerator of the gauge boson propagator is $-g^{\mu\nu}$. We can write this in terms of polarization vectors as

$$-g^{\mu\nu} = \sum_{i=1,2,3} \epsilon_i^\mu(k)\epsilon_i^{\nu*}(k) - \frac{k^\mu k^\nu}{m^2}. \tag{21.68}$$

The last term is the contribution from unphysical timelike polarization states. The unitarity of the S-matrix requires that, when a Cutkosky cut through a diagram puts a gauge boson propagator on-shell, the contribution of this piece

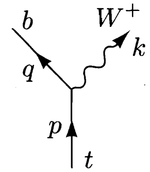

Figure 21.4. Decay of a t quark into $W^+ + b$.

must be canceled by a Cutkosky cut that runs through a Goldstone boson line. The required cancellation is

$$-\left|\frac{k_\mu}{m}\Gamma^\mu(k)\right|^2 + \left|\Gamma(k)\right|^2 = 0, \tag{21.69}$$

or, diagrammatically,

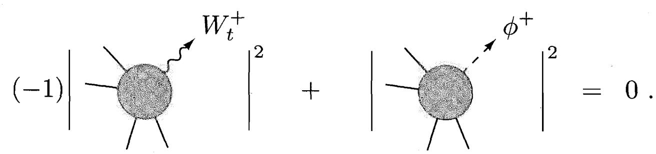

Once again, since $\Gamma^\mu(k)$ is a one-particle-irreducible vertex, we can use (21.60) to replace (k^μ/m) by the longitudinal polarization vector $\epsilon^\mu_L(k)$ for a high-energy gauge boson. Then (21.69) becomes just the square of (21.67).

Through these formal arguments, we can see, at least to the tree level in processes with single gauge boson emission, that the equivalence theorem must be valid. However, it is much more illuminating to see the equivalence theorem at work in explicit calculations for interesting physical processes. We will now illustrate its influence in two examples.

Top Quark Decay

The first example is the weak decay of the top quark. This charge $+2/3$ quark is sufficiently heavy that it can decay to a real W^+ through $t \to W^+ + b$. The diagram for this decay is given by the simple gauge vertex shown in Fig. 21.4.

Let us first try to guess the magnitude of the top quark width. The squared matrix element will contain a factor of g^2, times some expression with dimensions of mass. Since the width should be large if the top quark mass is heavy, a first guess might be

$$\Gamma \sim \frac{g^2}{4\pi} m_t. \tag{21.70}$$

The correct expression, however, turns out to be enhanced by a factor of $(m_t/m_W)^2$.

The amplitude for this decay can be read from Eq. (20.80):

$$i\mathcal{M} = \frac{ig}{\sqrt{2}}\bar{u}(q)\gamma^\mu\left(\frac{1-\gamma^5}{2}\right)u(p)\epsilon^*_\mu(k). \tag{21.71}$$

(We set the relevant CKM factor equal to 1.) We will now turn this amplitude into an expression for the decay rate of the top quark. For simplicity, we will ignore the mass of the b quark in this computation.

Squaring the amplitude in (21.71) according to our standard methods, and then averaging over initial and summing over final spins, we find

$$\frac{1}{2}\sum_{\text{spins}}|\mathcal{M}|^2 = \frac{g^2}{2}\left[q^\mu p^\nu + q^\nu p^\mu - g^{\mu\nu} q\cdot p\right] \sum_{\text{polarizations}} \epsilon^*_\mu(k)\epsilon_\nu(k). \tag{21.72}$$

We can sum explicitly over physical gauge boson polarizations by inserting the expression (21.26) for the polarization sum. This gives

$$\begin{aligned}\frac{1}{2}\sum_{\text{spins}}|\mathcal{M}|^2 &= \frac{g^2}{2}\left[q^\mu p^\nu + q^\nu p^\mu - g^{\mu\nu} q\cdot p\right]\left[-g_{\mu\nu} + \frac{k_\mu k_\nu}{m_W^2}\right] \\ &= \frac{g^2}{2}\left[q\cdot p + 2\frac{(k\cdot q)(k\cdot p)}{m_W^2}\right].\end{aligned} \tag{21.73}$$

For $m_b = 0$,

$$2q\cdot p = 2q\cdot k = m_t^2 - m_W^2, \qquad 2k\cdot p = m_t^2 + m_W^2. \tag{21.74}$$

Then

$$\frac{1}{2}\sum_{\text{spins}}|\mathcal{M}|^2 = \frac{g^2}{4}\frac{m_t^4}{m_W^2}\left(1 - \frac{m_W^2}{m_t^2}\right)\left(1 + 2\frac{m_W^2}{m_t^2}\right). \tag{21.75}$$

After multiplying by phase space, we find

$$\Gamma = \frac{g^2}{64\pi}\frac{m_t^3}{m_W^2}\left(1 - \frac{m_W^2}{m_t^2}\right)^2\left(1 + 2\frac{m_W^2}{m_t^2}\right). \tag{21.76}$$

This is larger than our initial estimate (21.70) by a factor $(m_t/m_W)^2$.

It is not difficult to find the origin of this enhancement, by using the Goldstone boson equivalence theorem. In the gauge theory of weak interactions, the top quark obtains its mass from its coupling to the Higgs sector. The relation between the top-Higgs coupling λ_t and the top quark mass is written in Eq. (20.103). The top quark can be heavy only if λ_t is large. But then the amplitude for the top quark to decay to a Goldstone boson will be enhanced above (21.70) by the factor

$$\frac{\lambda_t^2}{g^2} = \frac{m_t^2}{2m_W^2}, \tag{21.77}$$

which is in fact the enhancement we found in (21.76).

To make the comparison more precise, we will now compute the prediction of the equivalence theorem for the top quark decay rate into a longitudinally polarized W^+ boson. Recall from (20.101) that the term in the weak interaction Lagrangian that couples t and b to the Higgs field is

$$\Delta\mathcal{L} = -\lambda_t \epsilon^{ab}\overline{Q}_{La}\phi_b^\dagger t_R + \text{h.c.} \tag{21.78}$$

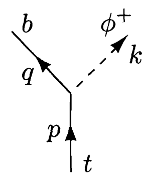

Figure 21.5. Decay of a t quark into a Goldstone boson and a b quark.

Decompose the Higgs field as in (21.38), and write

$$\phi^{\pm} = \frac{1}{\sqrt{2}}(\phi^1 \pm i\phi^2). \tag{21.79}$$

These are the fields of the charged Goldstone bosons that are eaten by the $W^{\pm}$. Including the Goldstone boson in the theory adds a process $t \to \phi^+ + b$, shown in Fig. 21.5. This process is mediated by the Lagrangian term

$$\Delta\mathcal{L} = \lambda_t \bar{b}_L \phi^+ t_R, \tag{21.80}$$

which leads to the decay amplitude

$$i\mathcal{M} = i\lambda_t \bar{u}(q)\Big(\frac{1+\gamma^5}{2}\Big)u(p). \tag{21.81}$$

From this expression, we easily find

$$\tfrac{1}{2}\sum_{\text{spins}} |\mathcal{M}|^2 = \lambda_t^2\, q\cdot p. \tag{21.82}$$

If we now ignore the mass of the Goldstone boson, or, equivalently, consider the limit $m_t \gg m_W$, we find for the top quark decay rate

$$\Gamma = \frac{\lambda_t^2}{32\pi} m_t = \frac{g^2}{64\pi}\frac{m_t^3}{m_W^2}, \tag{21.83}$$

in agreement with the leading term of (21.76) in this limit. Our results imply that only the production of the longitudinal polarization state of the W^+ is enhanced; this is easily checked directly by substituting explicit polarization vectors into (21.72).

In our derivation of (21.76), we summed over the physical polarization states of the emitted W^+; one might say that we used the prescription of the U gauge to sum over polarizations. We could equally well have used the prescription of Feynman-'t Hooft gauge, replacing

$$\sum_i \epsilon_\mu^*(k)\epsilon_\nu(k) \to -g_{\mu\nu}, \tag{21.84}$$

and also adding the contribution of the Goldstone boson emission diagram, treating the Goldstone boson as a massive particle with mass m_W. With these prescriptions, the gauge boson matrix element gives

$$\tfrac{1}{2}\sum_{\text{spins}} |\mathcal{M}|^2 = \frac{g^2}{2}(2q\cdot p) = \frac{g^2}{2}(m_t^2 - m_W^2). \tag{21.85}$$

The Goldstone boson emission diagram gives

$$\tfrac{1}{2}\sum_{\text{spins}} |\mathcal{M}|^2 = \lambda_t^2\, q\cdot p = \frac{g^2}{4}\frac{m_t^2}{m_W^2}(m_t^2 - m_W^2). \tag{21.86}$$

The sum of these contributions indeed reproduces (21.75) and thus gives the same result (21.76) for the total decay rate. In Feynman-'t Hooft gauge, the enhancement due to the large coupling of the top quark to the Higgs sector shows up explicitly in the Goldstone boson emission contributions to the total rate of W^+ production.

$e^+e^- \to W^+W^-$

Our second example is more complicated, but also contains more interesting physics. This is the reaction $e^+e^- \to W^+W^-$. In this reaction, the equivalence theorem does not lead to an enhancement of the cross section, but, rather, directs a cancellation between Feynman diagrams. As we will see, this cancellation is essential for the internal consistency of the theory.

In Problem 9.1, we computed the cross section for e^+e^- annihilation into a pair of charged scalar particles, as in Fig. 21.6(a), and found the result

$$\frac{d\sigma}{d\cos\theta}(e^+e^- \to \phi^+\phi^-) = \frac{\pi\alpha^2}{4s}\sin^2\theta \tag{21.87}$$

at energies much larger than the scalar mass. Just as for e^+e^- annihilation to fermion pairs, this cross section falls as $1/s$ at high energy. It can be shown that this behavior is required by unitarity: Since the electron and positron annihilate through a pointlike vertex, the annihilation takes place in only one partial wave. Unitarity puts a limit on the amplitude in this partial wave, requiring that $\mathcal{M}$ be bounded by a constant, and thus that σ be bounded by $1/s$ at high energy.*

The same unitarity argument applies to e^+e^- annihilation to vector bosons. Here, however, it is much less obvious that Feynman diagrams actually produce a cross section consistent with unitarity. Consider the contribution of Fig. 21.6(b). We would expect that the square of this diagram should contain a contribution to the cross section of the form of the scalar contribution (21.87) multiplied by the dot product of polarization vectors:

$$\frac{d\sigma}{d\cos\theta}(e^+e^- \to W^+W^-) \sim \frac{\pi\alpha^2}{4s}\cdot \left|\epsilon(k_+)\cdot\epsilon(k_-)\right|^2, \tag{21.88}$$

*Partial-wave analysis for relativistic collisions is discussed in Perkins (1987), Chapter 4.

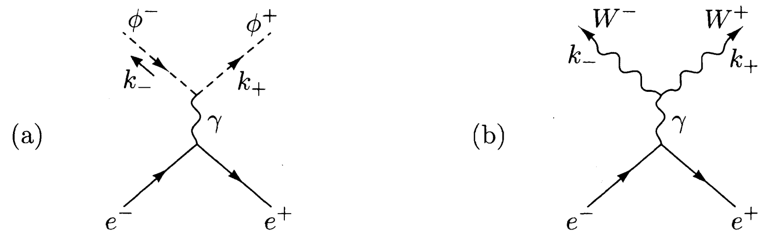

Figure 21.6. Electron-positron annihilation through a virtual photon (a) to charged scalar bosons, (b) to W bosons.

where k_+ and k_- are the momenta of the outgoing W bosons. For transversely polarized W bosons, this term is well behaved, but for longitudinally polarized W's it leads to problems. Using the approximation (21.60) for the longitudinal polarization vectors, we find

$$\epsilon(k_+) \cdot \epsilon(k_-) \to \frac{k_+ \cdot k_-}{m_W^2} \to \frac{s}{4m_W^2} \tag{21.89}$$

for $s \gg m_W^2$. This leads to a cross section that grows much faster than is allowed by unitarity. In principle, the cross section could be brought back down to a proper behavior by the addition of contributions from higher orders in perturbation theory, but this would be a most unpleasant resolution. It would imply that the theory of W bosons becomes strongly coupled at energies such that

$$\frac{s}{4m_W^2} \sim \left(\frac{g^2}{4\pi}\right)^{-1}, \tag{21.90}$$

corresponding to center-of-mass energies of order 1000 GeV. But if the theory of W bosons is strongly coupled at short distances, it is hard to understand why, at large distances, it should become the simple, weak-coupling theory that we observe.

Fortunately, there is another possible resolution of this problem. In the weak interaction gauge theory, there are three Feynman diagrams that contribute to the amplitude for $e^+e^- \to W^+W^-$ at the tree level; these are shown in Fig. 21.7. Each diagram separately produces a cross section that grows in the same manner as (21.88). However, it is possible that the badly behaved terms might cancel among the three diagrams, leaving a more proper high-energy behavior. If this miraculous cancellation were to occur, it would allow the theory of W bosons to be consistently weakly coupled up to very high energies.

Although such a cancellation seems unlikely at first sight, it is actually required by the Goldstone boson equivalence theorem. The theorem states that, at high energy, the cross section for producing longitudinal W bosons should be equal to the cross section for producing the corresponding scalar Goldstone bosons. But we know that scalar cross sections behave as $1/s$, as

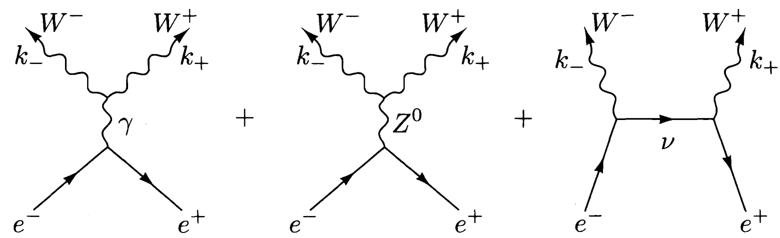

Figure 21.7. Diagrams contributing to $e^+e^- \to W^+W^-$ in the weak interaction gauge theory.

indicated in (21.87). Thus, somehow, the gauge boson cross section must also conspire to produce this result. We will now show this explicitly. We will see that the required cancellations are directed by the Ward identities of the gauge theory.

To prepare for this calculation, we need the Feynman rules for the vertices shown in Fig. 21.8. The Feynman rules for the couplings of the electron to W, Z, and γ can be read directly from (20.80). The relative strengths of these couplings are determined by the $SU(2) \times U(1)$ quantum numbers of the left- and right-handed components of the electron. It is equally straightforward to construct the couplings of the Goldstone bosons to Z and γ. Since the boson ϕ^+ has electric charge 1, the photon coupling is just that found in Problem 9.1. The Z coupling is determined with the additional information that the ϕ^+ has $I^3 = +1/2$. All of these expressions are shown in Fig. 21.8.

The three-gauge-boson vertices that appear in Fig. 21.7 arise from the cubic terms in the gauge field action. Since the $U(1)$ field strength is linear in gauge fields, these come only from the kinetic term of the $SU(2)$ gauge field. To identify the specific pieces we need, we must rewrite this cubic term in the basis of mass eigenstates given by (20.63) and (20.64). This can be done as follows:

$$\begin{aligned}
-\tfrac{1}{4}(F^a_{\mu\nu})^2 &\to -\tfrac{1}{2}(\partial_\mu A^a_\nu - \partial_\nu A^a_\mu) g\epsilon^{abc} A^{\mu b} A^{\nu c} \\
&= -g(\partial_\mu A^1_\nu - \partial_\nu A^1_\mu)A^{\mu 2}A^{\nu 3} + g(\partial_\mu A^2_\nu - \partial_\nu A^2_\mu)A^{\mu 1}A^{\nu 3} \\
&\qquad - g(\partial_\mu A^3_\nu - \partial_\nu A^3_\mu)A^{\mu 1}A^{\nu 2} \\
&= ig\big[(\partial_\mu W^+_\nu - \partial_\nu W^+_\mu)W^{\mu -}A^{\nu 3} - (\partial_\mu W^-_\nu - \partial_\nu W^-_\mu)W^{\mu +}A^{\nu 3} \\
&\qquad + \tfrac{1}{2}(\partial_\mu A^3_\nu - \partial_\nu A^3_\mu)(W^{\mu +}W^{\nu -} - W^{\mu -}W^{\nu +})\big]. \qquad (21.91)
\end{aligned}$$

Finally, inserting $A^3_\mu = \cos\theta_w Z_\mu + \sin\theta_w A_\mu$ and $g = e/\sin\theta_w$, we find the Feynman rules shown in Fig. 21.9.

Before examining the amplitude for e^+e^- annihilation to vector boson

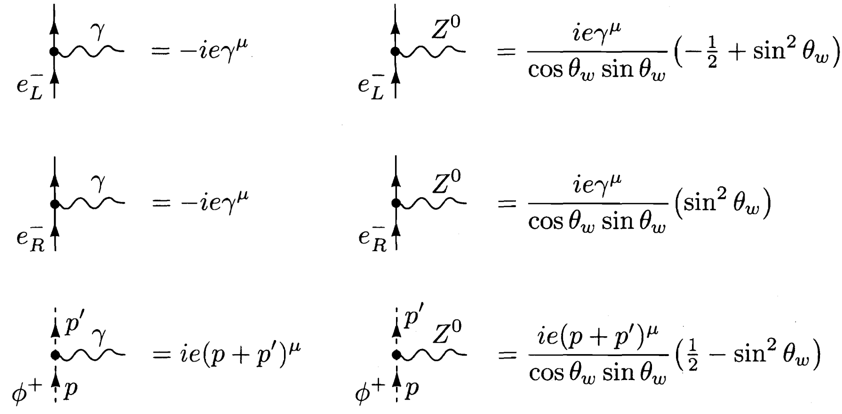

Figure 21.8. Feynman rules of the weak-interaction gauge theory for electrons and scalars coupling to photons and Z bosons.

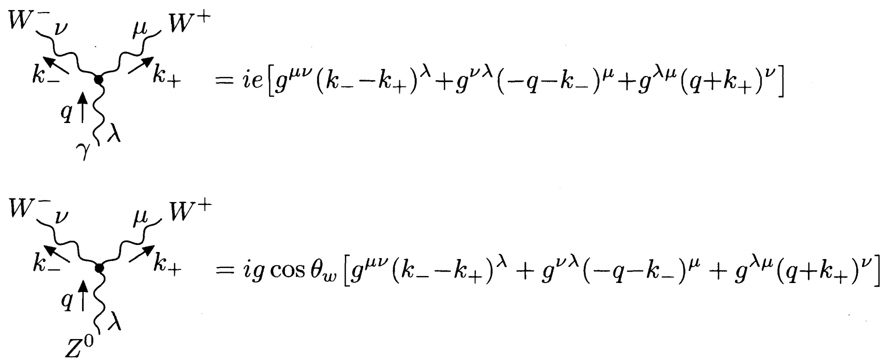

Figure 21.9. Feynman rules of the weak-interaction gauge theory for $WW\gamma$ and WWZ vertices.

pairs, we will first work out the amplitude for production of a pair of charged scalars. The equivalence theorem predicts that the amplitude for production of two longitudinal W bosons should become equal to this amplitude at high energy. Assembling vertices from Fig. 21.8, we find that, for an electron of either helicity, the amplitude to annihilate to scalars through a virtual photon is

$$i\mathcal{M}(ee \to \gamma^* \to \phi^+\phi^-) = ie^2\bar{v}\gamma_\mu u \frac{1}{q^2}(k_+ - k_-)^\mu, \tag{21.92}$$

where k_+, k_- are the momenta of the scalars and $q = k_+ + k_-$. The corresponding amplitude for annihilation through a virtual Z^0 depends on the e^+e^- helicities. Adding these contributions to the preceding expression, we find

$$i\mathcal{M}(e_L^- e_R^+ \to \phi^+\phi^-) = ie^2\bar{v}_L\gamma_\mu u_L\left[\frac{1}{q^2} + \frac{(\frac{1}{2}-\sin^2\theta_w)^2}{\sin^2\theta_w\cos^2\theta_w}\frac{1}{q^2-m_Z^2}\right](k_+-k_-)^\mu,$$
$$i\mathcal{M}(e_R^- e_L^+ \to \phi^+\phi^-) = ie^2\bar{v}_R\gamma_\mu u_R\left[\frac{1}{q^2} - \frac{(\frac{1}{2}-\sin^2\theta_w)}{\cos^2\theta_w}\frac{1}{q^2-m_Z^2}\right](k_+-k_-)^\mu. \tag{21.93}$$

Notice that, in the high-energy limit, the amplitude for the annihilation of right-handed electrons cancels down to

$$i\mathcal{M}(e_R^- e_L^+ \to \phi^+\phi^-) \to i\frac{e^2}{2\cos^2\theta_w}\bar{v}_R\gamma_\mu u_R\frac{1}{q^2}(k_+ - k_-)^\mu, \tag{21.94}$$

which is just the amplitude for an e_R^-, with $Y = -1$, to couple to a ϕ^+, with $Y = 1/2$, through the $U(1)$ gauge boson B_μ with coupling constant $g' = e/\cos\theta_w$. This expression reflects the fact that the e_R^- has no direct coupling to the $SU(2)$ gauge bosons. Similarly, the amplitude for left-handed electrons tends to

$$i\mathcal{M}(e_L^- e_R^+ \to \phi^+\phi^-) \to ie^2\left[\frac{1}{4\cos^2\theta_w} + \frac{1}{4\sin^2\theta_w}\right]\bar{v}_L\gamma_\mu u_L\frac{1}{q^2}(k_+ - k_-)^\mu \tag{21.95}$$

in the high-energy limit. This has the structure of a coherent sum of amplitudes with B_μ and A_μ^3 exchange. In just the way that we saw in Chapter 11, the symmetry structure of a gauge theory with spontaneously broken symmetry is recovered in the high-energy limit.

Now let us compare these results to a direct calculation of the W^+W^- production amplitude in the weak interaction gauge theory. Begin with the case of an initial e_R^-. Since the coupling of the electron to the W^- is purely left-handed, the third diagram of Fig. 21.7 vanishes in this case, so the computation is a bit easier. The first two diagrams of Fig. 21.7 have exactly the same structure and sum to

$$i\mathcal{M}(e_R^- e_L^+ \to W^+W^-) = \bar{v}_R\gamma_\lambda u_R\left[(-ie)\frac{-i}{q^2}(ie) + \frac{ie\sin\theta_w}{\cos\theta_w}\frac{-i}{q^2-m_Z^2}\frac{ie\cos\theta_w}{\sin\theta_w}\right]$$
$$\cdot\left[g^{\mu\nu}(k_--k_+)^\lambda + g^{\lambda\nu}(-q-k_-)^\mu + g^{\lambda\mu}(k_++q)^\nu\right]\epsilon_\mu^*(k_+)\epsilon_\nu^*(k_-). \tag{21.96}$$

This equation is valid in any of the R_ξ gauges, since, if we ignore the electron mass,

$$q^\lambda\bar{v}_R\gamma_\lambda u_R = 0. \tag{21.97}$$

The second line of Eq. (21.96) contains the enhancement for longitudinal W bosons mentioned above. If we approximate the longitudinal polarization vectors by (21.60) and drop terms that do not grow as $s \to \infty$, this line becomes

$$\left[g^{\mu\nu}(k_- - k_+)^\lambda + g^{\lambda\nu}(-q - k_-)^\mu + g^{\lambda\mu}(k_+ + q)^\nu\right]\frac{k_{+\mu}}{m_W}\frac{k_{-\nu}}{m_W}$$

$$= \frac{1}{m_W^2}\left[k_+\cdot k_-(k_- - k_+)^\lambda - 2k_-\cdot k_+ k_-^\lambda + 2k_+\cdot k_- k_+^\lambda\right] + \mathcal{O}(1)\cdot(k_- - k_+)^\lambda$$
$$= \frac{s}{2m_W^2}(k_+ - k_-)^\lambda + \cdots . \tag{21.98}$$

On the other hand, the expression in brackets in the first line of (21.96) cancels almost completely, to

$$-ie^2\left(\frac{1}{q^2} - \frac{1}{q^2 - m_Z^2}\right) = +ie^2\frac{m_Z^2}{q^2(q^2 - m_Z^2)}.$$

Using both of these simplifications, we find

$$i\mathcal{M}(e_R^- e_L^+ \to W_L^+ W_L^-) = \bar{v}_R\gamma_\lambda u_R\left[(ie^2)\frac{m_Z^2}{s^2}\right]\frac{s}{2m_W^2}(k_+ - k_-)^\lambda. \tag{21.99}$$

By inserting the relation $m_W = m_Z\cos\theta_w$, we see that this amplitude is identical to (21.94), as required by the equivalence theorem.

For the amplitude with an initial e_L^-, the computation is somewhat more involved. Now all three diagrams of Fig. 21.7 contribute, and since the last diagram has a different kinematic structure, it will be less clear how the diagrams combine together. In what follows, we will demonstrate the cancellation of the unitarity-violating enhanced terms, and we will indicate how the terms one order smaller in m_W^2/s assemble into the correct structure. However, we will not account rigorously for all of these smaller terms. The full calculation of these diagrams is the subject of Problem 21.2.

For the case of an initial e_L^-, the first two diagrams of Fig. 21.7 sum to the expression

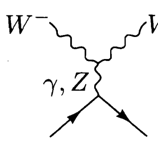

$$= \bar{v}_L\gamma_\lambda u_L\left[(-ie)\frac{-i}{q^2}(ie) + \frac{ie(-\frac{1}{2}+\sin^2\theta_w)}{\sin\theta_w\cos\theta_w}\frac{-i}{q^2 - m_Z^2}\frac{ie\cos\theta_w}{\sin\theta_w}\right]$$
$$\cdot\left[g^{\mu\nu}(k_- - k_+)^\lambda + g^{\lambda\nu}(-q - k_-)^\mu + g^{\lambda\mu}(k_+ + q)^\nu\right]\epsilon_\mu^*(k_+)\epsilon_\nu^*(k_-), \tag{21.100}$$

which differs from (21.96) only in the coupling of the electron to the virtual Z^0. For longitudinal W bosons, we can simplify this expression as we did (21.96), obtaining

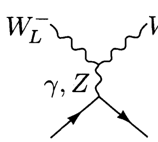

$$= \bar{v}_L\gamma_\lambda u_L(ie^2)\left[\frac{m_Z^2}{s(s - m_Z^2)} - \frac{1}{2\sin^2\theta_w}\frac{1}{s - m_Z^2}\right]\frac{s}{2m_W^2}(k_+ - k_-)^\lambda. \tag{21.101}$$

The second term in brackets is a potentially dangerous contribution, which must be canceled by the diagram with t-channel neutrino exchange. This diagram has the value

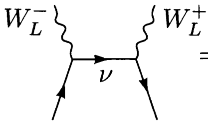

$$= \left(\frac{ig}{\sqrt{2}}\right)^2 \bar{v}_L \gamma^\mu \frac{i(\not{\ell} - \not{k}_-)}{(\ell - k_-)^2} \gamma^\nu u_L(\ell) \epsilon^*_\mu(k_+) \epsilon^*_\nu(k_-), \tag{21.102}$$

where ℓ is the initial electron momentum. Approximating the longitudinal polarization vectors as before, we have

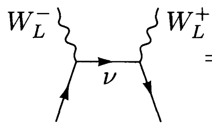

$$= -i\frac{g^2}{2} \bar{v}_L \frac{\not{k}_+}{m_W} \frac{(\not{\ell} - \not{k}_-)}{(\ell - k_-)^2} \frac{\not{k}_-}{m_W} u_L(\ell). \tag{21.103}$$

Now we manipulate this expression as if we were proving a Ward identity. Using the fact that $u_L(\ell)$ satisfies the Dirac equation,

$$(\not{\ell} - \not{k}_-)\not{k}_- u_L(\ell) = -(\not{\ell} - \not{k}_-)^2 u_L(\ell) = -(\ell - k_-)^2 u_L(\ell), \tag{21.104}$$

expression (21.103) reduces to

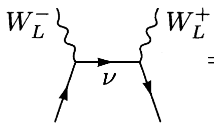

$$= i\frac{g^2}{2} \bar{v}_L \frac{\not{k}_+}{m_W^2} u_L(\ell). \tag{21.105}$$

Finally, using Eq. (21.97), we can rewrite this expression as

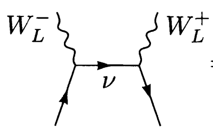

$$= ie^2 \frac{1}{2\sin^2\theta_w} \frac{1}{2m_W^2} \bar{v}_L \gamma_\lambda u_L(\ell)(k_+ - k_-)^\lambda. \tag{21.106}$$

This term cancels the dangerous high-energy behavior of (21.101). To see that the sum of diagrams has the correct high-energy limit, however, the approximations that we have used are not quite adequate. In particular, the correction to relation (21.60) for the polarization vectors is of order m_W^2/s and must be taken into account. When all of the corrections of order m_W^2/s are included, it turns out that the sum of the s-channel diagrams (21.101) is unchanged, while the expression for the neutrino exchange diagram (21.106) is multiplied by the factor $(1 + 2m_W^2/s)$. Then the sum of all three diagrams gives

$$\begin{aligned} i\mathcal{M}(e^-_L e^+_R \to W^+_L W^-_L) &= ie^2 \bar{v}_L \gamma_\lambda u_L (k_+ - k_-)^\lambda \frac{1}{s} \\ &\cdot \left[\frac{1}{2\cos^2\theta_w} - \frac{1}{4\cos^2\theta_w \sin^2\theta_w} + \frac{1}{2\sin^2\theta_w}\right]. \end{aligned} \tag{21.107}$$

The middle term in brackets cancels half of each of the other two terms, to give an expression that agrees precisely with Eq. (21.95).

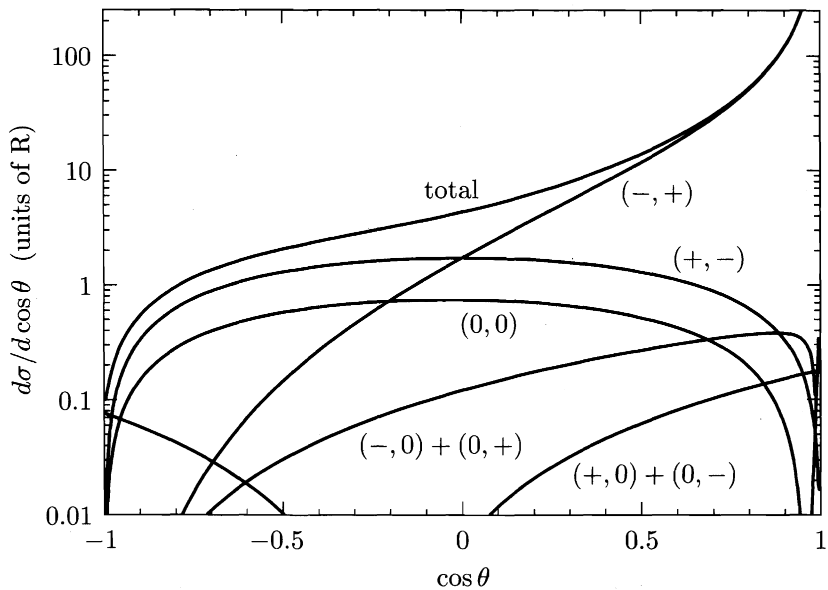

Figure 21.10. The differential cross section for $e^-_L e^+_R \to W^+W^-$, in units of R (Eq. (5.15)), at $E_{\text{cm}} = 1000$ GeV. The various curves show the contributions to the total from individual helicity states of W^- and W^+; these are denoted (h_-, h_+), where each helicity takes the values $(+, -, 0)$. The contributions from the $(+,+)$ and $(-,-)$ states are too small to be visible. Notice that both the $W^-_L W^+_L$ cross section, denoted $(0,0)$, and the $(+,-)$ cross section become proportional to $\sin^2\theta$ at very high energy.

The calculation of Problem 21.2 gives for the complete annihilation amplitude

$$\begin{aligned} i\mathcal{M}(e^-_L e^+_R \to W^+_L W^-_L) &= ie^2 \bar{v}_L \gamma_\lambda u_L (k_+ - k_-)^\lambda \frac{1}{s} \\ &\cdot \left[\frac{1}{2\sin^2\theta_w} \left\{ -\frac{s}{s-m_Z^2}\left(\frac{m_Z^2}{2m_W^2}+1\right) + \frac{2}{\beta^2} \right. \right. \\ &\left.\left. - \frac{8m_W^2}{s\beta^2(1+\beta^2-2\beta\cos\theta)} \right\} + \frac{m_Z^2}{m_W^2}\left(\frac{\frac{1}{2}s+m_W^2}{s-m_Z^2}\right) \right], \end{aligned} \tag{21.108}$$

where $\beta = (1 - 4m_W^2/s)^{1/2}$ is the W boson velocity. The high-energy limit of this expression indeed reproduces (21.107). The contributions to the differential cross section for $e^-_L e^+_R \to W^+W^-$ from this and the other possible helicity states are plotted in Fig. 21.10.

These cancellations among the diagrams of Fig. 21.7 occur by virtue of the Ward identities of the gauge theory. That is, they occur only because the theory has an underlying local gauge invariance. At the beginning of our discussion, we argued that these cancellations are necessary to insure that the theory remains, in a consistent way, weakly coupled up to arbitrarily high energy. In Section 20.1, we showed that one can generate masses for vector bosons by spontaneously breaking local gauge invariance. We have now argued the converse of that result: that the only theories of massive vector bosons that do not have violent high-energy behavior are those that result from spontaneously broken gauge theories.†

21.3 One-Loop Corrections to the Weak-Interaction Gauge Theory

The final topic in our study of spontaneously broken gauge theories is the computation of one-loop corrections in the weak-interaction gauge theory. As we discussed in Section 20.2, tree-level diagrams produce a number of intricate predictions for the couplings of the Z^0 and the cross sections for neutral current reactions. In general, these predictions are modified by the effects of one-loop diagrams. In this section we will study some examples of these one-loop corrections.

As in any renormalizable field theory, the one-loop diagrams of the electroweak gauge theory are typically ultraviolet divergent. These divergences can be absorbed by adjusting the underlying parameters of the theory. These adjustments define a set of counterterms which, by renormalizability, render the full set of one-loop diagrams of the theory finite. Those amplitudes that are not adjusted by hand then become predictions of the theory.

In Chapter 11, we saw that this general procedure, which applies to any renormalizable field theory, gives especially rich information when applied to a theory with spontaneous symmetry breaking. In a theory with spontaneously broken symmetry, the amplitudes of the theory vary markedly for different particles in the same multiplet of the original symmetry. However, the counterterms of the theory respect the symmetry relations. Thus, the adjustment of an amplitude for one particle leads to definite predictions for other particles that are not related by any manifest symmetry.

Theoretical Orientation, and a Specific Problem

At the end of Section 11.6, we presented a useful framework for organizing calculations of the predictions of renormalizable theories with spontaneous symmetry breaking. We defined a *zeroth-order natural relation* to be a relation among observable quantities in the theory that is true for any values of the parameters in the Lagrangian. Since the counterterms of the theory shift the values of the underlying parameters without adding new terms, a zeroth-order natural relation will not be corrected by these counterterms. Thus, if the theory is renormalizable, the one-loop corrections to a zeroth-order natural

†This statement is proved systematically in the paper of Cornwall, Levin, and Tiktopoulos cited at the beginning of this section.

relation will be finite, and will in fact be definite predictions from the quantum structure of the field theory. Though we discussed this idea originally in theories with spontaneously broken global symmetry, it applies equally well to theories with spontaneously broken gauge symmetry. In this section, we will apply this idea to derive finite one-loop corrections to relations in the weak-interaction gauge theory.

It is easy to find zeroth-order natural relations in the electroweak theory. The leading-order predictions given in Section 20.2 involve a relatively small number of free parameters. Many of these predictions are made for energies at which the quark and lepton masses can be ignored; then they depend only on the coupling constants g and g' and the vacuum expectation value v, which sets the scale of spontaneous symmetry breaking. The remaining ingredients of the weak-interaction theory are given in terms of these parameters; for example,

$$\begin{aligned} m_W &= g\frac{v}{2}, \qquad & m_Z &= \sqrt{g^2+g'^2}\frac{v}{2}, \\ e &= \frac{gg'}{\sqrt{g^2+g'^2}}, \qquad & \frac{G_F}{\sqrt{2}} &= \frac{g^2}{8m_W^2} = \frac{1}{2v^2}. \end{aligned} \tag{21.109}$$

Even in this set of quantities, we have four relations that depend on three underlying parameters, so there is one relation of observable quantities that is independent of the parameters of the Lagrangian.

Since many of the predictions of the weak interaction gauge theory are determined by the parameter $\sin^2\theta_w$, it is useful to define $\sin^2\theta_w$ in terms of observables and then use this definition as a basis for constructing natural relations. In our discussion of the precision tests of electroweak theory in Section 20.2, we used the definition

$$s_W^2 \equiv 1 - \frac{m_W^2}{m_Z^2} \tag{21.110}$$

as a standard for comparison of different experiments. But since the three most accurately known weak-interaction observables are α, G_F, and m_Z, it is useful to construct another physical definition of $\sin^2\theta_w$ based on these three quantities. Define θ_0 such that

$$\sin 2\theta_0 \equiv \left(\frac{4\pi\alpha_*}{\sqrt{2}G_F m_Z^2}\right)^{1/2}, \tag{21.111}$$

where α_* is the running coupling constant of QED evaluated at the scale $Q^2 = m_Z^2$. The renormalization group insists that it is the value of the electric charge at the weak-interaction scale that enters precision electroweak predictions, and this observation is confirmed by summing radiative correction diagrams involving light quarks and leptons. The current best values of the quantities in Eq. (21.111) give

$$s_0^2 \equiv \sin^2\theta_0 = 0.2307 \pm 0.0005. \tag{21.112}$$

Thus, this quantity provides a very accurate standard of reference.

Once Eq. (21.111) is taken to define a reference value of $\sin^2\theta_w$, the equations of Section 20.2 that connect $\sin^2\theta_w$ to other observables become zeroth-order natural relations. For example, the tree-level equations

$$\frac{m_W^2}{m_Z^2} = \cos^2\theta_w, \qquad A_{LR}^e = \frac{(\frac{1}{2}-\sin^2\theta_w)^2 - (\sin^2\theta_w)^2}{(\frac{1}{2}-\sin^2\theta_w)^2 + (\sin^2\theta_w)^2} \tag{21.113}$$

are natural relations linking four observables of the weak interactions. The corrections to these relations will be well-defined predictions of the theory.

In principle, we could now compute all of the one-loop diagrams that correct the parameters m_W, m_Z, G_F, α, and A_{LR}^e. However, this is a very complicated exercise, requiring an extensive technical apparatus.‡ In this section we will focus on radiative corrections from one simple source that can be considered independently. Aside from the question of anomalies, the electroweak theory does not restrict the number of quark or lepton generations. Thus, it is sensible, and gauge invariant, to compute the one-loop corrections due to one quark or lepton doublet. For definiteness, we consider the effects of the (t, b) quark doublet.

By focusing on the radiative corrections due to heavy quarks, we dramatically simplify the calculational task before us. The various observables of the weak-interaction gauge theory are extracted from the measurement of scattering amplitudes with light fermions, leptons or quarks, in the initial and final states. For example, G_F is measured from the strength of a low-energy weak-interaction process, usually chosen to be the rate of muon decay: $\mu \to \nu_\mu e^- \bar{\nu}_e$. For any such process, there are one-loop corrections of many kinds, as shown in Fig. 21.11. In addition to corrections to the vector boson propagator, there are vertex corrections, box diagrams, and diagrams with real photon emission. In general, the contributions of the various classes of diagrams are not gauge invariant; rather, gauge invariance results from cancellations between the classes of diagrams in Fig. 21.11(b), (c), and (d). However, since heavy quarks do not couple directly to the light leptons, the (t, b) doublet contributes only the single diagram shown in Fig. 21.11(f), which must be gauge invariant by itself. This same conclusion applies to the (t, b) correction to other leptonic weak interaction processes. If we ignore the CKM angles that mix the t and b with other species, the conclusion extends also to weak-interaction processes involving light quarks.

A similar situation occurs with other species of particles, such as those of the Higgs sector. The coupling of Higgs sector particles to a light quark or lepton is proportional to the fermion's mass, which we can often ignore. Thus the most important contributions from Higgs-sector particles are propagator corrections. The case in which the spontaneous symmetry breaking is produced by a single scalar field ϕ is particularly straightforward to analyze;

‡A detailed theoretical discussion of one-loop corrections to the electroweak theory can be found in W. Hollik, *Fortscr. d. Physik* **38**, 165 (1990).

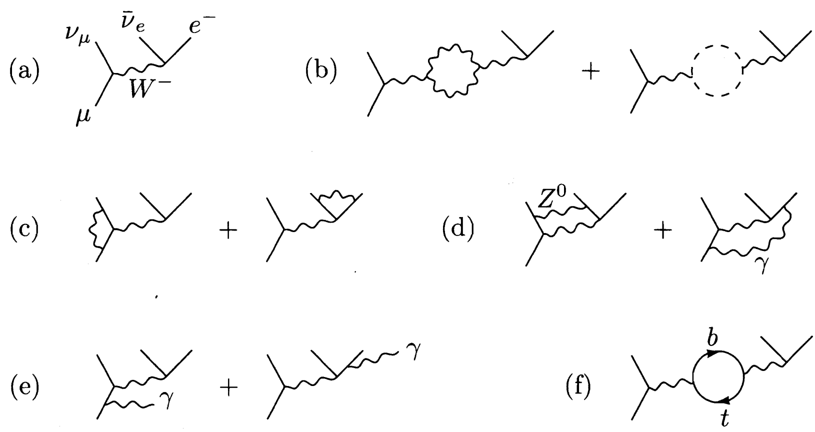

Figure 21.11. Examples of radiative corrections to μ decay in the weak interaction gauge theory: (a) lowest-order diagram; (b) propagator corrections; (c) vertex diagrams; (d) box diagrams; (e) real photon corrections; (f) the contribution of the (t, b) doublet.

this is done in Problem 21.4. Loop corrections from particles that do not couple directly to the external fermions are often termed *oblique*, since they enter the low-energy weak interactions only indirectly.

Influence of Heavy Quark Corrections

Our task, then, is to compute the corrections to relations (21.113) due to the (t, b) doublet. These two relations depend on five observable quantities—m_Z, m_W, A^e_{LR}, α, and G_F—with the last two parameters entering through θ_w and Eq. (21.111). We will express these five quantities as functions of the bare parameters g, g', and v, with corrections proportional to combinations of t and b vacuum polarization diagrams. The zeroth-order terms will naturally cancel out when we compute the corrections to the relations (21.113).

The loop amplitudes that we require are shown in Fig. 21.12. To deal with these contributions most straightforwardly, we introduce a uniform notation for vacuum polarization amplitudes. Denote the vacuum polarization amplitude involving the gauge bosons I and J as

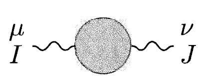

$$= i\Pi^{\mu\nu}_{IJ}(q), \tag{21.114}$$

where I and J may be γ, W, or Z. When the gauge bosons are massive, the vacuum polarization amplitudes need not be transverse by themselves, so $\Pi^{\mu\nu}_{IJ}(q)$ need not vanish at $q^2 = 0$. Thus, we will change our notation from the case of QED and write the decomposition of $\Pi^{\mu\nu}_{IJ}(q)$ into tensor structures as

$$\Pi^{\mu\nu}_{IJ}(q) = \Pi_{IJ}(q^2)g^{\mu\nu} - \Delta(q^2)q^\mu q^\nu. \tag{21.115}$$

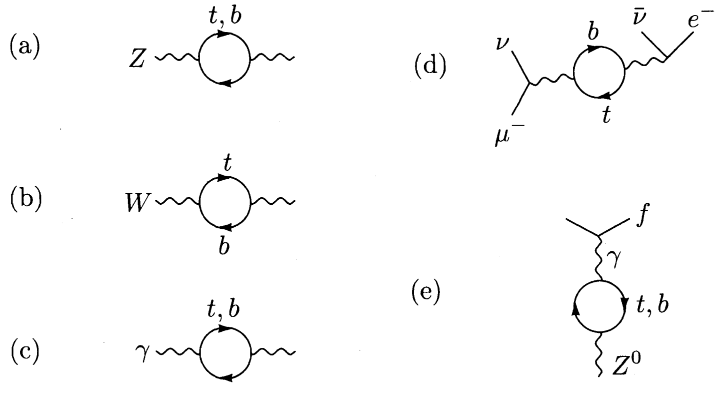

Figure 21.12. One-loop corrections from t and b to weak-interaction observables: (a) m_Z; (b) m_W; (c) α; (d) G_F; (e) A^e_{LR}.

In all of the examples to follow, the factors q^μ will dot into currents of light leptons, to give zero as in Eq. (21.97). Thus the form factor $\Delta(q^2)$ will drop out of our calculations. Our previous result that $\Pi^{\mu\nu}(q)$ vanishes in QED at $q^2 = 0$ appears in this formalism as the set of constraints

$$\Pi_{\gamma\gamma}(0) = \Pi_{\gamma Z}(0) = 0. \tag{21.116}$$

For the other amplitudes, our sign conventions are chosen so that a positive value of $\Pi_{IJ}(m^2)$ gives a positive mass shift to the gauge boson. Let us also define

$$\Pi'_{\gamma\gamma}(0) = \left.\frac{d\Pi_{\gamma\gamma}}{dq^2}\right|_{q^2=0}; \tag{21.117}$$

this is the quantity we called $\Pi(0)$ in Eq. (7.73).

Now we use this notation to write the loop corrections to each of the five observables. The first two diagrams in Fig. 21.12 are simply mass corrections, and so, straightforwardly,

$$\begin{aligned} m_Z^2 &= (g^2 + g'^2)\frac{v^2}{4} + \Pi_{ZZ}(m_Z^2), \\ m_W^2 &= g^2\frac{v^2}{4} + \Pi_{WW}(m_W^2). \end{aligned} \tag{21.118}$$

Note that both vacuum polarization amplitudes are evaluated at the poles in the respective propagators. To evaluate the shift of α by one-loop corrections, we consider the effect of Fig. 21.12(c) on the low-energy Coulomb potential. The values of the leading-order propagator and the one-loop correction combine to give the factors

$$\frac{-ie^2}{q^2}\Big(1 + i\Pi_{\gamma\gamma}(q^2)\cdot\frac{-i}{q^2}\Big), \tag{21.119}$$

where, in this equation, e^2 is given in terms of bare variables as in (21.109). Thus, the observed value of α, in the limit $q^2 \to 0$, is modified according to the relation

$$4\pi\alpha = \frac{g^2 g'^2}{g^2 + g'^2}\big(1 + \Pi'_{\gamma\gamma}(0)\big). \tag{21.120}$$

In a similar way, the diagrams of Fig. 21.12(d) give a modified strength of the 4-fermion weak interaction process that leads to μ decay. The leading and one-loop diagrams sum to

$$\frac{g^2}{q^2 - m_W^2}\Big(1 + i\Pi_{WW}(q^2)\frac{-i}{q^2 - m_W^2}\Big). \tag{21.121}$$

Then the effective strength of the weak interaction vertex at $q^2 = 0$ is shifted as follows:

$$\frac{G_F}{\sqrt{2}} = \frac{1}{2v^2}\Big(1 - \frac{\Pi_{WW}(0)}{m_W^2}\Big). \tag{21.122}$$

Notice that, in the approximation of keeping only oblique corrections, the strength of every low-energy weak interaction amplitude is corrected by this same factor.

Finally, the polarization asymmetry A^e_{LR} is corrected by a (t, b) loop diagram according to Fig. 21.12(e). The analogous diagram with an intermediate Z^0 is summed into the Z^0 propagator and does not affect the form of the vertex. At zeroth order, the coupling of the Z^0 to any left- or right-handed light fermion is given, according to Eq. (20.71), by

$$\sqrt{g^2 + g'^2}\Big(T^3 - \frac{g'^2}{g^2 + g'^2}Q\Big). \tag{21.123}$$

The coefficient of Q is the bare value of $\sin^2\theta_w$. The loop diagram in Fig. 21.12(e) adds to this a contribution

$$i\Pi_{Z\gamma}(q^2)\frac{-i}{q^2} \cdot (ieQ). \tag{21.124}$$

To discuss asymmetries at the Z^0 resonance, we set $q^2 = m_Z^2$. The term (21.124) adds to the piece of (21.123) proportional to Q; thus it shifts the bare value of $\sin^2\theta_w$. When we include this correction, the Z^0 coupling takes the form

$$\sqrt{g^2 + g'^2}\big(T^3 - s_*^2 Q\big), \tag{21.125}$$

where

$$s_*^2 = \frac{g'^2}{g^2 + g'^2} - \frac{e}{\sqrt{g^2 + g'^2}}\frac{\Pi_{\gamma Z}(m_Z^2)}{m_Z^2}. \tag{21.126}$$

The asymmetries at the Z^0 resonance discussed in Section 20.2 are computed as ratios of these couplings. Thus, to include the oblique radiative correction to A^f_{LR}, for any light fermion species f, we reevaluate formula (20.96), using s_*^2 in place of the zeroth-order $\sin^2\theta_w$.

We might, in fact, say that s_*^2 gives an additional way to define $\sin^2\theta_w$ from observable quantities, to be compared to the definitions s_W^2 given in (21.110) and s_0^2 given in (21.111). Speaking strictly, the value of $\sin^2\theta_w$ determined by the asymmetries at the Z^0 depends on the quark or lepton quantum numbers through vertex corrections that are not included in the analysis above. However, these species-dependent corrections are small and can be systematically subtracted to define a universal s_*^2 that determines the weak interaction asymmetries of all fermion species.*

The three definitions of $\sin^2\theta_w$ all agree at zeroth order but receive different radiative corrections. If we include only the oblique corrections, it is easy to produce compact formulae for the three quantities. From (21.126), we have

$$s_*^2 = \frac{g'^2}{g^2+g'^2} - \sin\theta_w\cos\theta_w\frac{\Pi_{\gamma Z}}{m_Z^2}. \tag{21.127}$$

In the prefactor of the one-loop correction, we can ignore the distinction between the bare and renormalized values of $\sin^2\theta_w$. We can obtain a similar expression for s_W^2 by taking the ratio of the two formulae in (21.118):

$$s_W^2 = \frac{g'^2}{g^2+g'^2} - \frac{1}{m_Z^2}\left(\Pi_{WW}(m_W^2) - \frac{m_W^2}{m_Z^2}\Pi_{ZZ}(m_Z^2)\right). \tag{21.128}$$

Finally, we can evaluate the oblique corrections to $\sin^2\theta_0$ defined by (21.111). This is most readily done by writing $\delta\theta_0$ for the difference between the true and the bare value of θ_0, and then expanding (21.111) as follows:

$$2\cos 2\theta_0\,\delta\theta_0 = \frac{1}{2}\sin 2\theta_0\left[\frac{\delta\alpha}{\alpha} - \frac{\delta G_F}{G_F} - \frac{\delta m_Z^2}{m_Z^2}\right]. \tag{21.129}$$

The shifts of α, G_F, and m_Z^2 can be read from (21.120), (21.122), and (21.118). Then we can reconstruct

$$\sin^2\theta_0 = \frac{g'^2}{g^2+g'^2} + 2\sin\theta_0\cos\theta_0\delta\,\theta_0. \tag{21.130}$$

Assembling the pieces and evaluating the coefficients of the vacuum polarization diagrams to zeroth order, we obtain

$$\begin{aligned}\sin^2\theta_0 = {} & \frac{g'^2}{g^2+g'^2} \\ & + \frac{\sin^2\theta_w\cos^2\theta_w}{\cos^2\theta_w-\sin^2\theta_w}\left[\Pi'_{\gamma\gamma}(0) + \frac{1}{m_W^2}\Pi_{WW}(0) - \frac{1}{m_Z^2}\Pi_{ZZ}(m_Z^2)\right].\end{aligned} \tag{21.131}$$

It is not difficult to discover that each of the equations (21.127), (21.128), and (21.131) contains ultraviolet divergences. However, if the weak interaction gauge theory is renormalizable, these divergences should cancel when we

*This is explained clearly in D. Kennedy and B. W. Lynn, *Nucl. Phys.* **B322**, 1 (1989).

compute the corrections to any zeroth-order natural relation. In the situation that we consider, renormalizability implies that the various definitions of $\sin^2\theta_w$ should differ only by expressions that are ultraviolet-finite.

We are now almost prepared to check this prediction explicitly. We can clarify the structure of the ultraviolet divergences in our relations for the various quantities $\sin^2\theta_w$ by recasting the vacuum polarization amplitudes to make more explicit the quantum numbers to which the gauge bosons couple. Recall from Eq. (20.71) that the Z boson couples to the combination of $SU(2)$ and electromagnetic quantum numbers $(T^3 - \sin^2\theta_w Q)$. Similarly, the W bosons couple to $T^\pm$, or, equivalently, to T^1, T^2. It is useful to break up the vacuum polarization amplitudes into terms that depend on these specific quantum numbers. We will also extract the coupling constants indicated in (20.71). Thus we replace

$$\begin{aligned}
\Pi_{\gamma\gamma} &= e^2\Pi_{QQ},\\
\Pi_{\gamma Z} &= \Big(\frac{e^2}{\sin\theta_w\cos\theta_w}\Big)\big[\Pi_{3Q} - \sin^2\theta_w\Pi_{QQ}\big],\\
\Pi_{ZZ} &= \Big(\frac{e}{\sin\theta_w\cos\theta_w}\Big)^2\big[\Pi_{33} - 2\sin^2\theta_w\Pi_{3Q} + \sin^4\theta_w\Pi_{QQ}\big],\\
\Pi_{WW} &= \Big(\frac{e}{\sin\theta_w}\Big)^2\Pi_{11},
\end{aligned}\tag{21.132}$$

where Q denotes the electric charge and $1, 2, 3$ denote the components of weak-interaction $SU(2)$.

A vacuum polarization amplitude can always be viewed as an expectation value of a pair of currents. From this viewpoint, the quantities on the right-hand side of (21.132) are expectation values of currents with definite quantum numbers. For example, Π_{33} is an expectation value of a pair of $SU(2)$ currents $J^{\mu 3}$. Acting on the standard fermions, J^μ_a is a left-handed current and J^μ_Q is a vector current.

The ultraviolet divergences in the expectation values of currents in (21.132) have the form

$$\begin{aligned}
\Pi_{33} &\sim \big(A + Bq^2\big)\log\Lambda^2,\\
\Pi_{11} &\sim \big(A + Bq^2\big)\log\Lambda^2,\\
\Pi_{3Q} &\sim \big(Bq^2\big)\log\Lambda^2,\\
\Pi_{QQ} &\sim \big(Cq^2\big)\log\Lambda^2.
\end{aligned}\tag{21.133}$$

We will demonstrate this explicitly later in this section. However, we can understand this structure from the following rough argument: Since the symmetry of the theory should be recovered at large momentum, the amplitudes Π_{33} and Π_{11}, which differ only by their orientation in the symmetry space, should have the same ultraviolet divergences. The divergence in the slope of Π_{3Q} should be related to that in the slope of Π_{33} because $Q = T^3 + Y$ and Π_{3Y} is unimportant asymptotically since $\mathrm{tr}[T^3 Y] = 0$. We pointed out in Eq. (21.116) that Π_{3Q} and Π_{QQ} vanish at $q^2 = 0$; thus they have no q^2-independent divergences.

Now we will rewrite the two zeroth-order natural relations in (21.113) in such a way that we can apply (21.133). To do this, we take the differences of Eqs. (21.127), (21.128), and (21.131) to obtain

$$\begin{aligned} s_*^2 - \sin^2\theta_0 &= \frac{\sin^2\theta_w\cos^2\theta_w}{\cos^2\theta_w - \sin^2\theta_w}\left\{\frac{\Pi_{ZZ}(m_Z^2)}{m_Z^2} - \frac{\Pi_{WW}(0)}{m_W^2} - \Pi'_{\gamma\gamma}(0)\right. \\ &\qquad\qquad \left. - \frac{\cos^2\theta_w - \sin^2\theta_w}{\sin\theta_w\cos\theta_w}\frac{\Pi_{\gamma Z}(m_Z^2)}{m_Z^2}\right\}, \\ s_W^2 - s_*^2 &= -\frac{\Pi_{WW}(m_W^2)}{m_Z^2} + \frac{m_W^2}{m_Z^2}\frac{\Pi_{ZZ}(m_Z^2)}{m_Z^2} + \sin\theta_w\cos\theta_w\frac{\Pi_{\gamma Z}(m_Z^2)}{m_Z^2}. \end{aligned} \tag{21.134}$$

Inserting (21.132), and also using the relation $m_W = m_Z\cos\theta_w$ in the coefficients of terms already of one-loop order, we find after some algebra

$$\begin{aligned} s_*^2 - \sin^2\theta_0 &= \frac{e^2}{(\cos^2\theta_w - \sin^2\theta_w)m_Z^2}\Big\{\big[\Pi_{33}(m_Z^2) - \Pi_{11}(0) - \Pi_{3Q}(m_Z^2)\big] \\ &\qquad\qquad + \sin^2\theta_w\cos^2\theta_w\big[\Pi_{QQ}(m_Z^2) - m_Z^2\Pi'_{QQ}(0)\big]\Big\}, \\ s_W^2 - s_*^2 &= \frac{e^2}{\sin^2\theta_w m_Z^2}\big[\Pi_{33}(m_Z^2) - \Pi_{11}(m_W^2) - \sin^2\theta_w\Pi_{3Q}(m_Z^2)\big]. \end{aligned} \tag{21.135}$$

If indeed the ultraviolet divergences of the vacuum polarization integrals have the structure of (21.133), then the divergent part of each expression in brackets in (21.135) vanishes, and the weak interaction gives definite, finite predictions for the differences of s_*^2, s_W^2, and $\sin^2\theta_0$.

Computation of Vacuum Polarization Amplitudes

We can verify the divergence structure (21.133) by computing the vacuum polarization diagrams for t and b quarks explicitly. Rather than computing these one by one, it is easiest to compute, once and for all, the most general fermionic vacuum polarization amplitudes, and then to recover the amplitudes required in the previous paragraph as special cases of these.

Consider, then, the two vacuum polarization amplitudes shown in Fig. 12.13. The diagrams are built from two fermion propagators with different masses m_1 and m_2, linked by left- or right-handed currents. We call the vacuum polarization amplitude with two left-handed currents $\Pi_{LL}^{\mu\nu}(q^2)$, and that with one left and one right-handed current $\Pi_{LR}^{\mu\nu}(q^2)$. Since the vacuum polarizations depend on only one momentum and two vector indices, there is no way that they can contain an invariant involving $\epsilon^{\mu\nu\rho\sigma}$. Thus, the amplitudes with other combinations of currents are related to these by

$$\Pi_{RR}^{\mu\nu}(q^2) = \Pi_{LL}^{\mu\nu}(q^2), \qquad \Pi_{RL}^{\mu\nu}(q^2) = \Pi_{LR}^{\mu\nu}(q^2). \tag{21.136}$$

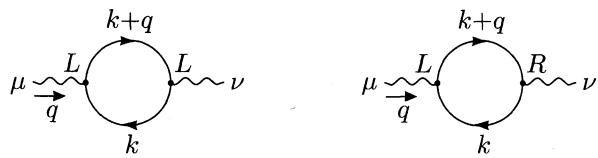

Figure 21.13. Elementary vacuum polarization amplitudes of fermionic currents.

In addition, there is no difficulty in regularizing these diagrams using dimensional regularization with an anticommuting γ^5, the regularization prescription we endorsed at the end of Section 19.4. The vacuum polarization of a vector current is reconstructed as

$$\Pi^{\mu\nu}_{VL}(q^2) = \Pi^{\mu\nu}_{LL}(q^2) + \Pi^{\mu\nu}_{RL}(q^2). \tag{21.137}$$

The vacuum polarization of purely left-handed currents is given by

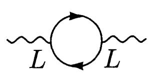

$$\begin{aligned} = (-1)\int \frac{d^4k}{(2\pi)^4}\, \mathrm{tr}\Big[(i\gamma^\mu)\Big(\frac{1-\gamma^5}{2}\Big)\frac{i(\not{k}+m_1)}{k^2-m_1^2} \\ \cdot (i\gamma^\nu)\Big(\frac{1-\gamma^5}{2}\Big)\frac{i(\not{k}+\not{q}+m_2)}{(k+q)^2-m_2^2}\Big] \\ = -\int \frac{d^4k}{(2\pi)^4}\, \mathrm{tr}\big[\gamma^\mu \not{k}\gamma^\nu(\not{k}+\not{q})\Big(\frac{1+\gamma^5}{2}\Big)\big] \cdot \frac{1}{(k^2-m_1^2)((k+q)^2-m_2^2)}. \end{aligned} \tag{21.138}$$

The prefactor (-1) comes from the fermion loop. There is no possible tensor structure antisymmetric in μ and ν, so we can now drop the γ^5 term. From here, the calculation proceeds as in Section 7.5. We combine denominators using

$$\frac{1}{(k^2-m_1^2)((k+q)^2-m_2^2)} = \int_0^1 dx\, \frac{1}{(\ell^2-\Delta)^2}, \tag{21.139}$$

where

$$\ell = k + xq, \qquad \Delta = xm_2^2 + (1-x)m_1^2 - x(1-x)q^2. \tag{21.140}$$

Then, integrating with dimensional regularization and following the steps leading to Eq. (7.90), we find

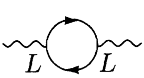

$$\begin{aligned} = -\frac{4i}{(4\pi)^{d/2}}\int_0^1 dx\, \frac{\Gamma(2-\frac{d}{2})}{\Delta^{2-d/2}}\big[g^{\mu\nu}\big(x(1-x)q^2 \\ - \tfrac{1}{2}(xm_2^2+(1-x)m_1^2)\big) - x(1-x)q^\mu q^\nu\big]. \end{aligned} \tag{21.141}$$

Notice that both $\Pi^{\mu\nu}_{LL}$ and its first derivative with respect to q^2 are logarithmically divergent.

The vacuum polarization amplitude $\Pi_{LR}^{\mu\nu}$ can be obtained in a very similar fashion. From the Feynman rules,

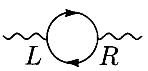

$$= (-1)\int \frac{d^4k}{(2\pi)^4}\,\mathrm{tr}\Big[(i\gamma^\mu)\Big(\frac{1-\gamma^5}{2}\Big)\frac{i(\not k+m_1)}{k^2-m_1^2} \cdot (i\gamma^\nu)\Big(\frac{1+\gamma^5}{2}\Big)\frac{i(\not k+\not q+m_2)}{(k+q)^2-m_2^2}\Big]$$

$$= -\int \frac{d^4k}{(2\pi)^4}\,\mathrm{tr}\Big[\gamma^\mu m_1\gamma^\nu m_2\Big(\frac{1+\gamma^5}{2}\Big)\Big]\frac{1}{(k^2-m_1^2)((k+q)^2-m_2^2)}. \tag{21.142}$$

From here, the same manipulations as in the previous paragraph lead to

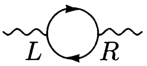

$$= -\frac{2i}{(4\pi)^{d/2}}\int_0^1 dx\,\frac{\Gamma(2-\frac{d}{2})}{\Delta^{2-d/2}}\big[g^{\mu\nu}m_1m_2\big]. \tag{21.143}$$

As a check, we can use (21.141), (21.143), and (21.136), setting $m_1 = m_2 = m$, to assemble the QED vacuum polarization of vector currents. We find

$$\begin{aligned}\Pi_{VV}^{\mu\nu}(q^2) &= e^2\big[\Pi_{LL}^{\mu\nu}+\Pi_{LR}^{\mu\nu}+\Pi_{RL}^{\mu\nu}+\Pi_{RR}^{\mu\nu}\big]\\ &= \frac{-8e^2}{(4\pi)^{d/2}}\int_0^1 dx\,\frac{\Gamma(2-\frac{d}{2})}{\Delta^{2-d/2}}\big[x(1-x)q^2g^{\mu\nu}-x(1-x)q^\mu q^\nu\big],\end{aligned} \tag{21.144}$$

where now $\Delta = m^2 - x(1-x)q^2$. This coincides precisely with our result from Section 7.5.

As we argued below (21.115), only the terms in the vacuum polarization amplitudes proportional to $g^{\mu\nu}$ will enter our expressions for weak-interaction radiative corrections. Thus, we can summarize the calculation of the basic vacuum polarization amplitudes by quoting the results for this leading form factor:

$$\begin{aligned}\Pi_{LL}(q^2) = \Pi_{RR}(q^2) &= -\frac{4}{(4\pi)^{d/2}}\int_0^1 dx\,\frac{\Gamma(2-\frac{d}{2})}{\Delta^{2-d/2}}\big[x(1-x)q^2\\ &\qquad\qquad -\tfrac{1}{2}(xm_2^2+(1-x)m_1^2)\big];\\ \Pi_{LR}(q^2) = \Pi_{RL}(q^2) &= -\frac{2}{(4\pi)^{d/2}}\int_0^1 dx\,\frac{\Gamma(2-\frac{d}{2})}{\Delta^{2-d/2}}\big[m_1m_2\big].\end{aligned} \tag{21.145}$$

From these terms, we can assemble any desired vacuum polarization of t and b quarks in the weak-interaction gauge theory. To make use of these expressions more easily, we will expand the quantities (21.145) in the limit $d \to 4$. If we set $\epsilon = 4 - d$, the integrands of the expressions above simplify according to

$$\frac{1}{(4\pi)^{d/2}} \frac{\Gamma(2-\frac{d}{2})}{\Delta^{2-d/2}} \to \frac{1}{(4\pi)^2}\left[\frac{2}{\epsilon} - \gamma + \log(4\pi) - \log\Delta\right]. \tag{21.146}$$

Let

$$E = \frac{2}{\epsilon} - \gamma + \log(4\pi) - \log(M^2), \tag{21.147}$$

where M is an arbitrary subtraction scale. It is useful to define

$$\begin{aligned} b_0(12X) &\equiv b_0(m_1^2, m_2^2, q_X^2) = \int_0^1 dx \, \log\bigl(\Delta(m_1^2, m_2^2, q_X^2)/M^2\bigr), \\ b_1(12X) &\equiv b_1(m_1^2, m_2^2, q_X^2) = \int_0^1 dx \, x \log\bigl(\Delta(m_1^2, m_2^2, q_X^2)/M^2\bigr), \\ b_2(12X) &\equiv b_2(m_1^2, m_2^2, q_X^2) = \int_0^1 dx \, x(1-x) \log\bigl(\Delta(m_1^2, m_2^2, q_X^2)/M^2\bigr). \end{aligned} \tag{21.148}$$

The abbreviated notation will prove useful below. In (21.148), X labels a momentum scale; we will need $q_X = 0, m_W, m_Z$. Note that for equal masses,

$$b_1(11X) = \tfrac{1}{2} b_0(11X). \tag{21.149}$$

With this notation,

$$\begin{aligned} \Pi_{LL}(q_X^2) = -\frac{4}{(4\pi)^2}\Bigl[&\bigl(\tfrac{1}{6}q_X^2 - \tfrac{1}{4}(m_1^2 + m_2^2)\bigr)E - q_X^2 b_2(12X) \\ &+ \tfrac{1}{2}\bigl(m_2^2 b_1(12X) + m_1^2 b_1(21X)\bigr)\Bigr] \end{aligned} \tag{21.150}$$

and

$$\Pi_{LR}(q_X^2) = -\frac{2}{(4\pi)^2}\bigl[m_1 m_2 E - m_1 m_2 b_0(12X)\bigr]. \tag{21.151}$$

We can now reconstruct all of the specific vacuum polarization amplitudes that appear in Eq. (21.135) in terms of divergences proportional to E and finite parts proportional to the b_i. The simplest is the expectation value of electromagnetic currents, which is given in our present notation by

$$\Pi_{QQ}(q_X^2) = -3 \cdot \frac{8}{(4\pi)^2}\Big[\big(\tfrac{2}{3}\big)^2\big(\tfrac{1}{6}q_X^2 E - q_X^2 b_2(ttX)\big) + \big(\tfrac{1}{3}\big)^2\big(\tfrac{1}{6}q_X^2 E - q_X^2 b_2(bbX)\big)\Big]. \tag{21.152}$$

The prefactor 3 is the trace over colors. As we expect from QED, (21.152) contains a divergence only in a term proportional to q_X^2. The divergent parts of the other amplitudes are

$$\begin{aligned}
\Pi_{33}(q_X^2) &= -\frac{12}{(4\pi)^2}\cdot \tfrac{1}{2}\big[\tfrac{1}{6}q_X^2 - \tfrac{1}{4}(m_t^2+m_b^2)\big]E + \cdots,\\
\Pi_{11}(q_X^2) &= -\frac{12}{(4\pi)^2}\cdot \tfrac{1}{2}\big[\tfrac{1}{6}q_X^2 - \tfrac{1}{4}(m_t^2+m_b^2)\big]E + \cdots,\\
\Pi_{3Q}(q_X^2) &= -\frac{12}{(4\pi)^2}\cdot \tfrac{1}{2}\big[\tfrac{1}{6}q_X^2\big]E + \cdots.
\end{aligned} \tag{21.153}$$

These divergences indeed follow the pattern claimed in Eq. (21.133), and thus the predictions of the weak interaction gauge theory given in (21.135) are free of ultraviolet divergences.

The Effect of m_t

Using the notation we have developed, we can write the finite parts of the relations (21.135) in a compact form. The first relation becomes

$$\begin{aligned}
s_*^2 - \sin^2\theta_0 = \frac{3\alpha}{\pi(\cos^2\theta_w - \sin^2\theta_w)}\Big\{&\big(\tfrac{1}{4}-\tfrac{1}{3}\big)b_2(ttZ) + \big(\tfrac{1}{4}-\tfrac{1}{6}\big)b_2(bbZ)\\
&- \tfrac{1}{4}\Big(\frac{m_t^2}{m_Z^2}[b_1(ttZ) - b_1(bt0)] + \frac{m_b^2}{m_Z^2}[b_1(bbZ) - b_1(tb0)]\Big)\\
&+ 2\sin^2\theta_w\cos^2\theta_w\big(\tfrac{4}{9}[b_2(ttZ) - b_2(tt0) - m_Z^2 b_2'(tt0)]\\
&+ \tfrac{1}{9}[b_2(bbZ) - b_2(bb0) - m_Z^2 b_2'(bb0)]\big)\Big\}.
\end{aligned} \tag{21.154}$$

Similarly, the second relation becomes

$$\begin{aligned}
s_W^2 - s_*^2 = \frac{3\alpha}{\pi\sin^2\theta_w}\Big\{&\big(\tfrac{1}{4}-\tfrac{1}{3}\sin^2\theta_w\big)b_2(ttZ) + \big(\tfrac{1}{4}-\tfrac{1}{6}\sin^2\theta_w\big)b_2(bbZ)\\
&- \tfrac{1}{4}\cos^2\theta_w b_2(tbW)\\
&- \tfrac{1}{4}\Big(\frac{m_t^2}{m_Z^2}[b_1(ttZ) - b_1(btW)] + \frac{m_b^2}{m_Z^2}[b_1(bbZ) - b_1(tbW)]\Big)\Big\}.
\end{aligned} \tag{21.155}$$

Though it is now straightforward to work out the complete expressions for the relations (21.154) and (21.155), we will content ourselves here with identifying the most important term in the limit in which the t quark mass becomes large. Notice that, in each of these expressions, there are terms with coefficients proportional to m_t^2/m_Z^2. These are easiest to understand within the simpler combination of vacuum polarization amplitudes

$$\begin{aligned}
\Pi_{11}(0) - \Pi_{33}(0) &= \frac{12}{(4\pi)^2}\frac{1}{4}\Big[m_t^2\big(b_1(tt0) - b_1(bt0)\big) + m_b^2\big(b_1(bb0) - b_1(tb0)\big)\Big] \\
&= \frac{3}{16\pi^2}\int_0^1 dx\,\Big\{xm_t^2\log\frac{m_t^2}{M^2} + (1-x)m_b^2\log\frac{m_b^2}{M^2} \\
&\qquad\qquad - \big(xm_t^2 + (1-x)m_b^2\big)\log\frac{xm_t^2 + (1-x)m_b^2}{M^2}\Big\} \\
&= -\frac{3}{16\pi^2}\int_0^1 dx\,\Big\{xm_t^2\log\frac{xm_t^2 + (1-x)m_b^2}{m_t^2} + \mathcal{O}(m_b^2)\Big\} \\
&= \frac{3}{16\pi^2}\cdot\frac{1}{4}m_t^2 + \mathcal{O}(m_b^2)
\end{aligned} \tag{21.156}$$

for $m_t \gg m_b$. If m_t is also much greater than m_Z, one can find a contribution proportional to m_t^2/m_Z^2 in each of the relations (21.154), (21.155) by replacing the argument $q_X^2 = m_Z^2$ with $q_X^2 = 0$, using (21.156), and ignoring all other contributions. One can show, by detailed examination of (21.154) and (21.155), that this procedure gives the complete leading term in m_t. The result is

$$\begin{aligned}
s_*^2 - \sin^2\theta_0 &= -\frac{3\alpha}{16\pi(\cos^2\theta_w - \sin^2\theta_w)}\frac{m_t^2}{m_Z^2} + \cdots, \\
s_W^2 - s_*^2 &= -\frac{3\alpha}{16\pi\sin^2\theta_w}\frac{m_t^2}{m_Z^2} + \cdots,
\end{aligned} \tag{21.157}$$

where the omitted terms are of order α with no enhancement.

The enhancement factor m_t^2/m_Z^2 is exactly the one that we found in our study of top quark decay in Section 21.2. It reflects the fact that some electroweak couplings of the top quark are effectively proportional to λ_t, the top quark coupling to the Higgs sector, instead of simply to the weak interaction coupling g.

The complete numerical evaluation of the formulae for s_*^2 and s_W^2 is shown in Fig. 21.14. To compare the results of this section to experiment, we have included, in addition to the top quark effect, the m_t-independent one-loop corrections from loops containing W and Z bosons and light quarks and leptons. In the figure, the predictions are compared to the value of s_*^2 obtained from the measurement of the Z^0 polarization and forward-backward asymmetries and the value of s_W^2 obtained from measurement of the W boson mass.

According to the figure, the weak interaction gauge theory requires the top quark mass radiative correction (or a similar radiative correction from some other heavy particle) for its consistency with experiment. The top quark is predicted to have a mass approximately equal to 170 GeV. A recent analysis

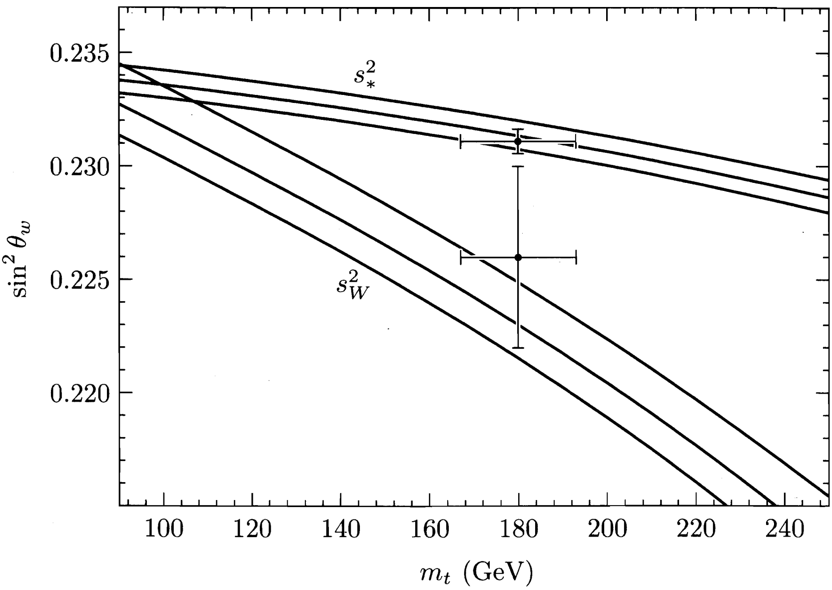

Figure 21.14. Dependence of s_*^2 and s_W^2 on the top quark mass, for fixed α, G_F, m_Z. The three curves in each group correspond to three different values of the Higgs boson mass: 100, 300, 1000 GeV from bottom to top. The curves are compared to values of s_*^2 and s_W^2, taken from the article of Langacker and Erler quoted in Table 20.1, and the CDF/D0 value of the top quark mass given in Eq. (21.159).

of all neutral current weak interaction data has given the prediction†

$$m_t = 169 \pm 24 \text{ GeV}. \tag{21.158}$$

Just as this book was being completed, the CDF and D0 experiments at Fermilab announced the observation of the production of top quark pairs in proton-antiproton scattering. From kinematic fits to events believed to contain top quarks, these experiments reported‡

$$m_t = 180 \pm 13 \text{ GeV}. \tag{21.159}$$

The discovery of the top quark in just the range required by precision electroweak measurements is quite remarkable. We can only conclude that, in the domain of weak interactions as well as those of electromagnetic, strong, and scalar interactions that we have studied earlier, the fluctuations predicted by quantum field theory make their imprint on the phenomena of Nature.

†P. Langacker and J. Erler, in *Review of Particle Properties, Phys. Rev.* **D50**, 1304 (1994).

‡F. Abe, et. al., *Phys. Rev. Lett.* **74**, 2626 (1995); S. Abachi, et. al., *Phys. Rev. Lett.* **74**, 2632 (1995).

Problems

21.1 Weak-interaction contributions to the muon $g-2$. The GWS model of the weak interactions leads to two new contributions to the anomalous magnetic moments of the leptons. Because these contributions are proportional to $G_F m_\ell^2$, they are extremely small for the electron, but for the muon they might possibly be observable. Both contributions are larger than the contribution of the Higgs boson discussed in Problem 6.3.

(a) Consider first the contribution to the muon electromagnetic vertex function that involves a W-neutrino loop diagram. In the R_ξ gauges, this diagram is accompanied by diagrams in which W propagators are replaced by propagators for Goldstone bosons. Compute the sum of these diagrams in the Feynman-'t Hooft gauge and show that, in the limit $m_W \gg m_\mu$, they contribute the following term to the anomalous magnetic moment of the muon:

$$a_\mu(\nu) = \frac{G_F m_\mu^2}{8\pi^2\sqrt{2}} \cdot \frac{10}{3}.$$

(b) Repeat the calculation of part (a) in a general R_ξ gauge. Show explicitly that the result of part (a) is independent of ξ.

(c) A second new contribution is that from a Z-muon loop diagram and the corresponding diagram with the Z replaced by a Goldstone boson. Show that these diagrams contribute

$$a_\mu(Z) = -\frac{G_F m_\mu^2}{8\pi^2\sqrt{2}} \cdot \left(\frac{4}{3} + \frac{8}{3}\sin^2\theta_w - \frac{16}{3}\sin^4\theta_w\right).$$

21.2 Complete analysis of $e^+e^- \to W^+W^-$.

(a) Using explicit polarization vectors, work out the amplitudes for $e^+e^- \to W^+W^-$ from left- and right-handed electrons to states in which the W^+ and W^- have definite helicity. For the cases in which both W bosons have longitudinal polarization, verify that Eq. (21.99) gives the correct high-energy limit for right-handed electrons, and verify the complete expression (21.108) for left-handed electrons. For the cases in which one W is longitudinally polarized and the second is transversely polarized, show that the individual diagrams give contributions to the amplitudes that grow like $\sqrt{s}$, but that the complete amplitudes fall as $1/\sqrt{s}$.

(b) Show that the contributions to $e_L^- e_R^+ \to W^-W^+$ found in part (a) reproduce Fig. 21.10, and that the differential cross section for $e_R^- e_L^+ \to W^-W^+$ is about 30 times smaller. How many of the qualitative features of the figure can you understand physically?

21.3 Cross section for $d\bar{u} \to W^-\gamma$. Compute the amplitudes for $d\bar{u} \to W^-\gamma$ for the various possible initial and final helicities. Ignore the quark masses. In this approximation, only the annihilation amplitude from $d_L\bar{u}_R$ is nonzero. Show that the scattering amplitudes for all final helicity combinations vanish at $\cos\theta = -1/3$, where θ is the scattering angle in the center-of-mass system. Compute the differential cross section as a function of $\cos\theta$.

21.4 Dependence of radiative corrections on the Higgs boson mass.

(a) Consider the contributions to weak-interaction radiative corrections involving the physical Higgs boson h^0 of the GWS model. The couplings of the h^0 were discussed near the end of Section 20.2. Show that, if we ignore terms proportional to the masses of light fermions, the Higgs boson contributes one-loop corrections to the processes considered in Section 21.3 only through vacuum polarization diagrams. It follows that the contributions to vacuum polarization amplitudes that depend on the Higgs boson mass are gauge invariant.

(b) Draw the vacuum polarization diagrams in Feynman-'t Hooft gauge that involve the Higgs boson, and compute the dependence of the various vacuum polarization amplitudes on the Higgs boson mass m_h.

(c) Show that, for $m_h \gg m_W$, the natural relations discussed in Section 21.3 receive corrections

$$s_*^2 - s_0^2 = \frac{\alpha}{\cos^2\theta_w - \sin^2\theta_w} \frac{(1 + 9\sin^2\theta_w)}{48\pi} \log\frac{m_h^2}{m_W^2},$$

$$s_W^2 - s_*^2 = \alpha\frac{5}{24\pi}\log\frac{m_h^2}{m_W^2}.$$

The effect of varying m_h is displayed in Fig. 21.14 and is included as a theoretical uncertainty in the prediction (21.158). More accurate experiments might allow one to predict m_h from its effect on electroweak radiative corrections.

Final Project

Decays of the Higgs Boson

At the end of Section 20.2, we discussed the mystery of the origin of spontaneous symmetry breaking in the weak interactions. The simplest hypothesis is that the $SU(2) \times U(1)$ gauge symmetry of the weak interactions is broken by the expectation value of a two-component scalar field ϕ. However, since we have almost no experimental information about the mechanism of this symmetry breaking, many other possibilities can be suggested.

Eventually, this problem should be resolved by experimental observation of the particles associated with the symmetry breaking. To form incisive experimental tests, we should compute the properties expected for these particles. We saw in Section 20.2 that, if the symmetry is indeed broken by a single scalar field ϕ, the symmetry-breaking sector contributes only one new particle, a scalar h^0 called the Higgs boson. The mass m_h of this particle is unknown. However, the couplings of the h^0 to known fermions and bosons are completely determined by the masses of those particles and the weak interaction coupling constants. Thus, it is possible to compute the amplitudes for production and decay of the h^0 in some detail. More complicated models of $SU(2) \times U(1)$ symmetry breaking typically contain one or more particles that share some properties with the h^0. Thus, this study is a useful starting point for the more general analysis of experimental tests of these models.

In this Final Project you will compute the amplitudes for the Higgs boson h^0 to decay to pairs of quarks, leptons, and gauge bosons. The computations beautifully illustrate the working of perturbation theory for non-Abelian gauge fields. Those decays of the Higgs boson that involve quarks and gluons bring in aspects of QCD. Thus, this exercise reviews all of the important technical methods of Part III. Except for a question raised at the end of part (a), the problem relies only on material from unstarred sections of Part III. The material in Chapter 20 plays an essential role. Material from Chapter 21 enters the analysis only in parts (b) and (f), and the other parts of the problem (except for the final summary in part (h)) do not rely on these. If you have studied Section 19.5, you will have some additional insight into the results of parts (c) and (f), but this insight is not necessary to work the problem.

Consider, then, the minimal form of the Glashow-Weinberg-Salam electroweak theory with one Higgs scalar field ϕ. The physical Higgs boson h^0 of this theory was discussed in Section 20.2, and we listed there the couplings of this particle to quarks, leptons, and gauge bosons. You can now use that information to compute the amplitudes for the various possible decays of the h^0 as a function of its mass m_h. You will discover that the decay pattern has a complicated dependence on the mass of the Higgs boson, with different decay modes dominating in different mass ranges. The dependences of the various decay rates on m_h illustrate many aspects of the physics of gauge theories that we have discussed in Part III.

In working this exercise, you should consider m_h as a free parameter. For the other parameters of weak-interaction theory, you might use the following values: $m_b = 5$ GeV, $m_t = 175$ GeV, $m_W = 80$ GeV, $m_Z = 91$ GeV, $\sin^2\theta_w = 0.23$, $\alpha_s(m_Z) = 0.12$.

(a) Compute first the rate for $h^0 \to f\bar{f}$, where f is a quark or lepton of the standard model. After a completely trivial computation, you should find

$$\Gamma(h^0 \to f\bar{f}) = \Big(\frac{\alpha m_h}{8\sin^2\theta_w}\Big) \cdot \frac{m_f^2}{m_W^2}\Big(1 - \frac{4m_f^2}{m_h^2}\Big)^{3/2} \cdot N_c(f),$$

where $N_c(f) = 1$ for leptons, 3 for quarks. If you have studied Chapter 18, you might improve this result for the case in which the fermion f is a quark, by computing the leading-log QCD corrections for the case $m_h \gg m_q$. Remember that the quark mass m_q is determined at the quark threshold $M^2 \sim m_q^2$.

(b) If $m_h > 2m_W$, the Higgs boson can decay to W^+W^-; if it is just a bit heavier, it can also decay to Z^0Z^0. Compute the decay widths to these final states. You can check your result in the following way: If $m_h \gg m_W$, the dominant contribution to the decay comes from production of longitudinally polarized W or Z bosons, and this contribution can be estimated at follows:

$$\Gamma(h^0 \to W^+W^-) \approx \Gamma(h^0 \to \phi^+\phi^-), \quad \Gamma(h^0 \to Z^0Z^0) \approx \Gamma(h^0 \to \phi^3\phi^3),$$

where $\phi^\pm$, ϕ^3 are the Goldstone bosons of the Higgs sector and the quantities on the right-hand sides of these relations are computed in the *ungauged* Higgs theory. Explain why this statement should be true, and verify it explicitly.

(c) The third important decay mode of the Higgs is the decay to 2 gluons. The amplitude for this decay is generated by diagrams involving quark loops. Compute these diagrams, using dimensional regularization. The diagrams will be finite, but nevertheless there is a subtle contribution which apparently depends on the regulator. Check that you have computed the amplitude correctly by verifying that it is gauge invariant. Then square the amplitude and construct the decay rate. You should find

$$\Gamma(h^0 \to 2g) = \Big(\frac{\alpha m_h}{8\sin^2\theta_w}\Big) \cdot \frac{m_h^2}{m_W^2} \cdot \frac{\alpha_s^2}{9\pi^2} \cdot \Big|\sum_q I\Big(\frac{m_h^2}{m_q^2}\Big)\Big|^2,$$

where the sum runs over all quark species and $I(m_h^2/m_q^2)$ is a form factor with the property that $I(x) \to 1$ as $x \to 0$ and $I(x) \to 0$ as $x \to \infty$. This property implies that the dominant contribution to the decay rate comes from very heavy quarks. You need not evaluate $I(x)$ explicitly at this stage; just leave it in the form of a Feynman parameter integral.

(d) The existence of the process $h^0 \to 2g$ implies the existence of the inverse process $g+g \to h^0$, which is a mechanism for production of Higgs bosons in proton-proton collisions. Using the parton model, derive a relation between the partial width $\Gamma(h^0 \to 2g)$ and the total cross section for $pp \to h^0 + X$. Compute this cross section numerically (in nanobarns) for a 30 GeV Higgs for pp collisions of center of mass energy 1–40 TeV. (1 TeV $= 10^3$ GeV.) For the purposes of this problem set (though this is not actually a good approximation) you may ignore the Q^2 dependence of the gluon distribution function and take simply

$$f_g(x) = 8 \cdot \frac{1}{x}(1-x)^7.$$

You may also set $I(m_h^2/m_t^2) = 1$; this is correct to about 10%.

(e) The final decay mode that you should consider is $h^0 \to 2\gamma$. Consider first the contribution from the loop diagrams involving quarks and leptons. Show that the result is simply expressed in terms of the form factor $I(m_h^2/m^2)$ that you derived in part (c).

(f) Next, compute the contribution to this decay amplitude from the loop diagram involving W bosons, and the various diagrams one must add to this to obtain a gauge-invariant result. It is easiest to work in Feynman-'t Hooft gauge. Add this contribution to that of very heavy quarks and leptons, each with electric charge Q_f. Your result should reduce to the following expression in the limit $m_h \ll m_W$:

$$\Gamma(h^0 \to 2\gamma) = \left(\frac{\alpha m_h}{8\sin^2\theta_w}\right) \cdot \frac{m_h^2}{m_W^2} \cdot \frac{\alpha^2}{18\pi^2} \cdot \left|\sum_f Q_f^2 N_c(f) - \frac{21}{4}\right|^2.$$

(g) Now work out the detailed behavior of the form factor $I(x)$ defined in part (c). Reduce your expression from part (c) to a one-parameter integral. then evaluate this integral numerically. Plot $I(m_h^2/m_t^2)$ over the range 50 GeV $< m_h <$ 500 GeV, and compute the decay width $\Gamma(h^0 \to 2g)$ numerically (in keV) over this range. The computation of part (f) introduces an addition form factor; compute this function in the same way.

(h) Finally, put together all the pieces. Find the branching fraction of the h^0 into each of its five major decay modes $b\bar{b}$, $t\bar{t}$, gg, W^+W^-, Z^0Z^0. for Higgs bosons of mass 50 GeV – 500 GeV.

Epilogue

Chapter 22

Quantum Field Theory at the Frontier

In this textbook we have surveyed the most important ideas of quantum field theory. Working from the basic concepts that come from fusing relativity, quantum mechanics, and fields, we have built an elaborate structure, which includes such remarkable elements as coupling constant renormalization and non-Abelian gauge fields. We have seen at many points that the strange and abstract elements of this structure actually intersect with observation and even produce explanations for unexpected aspects of the behavior of elementary particles.

In the course of our study, we have arrived at a complete theory of the strong, weak, and electromagnetic interactions of elementary particles. Each element of this theory has been described as a quantum field theory, and these quantum field theories have turned out to have very similar structure as gauge theories coupled to fermions. At various points in our discussion, we have noted that these theories have passed stringent quantitative experimental tests. We have not had space to describe the wide variety of experiments that contribute to our faith in these theories, but today almost all particle physicists consider this $SU(3) \times SU(2) \times U(1)$ gauge theory as established. In fact, most of these people refer to this theory condescendingly as 'the standard model'.

Though the best data to support the standard model have come from experiments of the past five years, the ideas behind it are much older. Most of the theoretical developments described in this book were concluded in the 1970s, a generation removed from the current frontier of physics. But this does not mean that quantum field theory is irrelevant to that frontier, any more than quantum mechanics and electrodynamics have lost their relevance after many years of exploration. On the contrary, the theory of elementary particles—like other areas of physics that depend on quantum fluctuations in continua—still holds deep mysteries, and quantum field theory remains the principal tool for exploration of these questions.

In this final chapter, we will flash forward to the present day and discuss the relevance of quantum field theory to current questions in the physics of the fundamental interactions. We will present what are, in our view, the outstanding unsolved problems of elementary particle physics and describe how quantum field theory is being used to confront these problems. Many of these applications involve aspects of quantum field theory that are beyond the scope of this book. These include the use of quantum field theory in the regime beyond the reach of perturbation theory and the use of quantum field theory to explore the special properties of theories with higher spin and local symmetry. In these areas our discussion will be mainly qualitative, but we will give references that provide points of entry into each of these subjects.

It should be obvious that our discussion in this final chapter will express our personal opinions and by no means represents the consensus of experts in quantum field theory. In addition, any collection of 'current problems' in a rapidly developing area of research should quickly become dated. In fact, we hope the readers of this book will quickly make this chapter obsolete by solving the problems that we highlight here.

22.1 Strong Strong Interactions

One paradoxical aspect of our discussion of the strong interactions is that all of our concrete results were obtained by assuming that these interactions are weak. At large momentum transfer, we argued, this assumption is actually valid due to asymptotic freedom. Still, it is uncomfortable that we have left the most obvious questions about strongly interacting particles—for example, their masses and low-energy interactions—in a mysterious regime excluded from our analysis.

To work with QCD in the region where the strong interactions are strong, we need to answer three questions: First, how do we describe the forces that bind quarks together into hadrons? Second, what is an appropriate description of the quark-antiquark and three-quark systems bound by those forces? And finally, how do we compute scattering amplitudes and matrix elements of currents using these bound states?

At this moment, there is no derivation of the complete force between quarks from the QCD Lagrangian. Explicit calculations can be done only in the limits of weak and strong coupling. In the weak-coupling limit, the result is a Coulomb potential with an asymptotically free coupling constant. The strong coupling limit, on the other hand, gives a linear potential which confines color in the way that we described, but did not derive, at the end of Section 17.1. The derivation of this result is quite unusual and brings in a new set of mathematical methods.

So far in this book, we have not discussed a strong coupling approximation to a quantum field theory. There is a simple reason for this: In a quantum field theory in which the coupling g^2 is very large, the elementary particles or their bound states typically acquire masses that grow with g^2. For $g^2 \to \infty$, these masses become comparable to the cutoff Λ and the field theory ceases to have a local continuum description.

Wilson proposed to solve this problem in a radical way, by replacing spacetime with a lattice of discretely spaced points. Such a lattice is easiest to visualize in Euclidean spacetime, and so we can use a functional integral over fields on a lattice to approximate Euclidean Green's functions. Such a theory can have a well-defined strong coupling limit. A theory of this type is very similar to a lattice model of a magnetic system.

In fact, we can understand this construction of a quantum field theory by using the concepts of Chapter 13. A lattice theory with fluctuating spin variables at each lattice site is described in the large by a quantum field theory of scalar fields with the symmetry of the underlying spin variables. Typically, the strong-coupling limit of the quantum field theory corresponds to the high-temperature limit of the magnet, in which the correlation length is much smaller than the lattice spacing. Decreasing the coupling constant corresponds to decreasing the temperature. Eventually, the coupling constant comes close to a fixed point of the renormalization group, and one can use this fixed point to define a limit of the lattice functional integral in which the lattice spacing is taken to zero.

To build a lattice model of the strong interactions, one needs to find a set of variables on the discrete lattice that correspond in the large to non-Abelian gauge fields. Wilson proposed that the fundamental variables for such a theory should be the line elements from one lattice vertex v_1 to a neighboring vertex v_2,

$$U(v_2, v_1) = P\exp\left[ig\int dx^\mu\, A^a_\mu t^a\right]. \tag{22.1}$$

To construct the lattice gauge theory with gauge group G, one should integrate over a finite group transformation U for each link of the lattice. Taking a product of these U matrices around a closed path, one can construct gauge-invariant observables, just as we did in Section 15.3. An appropriate Lagrangian can also be constructed as a sum of gauge-invariant products of the U matrices about elementary closed loops of the lattice.*

In a spin system, the defining property of the high-temperature phase is the exponential decay of correlations

$$\langle \vec{s}(0)\cdot\vec{s}(\mathbf{x})\rangle \sim \exp\bigl[-|\mathbf{x}|/\xi\bigr] \tag{22.2}$$

as $|\mathbf{x}| \to \infty$. The analogous property of the gauge-invariant correlation function of U matrices around a closed path P is

$$\Bigl\langle \prod_P U \Bigr\rangle \sim \exp\bigl[-A/\xi^2\bigr], \tag{22.3}$$

where A is the area spanned by the path. This behavior is in fact seen explicitly in the expansion of Wilson's lattice gauge theory for strong coupling. A pair of color sources that stand a distance R apart for a Euclidean time T are represented by a large rectangular loop of width R and length T. For such a

*This construction was introduced by K. Wilson, *Phys. Rev.* **D10**, 2445 (1974). The construction is described pedagogically in M. Creutz, *Quarks, Gluons, and Lattices* (Cambridge University Press, Cambridge, 1983).

loop, we can compare the result (22.3) to the expression for the energy of an excited state in Euclidean time,

$$\langle \exp[-H_E T] \rangle \sim \exp[-RT/\xi^2]. \tag{22.4}$$

Then we see that static sources of gauge charge, in the strong-coupling limit, are attracted to one another by a potential energy

$$V(R) \sim R/\xi^2 \tag{22.5}$$

at sufficiently large R. Similarly, when one introduces dynamical quarks into a lattice gauge theory and studies their properties in the strong-coupling limit, configurations with large separation of color sources are suppressed in the Euclidean functional integral by factors of the form of (22.3). The strong-coupling limit then predicts the permanent confinement of quarks into color-singlet bound states.

The argument we have just given applies equally well to gauge theories based on Abelian or non-Abelian symmetry groups. But non-Abelian gauge theories have the important additional property of asymptotic freedom. In this context, that implies that a theory with weak coupling at short distances flows to a theory with strong coupling at large distances. If we imagine integrating out short-distance degrees of freedom as we described in Section 12.1, and if there is no zero of the β function or other barrier to the renormalization group flow, we should eventually arrive at an effective theory for which the strong-coupling expansion is a good approximation. Thus, in the particular case of non-Abelian gauge theories, asymptotic freedom allows us to connect a short-distance picture based on free quarks and gluons to a large-distance picture based on color confinement.

It would be wonderful if the strong-coupling picture that we have described led to mathematical equations in continuum spacetime describing the motion of permanently confined quarks and antiquarks. Many authors have tried to write such equations by imagining the area suppression of the Wilson loop correlation function (22.3) to result from a physical surface that spans the loop. For the large rectangular loop associated with color sources, this surface can be interpreted physically as the lines of color electric flux that run from one source to the other (as in Fig. 17.1), swept out through Euclidean time. At one moment of Euclidean time, this surface can be idealized as an abstract one-dimensional excitation, often called a *string*. Unfortunately, the quantum properties of an idealized string turn out to be very complicated, since each small element of the string must be considered as an independent quantum degree of freedom. The only systems of string equations that have actually been solved have bizarre features, including unwanted massless particles. Up to now, no one has succeeded in writing an equation for the quark-confining string that is useful for quantitative calculations of quark bound states.†

†For one approach to color confinement from a picture involving Wilson loops and strings, see A. A. Migdal, *Phys. Repts.* **102**, 199 (1983).

However, the lattice regularization of a non-Abelian gauge theory suggests another approach to quantitative calculations in strong-interaction theory. By approximating QCD by a lattice gauge theory with a nonzero lattice spacing and a finite spacetime volume, we reduce the functional integral to a finite number of bounded integrations, that is, an integral over $SU(3)$ group matrices for each of the finite number of links in the lattice. A lattice of size, for example, 20^4 allows the lattice spacing to be smaller than the size of a hadron while the full size of the lattice is much larger than a hadronic radius. Then one can compute correlation functions by evaluating the integrals numerically, by the Monte Carlo method. Since the functional integral with a finite lattice spacing is related to the original functional integral with zero lattice spacing by integrating out short-distance degrees of freedom, the lattice approximation can be systematically improved by computing the short-distance effects perturbatively, using asymptotic freedom to justify a weak-coupling analysis.‡

This numerical method has now become the principal theoretical tool for quantitative calculations in hadron physics. This method currently gives the masses of the low-lying mesons and baryons to accuracies of 10–20%; it also allows the calculation of weak interaction matrix elements of hadrons at the 25% level. As computers become more powerful, this numerical method can be pushed to higher accuracy.

Eventually, it will be interesting to ask whether these nonperturbative numerical calculations are consistent with our precision knowledge of the perturbative region of QCD. At the time of this writing, the first such comparison has been made: We have listed in Table 17.1 a value of α_s from ψ and Υ spectroscopy. In this calculation, the experimentally determined masses of $\bar{c}c$ and $\bar{b}b$ bound states are compared to values computed numerically with lattice regularization. The comparison of these values gives the required bare coupling constant of the lattice theory, which can be converted to a value of $\alpha_s(m_Z)$ in the convention of the table. The resulting estimate for $\alpha_s(m_Z)$ does agree reasonably well with purely perturbative determinations.

What is the future of nonperturbative calculations in hadron physics? On the one hand, we expect to see further development of numerical lattice methods. These methods have hardly begun to address problems of hadron-hadron scattering and multiparticle matrix elements, and this seems an important direction for the future. In addition, these methods should eventually supply an engineering understanding of hadrons at the percent level or better. On the other hand, we hope also to see a quantitative continuum approach to hadron structure, in which dynamical quarks interact with some appropriate type of string degrees of freedom.

‡For an introduction to numerical lattice gauge theory, see *From Actions to Answers*, T. DeGrand and D. Toussaint, eds. (World Scientific, Singapore, 1990).

22.2 Grand Unification and its Paradoxes

If we put aside our questions about the low-energy, nonperturbative behavior of QCD, the $SU(3)\times SU(2)\times U(1)$ gauge theory gives an apparently complete description of elementary particle interactions at those energies that we have probed experimentally. But what happens beyond our current reach? Does this theory need modification, or could it continue to be valid at much higher energies?

The $SU(3)\times SU(2)\times U(1)$ gauge theory contains three independent gauge coupling constants, and the observed values of these couplings are larger for the larger components of the gauge group. This pattern can be explained by a bold hypothesis about the behavior of the gauge couplings at very high energy. If at some very large energy scale, these three couplings were equal, the values of the $SU(3)$ and $SU(2)$ couplings would increase at smaller momentum scales due to their asymptotically free renormalization group equations, while the value of the $U(1)$ coupling would decrease, resulting in the observed pattern of couplings at low energies. An even bolder hypothesis would be that the three gauge symmetries are subgroups of a single large symmetry group, which is spontaneously broken at very high energy scales. The simplest choice for this larger symmetry is $SU(5)$. In that theory, the coupling constants of $SU(3)\times SU(2)\times U(1)$ have the following relation to the underlying $SU(5)$ coupling at the scale of $SU(5)$ breaking:

$$g_5 = g_3 = g = \sqrt{\frac{5}{3}}\,g'. \tag{22.6}$$

The idea that the $SU(3)\times SU(2)\times U(1)$ gauge group is embedded in a larger simple group is known as *grand unification*; the particular choice of $SU(5)$ as the unifying group is due to Georgi and Glashow.* The observed quarks and leptons can be seen to fit neatly into an anomaly-free chiral representation of $SU(5)$; this embedding leads to a natural explanation of the fractional charges of quarks.†

Within this framework, we can extrapolate the values of the three coupling constants from the energy scale of m_Z upward. The result of this extrapolation is shown as the solid lines in Fig. 22.1. The coupling constants do come close together at very high energies, though they do not actually meet. The dashed lines in the figure show the evolution with a modified set of renormalization group equations, to be explained in Section 22.4; with this choice, the three couplings meet accurately within their current uncertainties. In any event, the evolution of coupling constants occurs on a logarithmic scale in energy, so grand unification cannot be achieved without assuming an enormous value—of order 10^{16} GeV—for the symmetry-breaking scale.

---

*H. Georgi and S. L. Glashow, *Phys. Rev. Lett.*, **32**, 438 (1974). The remarkable hubris of this paper makes it required reading for every student.

†For a pedagogical introduction to grand unification, see Ross (1984).

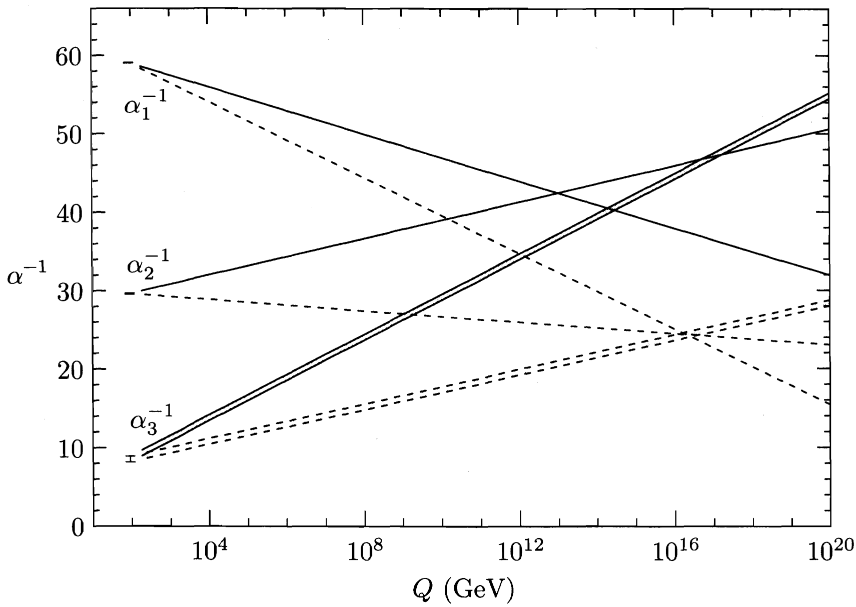

Figure 22.1. Extrapolation in energy of the coupling constants of the $SU(3) \times SU(2) \times U(1)$ gauge model, g_3, g, and $\sqrt{5/3}g'$. The solid lines are plotted using the β functions corresponding to the known set of elementary particles; the dashed lines are plotted using the β functions corresponding to a supersymmetric multiplet of particles.

The idea of a grand unification at such enormous energies raises many difficult questions, but it also suggests a wonderful opportunity. There is another enormous energy scale in quantum field theory, the scale at which the gravitational attraction of elementary particles becomes comparable to their strong, weak, and electromagnetic interactions. Conventionally, one defines the *Planck scale* as the energy for which the gravitational interaction of particles becomes of order 1:

$$m_{\text{Planck}} = (G_N/\hbar c)^{-1/2} \sim 10^{19} \text{ GeV}. \tag{22.7}$$

However, already at energies of order 10^{18} GeV, the gravitational attraction of particles is comparable to the gauge force due to the vector bosons of a grand unified theory. Though this scale is still slightly higher than the scale at which the standard model coupling constants meet, it is not unreasonable to hope that grand unification is somehow related to the unification of gravity with the forces of elementary particle physics.

On the other hand, the introduction of this large scale into physics leads to a number of conceptual problems. The first of these problems, which one meets immediately upon suggesting this extension of the standard model, is the Higgs boson mass. In our discussion at the end of Section 20.2, we came to a somewhat ambiguous conclusion about the nature of the Higgs boson. As a part of the gauge theory of weak interactions, we need some new sector that will cause the spontaneous breaking of $SU(2) \times U(1)$. This might be supplied by the vacuum expectation value of a scalar field, or by the more complicated dynamics of a new sector of particles. At this moment, we do not know which hypothesis is to be preferred.

If $SU(2) \times U(1)$ is broken by the vacuum expectation value of an elementary scalar field, that scalar field should be part of the grand unification. This leads to a serious conceptual problem. In order to produce a vacuum expectation value of the right size to give the observed W and Z boson masses, the Higgs scalar field must obtain a negative mass term, of the size

$$-\mu^2 \sim -(100 \text{ GeV})^2. \tag{22.8}$$

Unfortunately, the (mass)^2 of a scalar field receives additive renormalizations. In a theory with cutoff scale Λ, μ^2 can be much smaller than Λ^2 only if the bare mass of the scalar field is of order $-\Lambda^2$, and this value is canceled down to $-\mu^2$ by radiative corrections. If we envision that our theory of Nature contains the very large scales of grand unification, we must take seriously the idea that the appropriate value to take for Λ in this discussion is 10^{16} GeV or larger. This seems to require dramatic and even bizarre cancellations in the renormalized value of μ^2.

We met a situation of this type in the theory of phase transitions. At zero temperature, a ferromagnet typically has a spin expectation value of the order of the underlying atomic parameters. As the temperature is raised, or as some other variable in the system is changed, the magnetization decreases. Finally, by fine adjustment of the temperature, we can arrive at a situation where the system approaches a critical point. In the very near vicinity of this point, the expectation value of the spin field is much smaller than the value predicted from atomic parameters, and the system is described by an approximately massless continuum scalar field theory.

In statistical mechanics, this picture of the light scalar field makes sense because there is an experimenter sensitively adjusting a dial. In the theory of weak interactions, there is no one obviously making a fine adjustment that gives the (mass)^2 of the Higgs boson a value 28 orders of magnitude or more below its natural value. Thus, it is a mystery why the Higgs boson mass should be so small compared to the grand unification scale. Particle physicists refer to this question as the *gauge hierarchy problem*.

How can one naturally arrange a Higgs field mass term to be so much smaller than the underlying mass scale of the fundamental interactions? One possible strategy would be to arrange for a symmetry of the fundamental Lagrangian that forbids the Higgs boson mass term and that is very weakly broken. This idea turns out to be very difficult to implement. To build a theory of this type, one would need to create a scalar field theory in which additive radiative corrections to the Higgs boson mass must cancel to any foreseeable order in perturbation theory. But the Higgs mass term is very simple in form,

$$\Delta\mathcal{L} = \mu^2|\phi|^2, \tag{22.9}$$

and it is hard to imagine any principle that would keep this term from being generated by radiative corrections. There is one proposal for a symmetry with this property, but it requires the introduction of a profound principle called *supersymmetry* that entails deep modifications of fundamental physics. In particular, it requires a large number of new elementary particles, some of which should have masses below 1000 GeV, within the reach of the next generation of accelerators. We will discuss this possibility further in Section 22.4.

In this discussion, the problem of the Higgs mass stemmed from the hypothesis that the Higgs boson was an elementary particle. An alternative viewpoint, already suggested at the end of Section 20.2, is that the Higgs boson is a composite state bound by a new set of interactions. This idea also leads to observable experimental consequences, since the mass scale of these new interactions must be close to the weak interaction mass scale. In the simplest theories of this type, the symmetry breaking of the Higgs sector is modeled on the dynamical chiral symmetry breaking of the strong interactions, which we discussed in Section 19.3. The new strong interactions required by the theory lead to a spectrum of new particles with masses of about 1000 GeV.‡ Thus, the two conflicting hypotheses on the nature of the sector that breaks $SU(2) \times U(1)$ both lead to new phenomena observable at future accelerators, and possibly even at present ones.

Just as these two different theories of the Higgs sector present completely different answers to the question of why the weak-interaction symmetry $SU(2) \times U(1)$ should be spontaneously broken, they also imply completely different answers to the question of the origin of the quark and lepton masses. In a model in which the Higgs field is elementary, the quark and lepton masses are derived from the renormalizable couplings of fermions to the Higgs field. These couplings would presumably be part of the grand unification and could be predicted only by theories that made explicit reference to the grand unification scale. In principle, the knowledge of these couplings could give us clues as to the details of the grand unification. Even if the Higgs field is composite, we cannot avoid the fact that the generation of masses for the quarks and leptons requires the breaking of $SU(2) \times U(1)$. Thus, these mass terms must arise from couplings of the quarks and leptons to the Higgs sector of interactions. In this class of models, the interactions leading to the quark and lepton masses must arise at energies close to the scale of the Higgs sector strong interaction and may eventually be observable experimentally.

From either viewpoint, it is still mysterious why the spectrum of quarks

‡The properties of these models of the Higgs sector, known to specialists as *technicolor* models, are described in R. Kaul, *Rev. Mod. Phys.* **55**, 449 (1983) and K. D. Lane, in *The Building Blocks of Creation*, S. Raby, ed. (World Scientific, 1993).

and leptons covers 5 orders of magnitude, from the electron at 0.5 MeV to the top quark at 175 GeV. It is also not understood what gives rise to the pattern of quark mixings encoded in the CKM matrix and the magnitude of CP violation. Even with detailed confirmation of the standard model, these questions seem today very far from solution.

The enormous mass scale of grand unification can also enter one more physical quantity, one that poses an even greater paradox than that of the Higgs boson mass. When we first quantized a field in Section 2.3, we discovered that the energy density of the vacuum in free scalar field theory received an infinite positive contribution from the zero-point energies of the various modes of oscillation. With a cutoff scale Λ, this zero-point energy is given roughly by

$$\langle 0| H |0\rangle \sim \Lambda^4. \tag{22.10}$$

At many other points in our discussion, we found similarly large contributions to the vacuum energy. The filling of the Dirac sea in the quantization of the free fermion theory led to a downward shift in the vacuum energy with a similar ultraviolet divergence. Spontaneous symmetry breaking gives a finite but still possibly large shift in the vacuum energy density,

$$\Delta \langle 0| H |0\rangle \sim -cv^4, \tag{22.11}$$

with dimensionless c, for a field vacuum expectation value v. The spontaneous breaking of the weak interaction $SU(2)\times U(1)$ symmetry and of the strong interaction chiral symmetry both would be expected to shift the vacuum energy density in this way.

In elementary particle physics experiments, this shift of the vacuum energy is unobservable. Experimentally measured particle masses, for example, are energy differences between the vacuum and certain excited states of H, and the absolute vacuum energy cancels out in the calculation of these differences. However, there is a way that the absolute vacuum energy could potentially be observed, through the coupling of the vacuum energy to gravity. According to Einstein, the energy-momentum tensor of matter $\Theta^{\mu\nu}$ is the source of the gravitational field. A vacuum energy density $\langle 0| H |0\rangle = \lambda$ contributes to this source a term

$$\Theta^{\mu\nu} = N\big(\Theta^{\mu\nu}\big) + \lambda g^{\mu\nu}, \tag{22.12}$$

where the first term on the right is subtracted to have zero vacuum expectation value. The vacuum energy term has the form of Einstein's cosmological constant and thus potentially affects the expansion of the universe.

In fact, measurements of the cosmological expansion exclude a large cosmological constant. The current limit is

$$\lambda < 10^{-29}\ \mathrm{g/cm^3} \sim (10^{-11}\ \mathrm{GeV})^4. \tag{22.13}$$

We have no understanding of why λ is so much smaller than the vacuum energy shifts generated in the known phase transitions of particle physics, and so much again smaller than the underlying field zero-point energies. The discrepancy in λ between the experimental bound (22.13) and naive intuition is 120 orders of magnitude! The solution to this problem may come from one of many sources. It may be that the formalism of the quantum field theory of gravity requires that the vacuum energy be subtracted from the energy-momentum tensor that appears in Einstein's equations of gravity. It may be that there is a new physical mechanism coming from particle physics or from gravity itself that sets the total vacuum energy to zero. Or it may be that the overall scale of energy-momentum is genuinely ambiguous and is set by a cosmological boundary condition. At this moment, all of these possibilities are just guesses. All we know for certain is that the unification of quantum field theory and gravity cannot be straightforward, that there is some important concept still missing from our current understanding.*

22.3 Exact Solutions in Quantum Field Theory

From the idea of grand unification, with its great promise and mystery, we turn to the study of model quantum field theories that are so simple that they can be solved exactly. Throughout this book, we have stressed the intrinsic complexity of quantum field theory and the importance of using perturbation theory as a replacement for exact knowledge. But there are a variety of quantum field theories for which exact solutions are known. In this section, we will describe some of these and review the insights we have gained from them.

In searching for exact solutions to quantum field theory models, there is no reason to restrict our attention to four-dimensional spacetime. In fact, we have seen examples of two-dimensional theories with similar complexity of renormalization and short-distance behavior. At the same time, these theories occupy a one-dimensional space, and their degrees of freedom can be visualized as links in a chain. This allows some powerful simplifications.

In our discussion of the axial anomaly in two dimensions in Section 19.1, we showed that the photon of two-dimensional massless QED becomes a massive boson. More detailed examination of this theory shows that this boson is a noninteracting particle. The theory is originally formulated in terms of fermions, interacting through Coulomb forces. However, it is possible to exactly rewrite the theory as a theory of a scalar field that creates and destroys fermion-antifermion pairs. Heuristically, a particle and an antiparticle moving down the light-cone in one-dimensional space do not separate and therefore comprise one bosonic degree of freedom. In a wide class of models, the bosonic theories rewritten in this way are free-field theories. A remarkable model of this type is the *Thirring model*,

$$\mathcal{L} = \bar{\psi} i \partial\!\!\!/ \psi - \frac{g}{2} \bar{\psi}\gamma^{\mu}\psi\bar{\psi}\gamma_{\mu}\psi, \tag{22.14}$$

*The cosmological constant problem and a variety of unsuccessful solutions are reviewed in S. Weinberg, *Rev. Mod. Phys.* **61**, 1 (1989).

in two dimensions. In this model, the replacement of the fermion field by a boson field leads to a free field theory. Using this field theory, one can compute correlation functions of fermion bilinears explicitly and show directly that these operators have anomalous dimensions. In renormalization-group language, the model contains a line of fixed points parametrized by the coupling constant g.†

A more general class of two-dimensional models can be solved by visualizing them in a Hamiltonian picture as a one-dimensional chain of coupled field operators. The prototype of this method is a problem in the statistical mechanics of magnets, the one-dimensional chain of coupled spins. Consider a long chain of N discrete sites, with a spin-1/2 system at each site. The Pauli sigma matrices $\boldsymbol{\sigma}_i$ act on the two-dimensional Hilbert space at the site i. The Hamiltonian for the spin chain is then

$$H = \sum_i \left(-J\boldsymbol{\sigma}_i \cdot \boldsymbol{\sigma}_{i+1}\right). \tag{22.15}$$

Since

$$\boldsymbol{\sigma}_i \cdot \boldsymbol{\sigma}_{i+1} = 2(\sigma_i^+\sigma_{i+1}^- + \sigma_i^-\sigma_{i+1}^+) + \sigma_i^3\sigma_{i+1}^3, \tag{22.16}$$

this Hamiltonian conserves the number of up spins. The state with all spins down is an eigenstate of the Hamiltonian, and the states with one spin up in a state of definite momentum are also eigenstates. In 1934, Bethe analyzed the problem of two spins up and computed their S-matrix. He then discovered an amazing fact, that by multiplying the S-matrices for the two-spin problem, he could find the exact eigenstates of the Hamiltonian for any number of spins up. By considering $N/2$ spins up, he found the ground state of the system. This technique, now known as *Bethe's ansatz*, has been used to solve a wide variety of one-dimensional problems in condensed matter physics and quantum field theory. For example, this technique has been used by Andrei and Lowenstein to solve the Gross-Neveu model presented in Problem 11.3 and to demonstrate that the spectrum of this model has the properties expected from asymptotic freedom.‡

Even where it is not possible to solve a model for all values of its parameters, it is sometimes possible to find exact information about two-dimensional models at points where they contain massless fields. It is well known that a variety of classical two-dimensional partial differential equations can be solved by exploiting techniques of complex variables. For example, the two-dimensional Laplace equation $\nabla^2\phi = 0$ is invariant to conformal mappings $z \to w(z)$,

†For an introduction to these models, see S. Coleman, *Phys. Rev.* **D11**, 2088 (1975), *Ann. Phys.* **101**, 239 (1976).

‡For an introduction to Bethe's ansatz and its generalizations, see N. Andrei, K. Furuya, and J. H. Lowenstein, *Rev. Mod. Phys.* **55**, 331 (1983), L. D. Faddeev, in *Recent Advances in Field Theory and Statistical Mechanics*, J. B. Zuber and R. Stora, eds. (North-Holland, Amsterdam, 1984), and R. J. Baxter, *Exactly Solved Models in Statistical Mechanics* (Academic Press, London, 1982).

where $z = x + iy$. Two-dimensional quantum field theories with massless particles often have this conformal symmetry at the classical level, though generically it is anomalous. In special systems, however, these anomalies vanish and the quantum theory is invariant to conformal mapping. These theories typically contain operators with anomalous dimensions, indicating that each such theory is a new, nontrivial fixed point of the renormalization group. The conformal symmetry of the theory can be used to compute these anomalous dimensions.

As an example of this class of theories, consider the two-dimensional nonlinear sigma model in which the basic field is not a unit vector, as we discussed in Section 13.3, but rather a unitary matrix of a Lie group G. The Lagrangian of this theory is

$$\mathcal{L} = \frac{1}{4g^2}\int d^2x \; \mathrm{tr}\big[\partial_\mu U^\dagger \partial^\mu U\big]. \tag{22.17}$$

Like the theory of Section 13.3, this model is asymptotically free. However, Witten has shown that, by adding to this Lagrangian a particular perturbation of a rather complicated form first written by Wess and Zumino, one can find a fixed point of the renormalization group with manifest $G\times G$ global symmetry. This theory is conformally invariant, and all operator correlation functions can be computed using the conformal symmetry.*

One result of the nonperturbative exploration of quantum field theory was the realization that field theories can contain particle states that are not simply related to the quanta of the original fields. In the weak-coupling limit of a quantum field theory, such new states can appear as new solutions of the classical field equations. Consider, for example, ϕ^4 theory in two dimensions in the broken-symmetry phase. The equation of motion is

$$\frac{\partial^2}{\partial t^2}\phi - \frac{\partial^2}{\partial x^2}\phi - \mu^2\phi + \lambda\phi^3 = 0. \tag{22.18}$$

Treating this equation as a classical partial differential equation, we can find the time-independent solution

$$\phi(x) = \frac{\mu}{\sqrt{\lambda}}\tanh\frac{x\mu}{\sqrt{2}}. \tag{22.19}$$

This is a field configuration that begins in one well of the potential at $x = -\infty$ and crosses over to the other well as $x \to +\infty$. This solution has an energy of order μ/λ, larger by a factor of $1/\lambda$ than the mass of a ϕ quantum. Since the original equation (22.18) was Lorentz-covariant, the boosts of this solution must also be solutions to the classical partial differential equation. It is natural to suggest that, in the ϕ^4 quantum field theory, these solutions form a new set of massive particles. Such solutions, and the particles corresponding to

*For an introduction to conformally invariant two-dimensional quantum field theories, see P. Ginsparg, in *Fields, Strings, Critical Phenomena*, E. Brezin and J. Zinn-Justin, eds. (North-Holland, Amsterdam, 1989).

them, are often called *solitons*, borrowing a more specialized term from the literature on two-dimensional partial differential equations.†

Many examples are now known of particles that are associated in this way with classical solutions of a quantum field theory. In theories with spontaneously broken symmetry, the appearance of such particles is often related to the topology of the set of vacuum states; the ϕ^4 theory above gives a simple example of this relation. These examples are not limited to two dimensions but can also occur in theories that are potentially realistic. Such solutions can have magical properties. One interesting example is found in the $SU(2)$ gauge theory with a Higgs scalar field in the vector representation, the Georgi-Glashow model considered in Section 20.1. 't Hooft and Polyakov showed that this theory has a classical solution in which the Higgs field ϕ_a has the form

$$\phi_a(\mathbf{x}) = f(|\mathbf{x}|)x_a. \tag{22.20}$$

They showed that, when the gauge theory is interpreted as a unified model of weak and electromagnetic interactions, this solution is a magnetic monopole! In addition, particles that arise as heavy classical states in the weak coupling limit can have a more intricate relation to the dynamics of the theory when the coupling is increased. For example, in theories of the type of two-dimensional QED or the Thirring model in which fermions can be replaced by bosons, a weak-coupling limit is obtained by adding to the theory a large fermion mass. Then the original fermions are recovered from the bosonic representation of the theory as classical solutions very similar to that given in (22.19).

In some theories, one can find classical solutions of the Euclidean field equations. These solutions, called *instantons*, are localized in Euclidean time as well as in space. Thus, they are interpreted as quantum processes that modify the effective Hamiltonian of a quantum field theory. The most famous example of an instanton is found in four-dimensional non-Abelian gauge theories. It was shown by 't Hooft that this field configuration leads to a quantum process that violates the conservation of the $U(1)$ axial current in QCD. We have explained in Section 19.3 that this violation of current conservation is exactly what is needed to explain the spectrum of light mesons in QCD.

There is probably much more to be learned, especially about the strong-coupling behavior of gauge theories, by deeper analysis of the classical solutions to the field equations, and of the interrelations of the many exactly or partially solvable two-dimensional field theories.

---

†For an introduction to the use of solutions of the classical field equations in the analysis of problems in field theory, see S. Coleman (1985), Chaps. 6 and 7, and R. Rajaraman, *Solitons and Instantons* (North-Holland, Amsterdam, 1982).

22.4 Supersymmetry

Among the properties that a quantum field theory might possess to make it more beautiful or more mathematically tractable, there is one higher symmetry with particularly far-reaching implications. This is a symmetry that relates fermions and bosons, known (without hyperbole) as *supersymmetry.* In this section, we will introduce some of the purely mathematical consequences of supersymmetry, and then discuss the question of whether the true field equations of Nature could be supersymmetric.

A generator of supersymmetry is an operator that commutes with the Hamiltonian and converts bosonic into fermionic states. Such an operator must carry half-integer spin, in the simplest case spin 1/2. Let Q_α, with $\alpha = 1, 2$, be the left-handed spinor components of this operator. Their Hermitian conjugates, $Q^\dagger_\beta$, form a right-handed spinor. The anticommutator $\{Q_\alpha, Q^\dagger_\beta\}$ is a 2×2 matrix with positive diagonal elements; thus it cannot vanish. This matrix commutes with H but transforms nontrivially under Lorentz transformations. A Lorentz-covariant expression for this anticommutator is

$$\{Q_\alpha, Q^\dagger_\beta\} = 2\sigma^\mu_{\alpha\beta} P^\mu, \tag{22.21}$$

where P^μ is a conserved vector quantity. Such quantities are severely restricted; a theorem of Coleman and Mandula states that, if a quantum field theory in more than two dimensions has a second conserved vector quantity in addition to the energy-momentum 4-vector, the S-matrix equals 1 and no scattering is allowed. Thus the only possible choice for P^μ in Eq. (22.21) is the total energy-momentum. The Coleman-Mandula theorem also rules out any higher-spin conservation laws. This eliminates the possibility that a supersymmetry generator could have spin 3/2 or higher. The most general possibility is a collection of spin-1/2 operators with the anticommutation relations

$$\{Q^i_\alpha, Q^{j\dagger}_\beta\} = 2\delta^{ij}\sigma^\mu_{\alpha\beta} P^\mu, \tag{22.22}$$

with $i, j = 1, \ldots, N$. In the following discussion, we will mainly consider only the simplest case, $N = 1$.‡

The algebra (22.22) of conserved quantities has profound conseqences for the theory. Since the right-hand side of (22.22) is the total energy-momentum, it involves every field in the theory. To reproduce this algebra, the left-hand side must also involve every field. The representations of this algebra pair every bosonic state with a fermionic state at the same energy, and vice versa. If supersymmetry is an exact symmetry of the quantum field theory, it must act on every sector of the theory. In a realistic model, even the gravitational field must have a fermionic partner. This means that Einstein's equations of gravity must be generalized to a new set of geometrical equations that involve a fermionic (spin-3/2) field.

‡An excellent introduction to the formalism of supersymmetry is J. Wess and J. Bagger, *Supersymmetry and Supergravity* (Princeton University Press, 1983).

The first consequences of making a quantum field theory supersymmetric are easy to understand. For every (complex) scalar field, one must introduce a chiral fermion field. The self-interactions of the bosonic fields are related to the interactions of these fields with the fermions; for example, a possible interaction Lagrangian with coupling constant λ is

$$\Delta\mathcal{L} = -\lambda^2|\phi|^2 - \tfrac{1}{2}\lambda\psi^T\sigma^2\psi. \tag{22.23}$$

We have written a more general supersymmetric Lagrangian in Problem 3.5. Similarly, for every gauge field, one must introduce a chiral fermion in the adjoint representation of the gauge group. This fermion, called the *gaugino*, mediates interactions of the scalar fields with their fermionic partners whose strength is given by the gauge coupling g.

The special relation between the bosonic and fermionic interactions leads to great simplifications in the renormalization of supersymmetric theories. Some of these simplifications can be anticipated. Since supersymmetry requires that each scalar particle have a fermionic partner of the same mass, these particles must have the same mass renormalization. But we have seen that the fermion mass is multiplicatively renormalized and thus is only logarithmically divergent, while a scalar mass term is additively renormalized and thus can be quadratically divergent. Supersymmetry must imply that the quadratic divergences of scalar mass terms automatically vanish. In fact, these cancellations occur in every order of perturbation theory, with loop diagrams involving bosons canceling against diagrams with virtual fermions. To see another simplification required by supersymmetry, take the vacuum expectation value of the anticommutation relation (22.21). The vacuum state has zero momentum: $P^i|0\rangle = 0$. If the vacuum state is supersymmetric, $Q_\alpha|0\rangle = Q^\dagger_\beta|0\rangle = 0$. Then Eq. (22.21) implies

$$\langle 0|H|0\rangle = 0. \tag{22.24}$$

We have noted already that bosonic fields give positive contributions to the vacuum energy through their zero-point energy, and fermionic fields give negative contributions. We now see that, in a supersymmetric model, these contributions cancel exactly, not only at the leading order but to all orders in perturbation theory.

Deeper examination of supersymmetric theories leads to additional, and quite unexpected, cancellations in renormalization theory. For example, one can show that the coupling constants in scalar-fermion self-interactions, such as λ in (22.23), are renormalized only through field strength renormalizations. Thus the relative size of two different scalar interactions remains unchanged. If a particular type of renormalizable interaction is omitted, it cannot be generated by renormalization, in contrast to the case in ordinary field theory. The simplest supersymmetry does not constrain the renormalization of gauge couplings, but higher supersymmetries can have a profound effect: In $N = 2$ supersymmetric models, the β function vanishes if the leading-order term is arranged to be zero. In $N = 4$ supersymmetric models, this cancellation is automatic and $\beta(g) = 0$ exactly. These models give examples of four-dimensional quantum field theories with no ultraviolet divergences.*

Supersymmetry thus endows a quantum field theory with remarkable, even magical properties. But is it possible that the true equations of Nature could possess such a high degree of symmetry? Since we are certain that there is no charged boson with the same mass as the electron, we know that supersymmetry cannot be an exact symmetry of Nature. But it is tempting to guess that it might be a spontaneously broken symmetry of the underlying equations.

In fact, this conjecture has fruitful consequences for the grand unified theories that we discussed in Section 22.2. The problem of the Higgs boson mass that we highlighted in that section has an elegant solution in supersymmetry models. In a supersymmetric version of the standard model, the Higgs field is one of a large number of scalar fields with various $SU(3) \times SU(2) \times U(1)$ quantum numbers. For all of these scalar fields, the mass terms get only a logarithmic multiplicative renormalization. If supersymmetry were broken in such a way as to give mass differences of a few hundred GeV between the observed fermionic quarks and leptons and their scalar partners, one would also find a Higgs boson $(\text{mass})^2$ of the correct size. There are good reasons, which follow from more detailed properties of the theory, why it is the Higgs field, rather than some other scalar field, that obtains a vacuum expectation value.†

If this set of ideas is correct, the scalar partners of quarks and leptons would be light enough to be discovered experimentally in the near future. In that case, these scalar particles and the fermionic partners of gauge bosons would affect the renormalization of coupling constants between present energies and the grand unification scale. This might potentially disturb the prospects for grand unification, but, instead, it improves them: the dashed lines of Fig. 22.1, with a more impressive meeting of the three coupling constants, were generated by replacing the conventional β functions with ones including the supersymmetric partners.

The last of the problems discussed in Section 22.2 is also ameliorated by the introduction of supersymmetry. In a grand unified theory with broken supersymmetry, those momentum scales that are much larger than the mass differences of supersymmetry partners give no contribution to the vacuum energy. Thus the natural size of the cosmological constant in these theories is $\lambda \sim (100 \text{ GeV})^4$. This reduces the cosmological constant problem to a discrepancy of 50 orders of magnitude—but this is not nearly enough.

---

*Supersymmetric models with vanishing β function are reviewed by P. West, in *Shelter Island II*, R. Jackiw, N. N. Khuri, S. Weinberg, and E. Witten, eds. (MIT Press, Cambridge, 1985).

†Supersymmetric models of quarks and leptons, and their observable consequences, are reviewed in H. P. Nilles, *Phys. Repts.* **110**, 1 (1984), and in H. E. Haber and G. L. Kane, *Phys. Repts.* **117**, 75 (1985).

It is an exciting prospect that supersymmetric partners of the particles of the standard model might soon be seen in experiments. What we anticipate, in any event, is that the experiments of the next generation will make a definite choice between this hypothesis for the nature of the Higgs sector and the other possibilities discussed in Section 22.2. Either way, we will have advanced our knowledge one step toward the truly fundamental equations.

22.5 Toward an Ultimate Theory of Nature

What are these fundamental equations? Do they involve quantum field theory, or some very different organizing principle? Any answer to this question must be completely speculative. Nevertheless, there are some principles, and an example, that can guide this search.

For all the attention we have given in this book to the basic interactions of particle physics, we have given very little attention to gravity. In part, this is because the quantum theory of gravity has no known observational consequences. But it is also true that the quantum theory of gravity is still ill-formed and uncertain. If gravity is treated as a weak-coupling field theory with Feynman diagrams, one quickly finds that the divergences of these diagrams render the theory nonrenormalizable. This is no surprise, because gravity is a theory in which the coupling constant has inverse mass dimensions, with the mass scale m_{Planck} given by (22.7). In our general philosophy of renormalization, all of the complexity of this theory should be concentrated at the scale m_{Planck}.

At the scale where quantum fluctuations of the gravitational field are important, we must expect profound changes in physics. If these changes occur within the context of quantum field theory, they will at the least entail fluctuating spacetime geometry and topology. But it seems equally probable that quantum field theory will actually break down at this scale, with continuous spacetime replaced by a new discrete or nonlocal geometry.

One particular model for the behavior of spacetime at very small distances is *string theory*, the dynamics of abstract one-dimensional extended objects. In Section 22.1, we mentioned that such objects seemed to occur naturally in attempts to describe quark confinement in QCD, but that the detailed properties of these objects made them unsuitable for strong interaction phenomenology. Among the disappointing properties of these systems were the appearance of massless spin-2 states of the string, and a constraint that the dimension of spacetime must be increased unless the spectrum of the theory contained many massless spin-1 states. In 1974, Scherk and Schwarz made the remarkable suggestion that string theory was a correct mathematical description of a different problem, the unification of elementary particle interactions with gravity. They interpreted the spin-2 quantum as the graviton and the spin-1 quanta as gauge bosons of a gauge theory.‡ A decade later,

‡J. Scherk and J. H. Schwarz, *Nucl. Phys.* **B81**, 118 (1974).

Green and Schwarz put this conjecture on a firmer footing by showing that a particular string theory could be interpreted as a grand unified theory in ten spacetime dimensions, with all gravitational and gauge Ward identities automatically satisfied and all anomalies automatically canceling. Since that time, many other solutions to the constraint equations of string theory have been found, some of which correspond to unified models of gauge interactions and gravity in four dimensions. These models can naturally incorporate supersymmetry and, under that condition, give ultraviolet-finite results for all scattering amplitudes, including those of gravitons.*

String theories solve the ultraviolet divergence problems of quantum field theory by rejecting the idea that elementary particles are pointlike objects with contact interactions. Rather, in string theory, quarks, leptons, gauge bosons, and gravitons are extended loops of string excitation which thus interact nonlocally. Since particles cannot be definitely localized, spacetime itself takes on a nonlocal character. In some sense, distances much less than the Planck length $1/m_{\text{Planck}}$ do not exist in the string description of gravity. As yet, it is not clear how to understand intuitively the sort of geometry that string theory requires. This mathematical problem is now being actively investigated.

If indeed the truly fundamental geometry of Nature is nonlocal, discrete, or discontinuous in some other way, then the grand program for the fundamental interactions that we have set forth in this book must be altered in an essential way. The most elementary equations of Nature will not be gauge-invariant quantum field theories, but instead theories built from very different elements. Even the principles of model construction will be different from those based on gauge and Lorentz invariance that we have discussed here.

On the other hand, quantum field theory will still play an essential role in the interpretation of this structure. All of the processes we now observe, even the elementary particle processes at the highest energies currently accessible, occur over distances 15 orders of magnitude larger than the sizes of the strings or other fluctuating structures that appear in the underlying equations. The relation of experimental observations to these fundamental structures is thus very similar to the relation of macroscopic observations to the underlying atomic structure of matter. In the study of matter, we use a classical, Newtonian description of atoms to bridge this gap and to relate the properties of gases, liquids, and solids to underlying atomic properties. We might say that the quantum theory of atoms gives rise to a set of effective Newtonian equations that is extremely powerful in the macroscopic domain. Especially in the theory of gases, this Newtonian description was also used as a tool to realize the existence of atoms and to derive their properties.

*A technical introduction to string theory and its use in building unified models has been given by M. B. Green, J. H. Schwarz, and E. Witten, *Superstring Theory*, 2 vols. (Cambridge University Press, 1987).

Similarly, whatever the nature of Planck-scale physics, it leads to some effective continuum quantum field theory. This quantum field theory might well be an accurate approximation to the underlying physics already at distances of 100 Planck lengths, corresponding to momenta of 10^{17} GeV. From here to the scale of weak interactions, and from there up to the wavelength of light, and from there to the size of the universe, quantum field theory can be treated as the basic framework for the equations of physics. By recognizing the symmetries of the particular set of field equations that Nature has provided us, we can learn to compute all of the details of physical processes over this whole enormous domain. And, by contemplating the origin of these symmetries, perhaps we will also be able to see through to the next level and unlock the true structure of spacetime.

Appendix

Reference Formulae

This Appendix collects together some of the formulae that are most commonly used in Feynman diagram calculations.

A.1 Feynman Rules

In all theories it is understood that momentum is conserved at each vertex, and that undetermined loop momenta are integrated over: $\int d^4p/(2\pi)^4$. Fermion (including ghost) loops receive an additional factor of (-1), as explained on page 120. Finally, each diagram can potentially have a symmetry factor, as explained on page 93.

ϕ^4 theory: $\mathcal{L} = \frac{1}{2}(\partial_\mu\phi)^2 - \frac{1}{2}m^2\phi^2 - \frac{\lambda}{4!}\phi^4$

Scalar propagator: 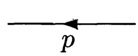

$$= \frac{i}{p^2 - m^2 + i\epsilon} \tag{A.1}$$

ϕ^4 vertex: 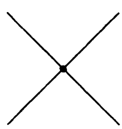
$$= -i\lambda \tag{A.2}$$

External scalar: 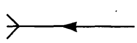
$$= 1 \tag{A.3}$$

(Counterterm vertices for loop calculations are given on page 325.)

Quantum Electrodynamics: $\mathcal{L} = \bar{\psi}(i\partial\!\!\!/ - m)\psi - \frac{1}{4}(F_{\mu\nu})^2 - e\bar{\psi}\gamma^\mu\psi A_\mu$

Dirac propagator: 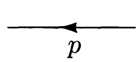

$$= \frac{i(p\!\!\!/ + m)}{p^2 - m^2 + i\epsilon} \tag{A.4}$$

Photon propagator: 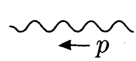

$$= \frac{-ig_{\mu\nu}}{p^2 + i\epsilon} \tag{A.5}$$

(Feynman gauge; see page 297 for generalized Lorentz gauge.)

QED vertex:

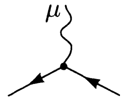

$$= iQe\gamma^\mu \tag{A.6}$$

($Q = -1$ for an electron)

External fermions:

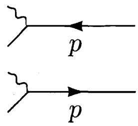

$$= u^s(p) \quad \text{(initial)}$$
$$= \bar{u}^s(p) \quad \text{(final)} \tag{A.7}$$

External antifermions:

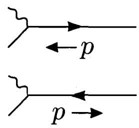

$$= \bar{v}^s(p) \quad \text{(initial)}$$
$$= v^s(p) \quad \text{(final)} \tag{A.8}$$

External photons:

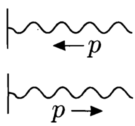

$$= \epsilon_\mu(p) \quad \text{(initial)}$$
$$= \epsilon^*_\mu(p) \quad \text{(final)} \tag{A.9}$$

(Counterterm vertices for loop calculations are given on page 332.)

Non-Abelian Gauge Theory:

$$\begin{aligned} \mathcal{L} = \bar{\psi}(i\not{\partial} - m)\psi - \tfrac{1}{4}(\partial_\mu A^a_\nu - \partial_\nu A^a_\mu)^2 + gA^a_\mu \bar{\psi}\gamma^\mu t^a \psi \\ - gf^{abc}(\partial_\mu A^a_\nu)A^{\mu b}A^{\nu c} - \tfrac{1}{4}g^2(f^{eab}A^a_\mu A^b_\nu)(f^{ecd}A^{\mu c}A^{\nu d}) \end{aligned}$$

The fermion and gauge boson propagators are the same as in QED, times an identity matrix in the gauge group space. Similarly, the polarization of external particles is treated the same as in QED, but each external particle also has an orientation in the group space.

Fermion vertex:

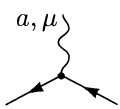

$$= ig\gamma^\mu t^a \tag{A.10}$$

3-boson vertex:

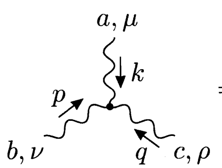

$$= \begin{aligned} gf^{abc}\big[g^{\mu\nu}(k-p)^\rho \\ + g^{\nu\rho}(p-q)^\mu \\ + g^{\rho\mu}(q-k)^\nu\big] \end{aligned} \tag{A.11}$$

4-boson vertex:

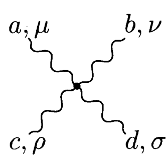

$$= \begin{aligned} -ig^2\big[f^{abe}f^{cde}(g^{\mu\rho}g^{\nu\sigma} - g^{\mu\sigma}g^{\nu\rho}) \\ + f^{ace}f^{bde}(g^{\mu\nu}g^{\rho\sigma} - g^{\mu\sigma}g^{\nu\rho}) \\ + f^{ade}f^{bce}(g^{\mu\nu}g^{\rho\sigma} - g^{\mu\rho}g^{\nu\sigma})\big] \end{aligned} \tag{A.12}$$

Ghost vertex:

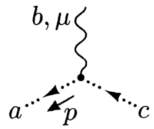

$$= -g f^{abc} p^{\mu} \tag{A.13}$$

Ghost propagator:

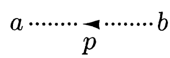

$$= \frac{i\delta^{ab}}{p^2 + i\epsilon} \tag{A.14}$$

(Counterterm vertices for loop calculations are given on pages 528 and 532.)

Other theories. Feynman rules for other theories can be found on the following pages:

Yukawa theory	page 118
Scalar QED	page 312
Linear sigma model	page 353
Electroweak theory	pages 716, 743, 753

A.2 Polarizations of External Particles

The spinors $u^s(p)$ and $v^s(p)$ obey the Dirac equation in the form

$$\begin{aligned} 0 &= (\not{p} - m)u^s(p) = \bar{u}^s(p)(\not{p} - m) \\ &= (\not{p} + m)v^s(p) = \bar{v}^s(p)(\not{p} + m), \end{aligned} \tag{A.15}$$

where $\not{p} = \gamma^\mu p_\mu$. The Dirac matrices obey the anticommutation relations

$$\{\gamma^\mu, \gamma^\nu\} = 2g^{\mu\nu}. \tag{A.16}$$

We use a chiral basis,

$$\gamma^\mu = \begin{pmatrix} 0 & \sigma^\mu \\ \bar{\sigma}^\mu & 0 \end{pmatrix}, \qquad \gamma^5 = \begin{pmatrix} -1 & 0 \\ 0 & 1 \end{pmatrix}, \tag{A.17}$$

where

$$\sigma^\mu = (1, \boldsymbol{\sigma}), \qquad \bar{\sigma}^\mu = (1, -\boldsymbol{\sigma}). \tag{A.18}$$

In this basis the normalized Dirac spinors can be written

$$u^s(p) = \begin{pmatrix} \sqrt{p\cdot\sigma}\,\xi^s \\ \sqrt{p\cdot\bar{\sigma}}\,\xi^s \end{pmatrix}, \qquad v^s(p) = \begin{pmatrix} \sqrt{p\cdot\sigma}\,\eta^s \\ -\sqrt{p\cdot\bar{\sigma}}\,\eta^s \end{pmatrix}, \tag{A.19}$$

where ξ and η are two-component spinors normalized to unity. In the high-energy limit these expressions simplify to

$$u(p) \approx \sqrt{2E}\begin{pmatrix} \frac{1}{2}(1 - \hat{p}\cdot\boldsymbol{\sigma})\xi^s \\ \frac{1}{2}(1 + \hat{p}\cdot\boldsymbol{\sigma})\xi^s \end{pmatrix}, \qquad v(p) \approx \sqrt{2E}\begin{pmatrix} \frac{1}{2}(1 - \hat{p}\cdot\boldsymbol{\sigma})\eta^s \\ -\frac{1}{2}(1 + \hat{p}\cdot\boldsymbol{\sigma})\eta^s \end{pmatrix}. \tag{A.20}$$

Using the standard basis for the Pauli matrices,

$$\sigma^1 = \begin{pmatrix} 0 & 1 \\ 1 & 0 \end{pmatrix}, \qquad \sigma^2 = \begin{pmatrix} 0 & -i \\ i & 0 \end{pmatrix}, \qquad \sigma^3 = \begin{pmatrix} 1 & 0 \\ 0 & -1 \end{pmatrix}, \tag{A.21}$$

we have, for example, $\xi^s = \binom{1}{0}$ for spin up in the z direction, and $\xi^s = \binom{0}{1}$ for spin down in the z direction. For antifermions the physical spin is opposite to that of the spinor: $\eta^s = \binom{1}{0}$ corresponds to spin *down* in the z direction, and so on.

In computing unpolarized cross sections one encounters the polarization sums

$$\sum_s u^s(p)\bar{u}^s(p) = \not{p} + m, \qquad \sum_s v^s(p)\bar{v}^s(p) = \not{p} - m. \tag{A.22}$$

For polarized cross sections one can either resort to the explicit formulae (A.19) or insert the projection matrices

$$\left(\frac{1+\gamma^5}{2}\right), \qquad \left(\frac{1-\gamma^5}{2}\right), \tag{A.23}$$

which project onto right- and left-handed spinors, respectively. Again, for antifermions, the helicity of the spinor is opposite to the physical helicity of the particle.

Many other identities involving Dirac spinors and matrices can be found in Chapter 3.

Polarization vectors for photons and other gauge bosons are conventionally normalized to unity. For massless bosons the polarization must be transverse:

$$\epsilon^\mu = (0, \boldsymbol{\epsilon}), \qquad \text{where } \mathbf{p} \cdot \boldsymbol{\epsilon} = 0. \tag{A.24}$$

If $\mathbf{p}$ is in the $+z$ direction, the polarization vectors are

$$\epsilon^\mu = \frac{1}{\sqrt{2}}(0, 1, i, 0), \qquad \epsilon^\mu = \frac{1}{\sqrt{2}}(0, 1, -i, 0), \tag{A.25}$$

for right- and left-handed helicities, respectively.

In computing unpolarized cross sections involving photons, one can replace

$$\sum_{\text{polarizations}} \epsilon^*_\mu \epsilon_\nu \longrightarrow -g_{\mu\nu}, \tag{A.26}$$

by virtue of the Ward identity. In the case of massless non-Abelian gauge bosons, one must also sum over the emission of ghosts, as discussed in Section 16.3. In the massive case, one must in addition include the emission of Goldstone bosons, as discussed in Section 21.1.

A.3 Numerator Algebra

Traces of γ matrices can be evaluated as follows:

$$\begin{aligned}
\mathrm{tr}(\mathbf{1}) &= 4 \\
\mathrm{tr}(\text{any odd \# of } \gamma\text{'s}) &= 0 \\
\mathrm{tr}(\gamma^\mu\gamma^\nu) &= 4g^{\mu\nu} \\
\mathrm{tr}(\gamma^\mu\gamma^\nu\gamma^\rho\gamma^\sigma) &= 4(g^{\mu\nu}g^{\rho\sigma} - g^{\mu\rho}g^{\nu\sigma} + g^{\mu\sigma}g^{\nu\rho}) \\
\mathrm{tr}(\gamma^5) &= 0 \\
\mathrm{tr}(\gamma^\mu\gamma^\nu\gamma^5) &= 0 \\
\mathrm{tr}(\gamma^\mu\gamma^\nu\gamma^\rho\gamma^\sigma\gamma^5) &= -4i\epsilon^{\mu\nu\rho\sigma}
\end{aligned} \tag{A.27}$$

Another identity allows one to reverse the order of γ matrices inside a trace:

$$\mathrm{tr}(\gamma^\mu\gamma^\nu\gamma^\rho\gamma^\sigma\cdots) = \mathrm{tr}(\cdots\gamma^\sigma\gamma^\rho\gamma^\nu\gamma^\mu). \tag{A.28}$$

Contractions of γ matrices with each other simplify to:

$$\begin{aligned}
\gamma^\mu\gamma_\mu &= 4 \\
\gamma^\mu\gamma^\nu\gamma_\mu &= -2\gamma^\nu \\
\gamma^\mu\gamma^\nu\gamma^\rho\gamma_\mu &= 4g^{\nu\rho} \\
\gamma^\mu\gamma^\nu\gamma^\rho\gamma^\sigma\gamma_\mu &= -2\gamma^\sigma\gamma^\rho\gamma^\nu
\end{aligned} \tag{A.29}$$

(These identities apply in four dimensions only; see the following section.) Contractions of the ϵ symbol can also be simplified:

$$\begin{aligned}
\epsilon^{\alpha\beta\gamma\delta}\epsilon_{\alpha\beta\gamma\delta} &= -24 \\
\epsilon^{\alpha\beta\gamma\mu}\epsilon_{\alpha\beta\gamma\nu} &= -6\delta^\mu{}_\nu \\
\epsilon^{\alpha\beta\mu\nu}\epsilon_{\alpha\beta\rho\sigma} &= -2\big(\delta^\mu{}_\rho\delta^\nu{}_\sigma - \delta^\mu{}_\sigma\delta^\nu{}_\rho\big)
\end{aligned} \tag{A.30}$$

In some calculations, it is useful to rearrange products of fermion bilinears by means of *Fierz identities.* Let $u_1, \ldots, u_4$ be Dirac spinors, and let $u_{iL} = \frac{1}{2}(1-\gamma^5)u_i$ be the left-handed projection. Then the most important Fierz rearrangement formula is

$$(\bar{u}_{1L}\gamma^\mu u_{2L})(\bar{u}_{3L}\gamma_\mu u_{4L}) = -(\bar{u}_{1L}\gamma^\mu u_{4L})(\bar{u}_{3L}\gamma_\mu u_{2L}). \tag{A.31}$$

Additional formulae can be generated by the use of the following identities for the 2×2 blocks of Dirac matrices:

$$(\sigma^\mu)_{\alpha\beta}(\sigma_\mu)_{\gamma\delta} = 2\epsilon_{\alpha\gamma}\epsilon_{\beta\delta}; \qquad (\bar{\sigma}^\mu)_{\alpha\beta}(\bar{\sigma}_\mu)_{\gamma\delta} = 2\epsilon_{\alpha\gamma}\epsilon_{\beta\delta}. \tag{A.32}$$

In non-Abelian gauge theories, the Feynman rules involve gauge group matrices t^a that form a representation r of a Lie algebra G. The symbol G also denotes the adjoint representation of the algebra. The matrices t^a obey

$$[t^a, t^b] = if^{abc}t^c, \tag{A.33}$$

where the structure constants f^{abc} are totally antisymmetric. The invariants $C(r)$ and $C_2(r)$ of the representation r are defined by

$$\operatorname{tr}[t^a t^b] = C(r)\delta^{ab}, \qquad t^a t^a = C_2(r)\cdot \mathbf{1}. \tag{A.34}$$

These are related by

$$C(r) = \frac{d(r)}{d(G)} C_2(r), \tag{A.35}$$

where $d(r)$ is the dimension of the representation. Traces and contractions of the t^a can be evaluated using the above identities and their consequences:

$$\begin{aligned} t^a t^b t^a &= [C_2(r) - \tfrac{1}{2}C_2(G)]t^b \\ f^{acd} f^{bcd} &= C_2(G)\delta^{ab} \\ f^{abc} t^b t^c &= \tfrac{1}{2} i C_2(G) t^a \end{aligned} \tag{A.36}$$

For $SU(N)$ groups, the fundamental representation is denoted by N, and we have

$$C(N) = \frac{1}{2}, \qquad C_2(N) = \frac{N^2-1}{2N}, \qquad C(G) = C_2(G) = N. \tag{A.37}$$

The following relation, satisfied by the matrices of the fundamental representation of $SU(N)$, is also very helpful:

$$(t^a)_{ij}(t^a)_{k\ell} = \frac{1}{2}\Big(\delta_{i\ell}\delta_{kj} - \frac{1}{N}\delta_{ij}\delta_{k\ell}\Big). \tag{A.38}$$

A.4 Loop Integrals and Dimensional Regularization

To combine propagator denominators, introduce integrals over Feynman parameters:

$$\frac{1}{A_1 A_2 \cdots A_n} = \int_0^1 dx_1 \cdots dx_n\, \delta(\textstyle\sum x_i - 1)\, \dfrac{(n-1)!}{\big[x_1 A_1 + x_2 A_2 + \cdots x_n A_n\big]^n} \tag{A.39}$$

In the case of only two denominator factors, this formula reduces to

$$\frac{1}{AB} = \int_0^1 dx\, \frac{1}{\big[xA + (1-x)B\big]^2}. \tag{A.40}$$

A more general formula in which the A_i are raised to arbitrary powers is given in Eq. (6.42).

Once this is done, the bracketed quantity in the denominator will be a quadratic function of the integration variables p_i^μ. Next, complete the square and shift the integration variables to absorb the terms linear in p_i^μ. For a one-loop integral, there is a single integration momentum p^μ, which is shifted to a momentum variable ℓ^μ. After this shift, the denominator takes the form

$(\ell^2 - \Delta)^n$. In the numerator, terms with an odd number of powers of ℓ vanish by symmetric integration. Symmetry also allows one to replace

$$\ell^\mu \ell^\nu \to \frac{1}{d}\ell^2 g^{\mu\nu}, \tag{A.41}$$

$$\ell^\mu \ell^\nu \ell^\rho \ell^\sigma \to \frac{1}{d(d+2)}(\ell^2)^2\big(g^{\mu\nu}g^{\rho\sigma} + g^{\mu\rho}g^{\nu\sigma} + g^{\mu\sigma}g^{\nu\rho}\big). \tag{A.42}$$

(Here d is the spacetime dimension.) The integral is most conveniently evaluated after Wick-rotating to Euclidean space, with the substitution

$$\ell^0 = i\ell_E^0, \qquad \ell^2 = -\ell_E^2. \tag{A.43}$$

Alternatively, one can use the following table of d-dimensional integrals in Minkowski space:

$$\int \frac{d^d\ell}{(2\pi)^d} \frac{1}{(\ell^2-\Delta)^n} = \frac{(-1)^n i}{(4\pi)^{d/2}} \frac{\Gamma(n-\frac{d}{2})}{\Gamma(n)} \left(\frac{1}{\Delta}\right)^{n-\frac{d}{2}} \tag{A.44}$$

$$\int \frac{d^d\ell}{(2\pi)^d} \frac{\ell^2}{(\ell^2-\Delta)^n} = \frac{(-1)^{n-1} i}{(4\pi)^{d/2}} \frac{d}{2} \frac{\Gamma(n-\frac{d}{2}-1)}{\Gamma(n)} \left(\frac{1}{\Delta}\right)^{n-\frac{d}{2}-1} \tag{A.45}$$

$$\int \frac{d^d\ell}{(2\pi)^d} \frac{\ell^\mu\ell^\nu}{(\ell^2-\Delta)^n} = \frac{(-1)^{n-1} i}{(4\pi)^{d/2}} \frac{g^{\mu\nu}}{2} \frac{\Gamma(n-\frac{d}{2}-1)}{\Gamma(n)} \left(\frac{1}{\Delta}\right)^{n-\frac{d}{2}-1} \tag{A.46}$$

$$\int \frac{d^d\ell}{(2\pi)^d} \frac{(\ell^2)^2}{(\ell^2-\Delta)^n} = \frac{(-1)^n i}{(4\pi)^{d/2}} \frac{d(d+2)}{4} \frac{\Gamma(n-\frac{d}{2}-2)}{\Gamma(n)} \left(\frac{1}{\Delta}\right)^{n-\frac{d}{2}-2} \tag{A.47}$$

$$\int \frac{d^d\ell}{(2\pi)^d} \frac{\ell^\mu\ell^\nu\ell^\rho\ell^\sigma}{(\ell^2-\Delta)^n} = \frac{(-1)^n i}{(4\pi)^{d/2}} \frac{\Gamma(n-\frac{d}{2}-2)}{\Gamma(n)} \left(\frac{1}{\Delta}\right)^{n-\frac{d}{2}-2} \times \frac{1}{4}\big(g^{\mu\nu}g^{\rho\sigma} + g^{\mu\rho}g^{\nu\sigma} + g^{\mu\sigma}g^{\nu\rho}\big) \tag{A.48}$$

If the integral converges, one can set $d = 4$ from the start. If the integral diverges, the behavior near $d = 4$ can be extracted by expanding

$$\left(\frac{1}{\Delta}\right)^{2-\frac{d}{2}} = 1 - (2-\tfrac{d}{2})\log\Delta + \cdots. \tag{A.49}$$

One also needs the expansion of $\Gamma(x)$ near its poles:

$$\Gamma(x) = \frac{1}{x} - \gamma + \mathcal{O}(x) \tag{A.50}$$

near $x = 0$, and

$$\Gamma(x) = \frac{(-1)^n}{n!}\left(\frac{1}{x+n} - \gamma + 1 + \cdots + \frac{1}{n} + \mathcal{O}(x+n)\right) \tag{A.51}$$

near $x = -n$. Here γ is the Euler-Mascheroni constant, $\gamma \approx 0.5772$. The following combination of terms often appears in calculations:

$$\frac{\Gamma(2-\frac{d}{2})}{(4\pi)^{d/2}}\left(\frac{1}{\Delta}\right)^{2-\frac{d}{2}} = \frac{1}{(4\pi)^2}\left(\frac{2}{\epsilon} - \log\Delta - \gamma + \log(4\pi) + \mathcal{O}(\epsilon)\right), \tag{A.52}$$

with $\epsilon = 4 - d$.

Notice that Δ is positive if it is a combination of masses and *spacelike* momentum invariants. If Δ contains timelike momenta, it may become negative. Then these integrals acquire imaginary parts, which give the discontinuities of S-matrix elements. To compute the S-matrix in a physical region, choose the correct branch of the function by the prescription

$$\left(\frac{1}{\Delta}\right)^{n-\frac{d}{2}} \to \left(\frac{1}{\Delta - i\epsilon}\right)^{n-\frac{d}{2}}, \tag{A.53}$$

where $-i\epsilon$ (not to be confused with ϵ in the previous paragraph!) gives a tiny negative imaginary part.

Traces in Eq. (A.27) that do not involve γ^5 are independent of dimensionality. However, since

$$g^{\mu\nu}g_{\mu\nu} = \delta^{\mu}{}_{\mu} = d \tag{A.54}$$

in d dimensions, the contraction identities (A.29) are modified:

$$\begin{aligned}
\gamma^\mu\gamma_\mu &= d \\
\gamma^\mu\gamma^\nu\gamma_\mu &= -(d-2)\gamma^\nu \\
\gamma^\mu\gamma^\nu\gamma^\rho\gamma_\mu &= 4g^{\nu\rho} - (4-d)\gamma^\nu\gamma^\rho \\
\gamma^\mu\gamma^\nu\gamma^\rho\gamma^\sigma\gamma_\mu &= -2\gamma^\sigma\gamma^\rho\gamma^\nu + (4-d)\gamma^\nu\gamma^\rho\gamma^\sigma
\end{aligned} \tag{A.55}$$

A.5 Cross Sections and Decay Rates

Once the squared matrix element for a scattering process is known, the differential cross section is given by

$$\begin{aligned}
d\sigma = {}& \frac{1}{2E_{\mathcal{A}}2E_{\mathcal{B}}\,|v_{\mathcal{A}}-v_{\mathcal{B}}|}\left(\prod_f \frac{d^3p_f}{(2\pi)^3}\frac{1}{2E_f}\right) \\
& \times \left|\mathcal{M}(p_{\mathcal{A}}, p_{\mathcal{B}} \to \{p_f\})\right|^2 (2\pi)^4\delta^{(4)}(p_{\mathcal{A}}+p_{\mathcal{B}} - \textstyle\sum p_f).
\end{aligned} \tag{A.56}$$

The differential decay rate of an unstable particle to a given final state is

$$d\Gamma = \frac{1}{2m_{\mathcal{A}}}\left(\prod_f \frac{d^3p_f}{(2\pi)^3}\frac{1}{2E_f}\right)\left|\mathcal{M}(m_{\mathcal{A}} \to \{p_f\})\right|^2 (2\pi)^4\delta^{(4)}(p_{\mathcal{A}} - \textstyle\sum p_f). \tag{A.57}$$

For the special case of a two-particle final state, the Lorentz-invariant phase space takes the simple form

$$\left(\prod_f \int \frac{d^3p_f}{(2\pi)^3}\frac{1}{2E_f}\right)(2\pi)^4\delta^{(4)}(\textstyle\sum p_i - \sum p_f) = \displaystyle\int \frac{d\Omega_{\text{cm}}}{4\pi}\frac{1}{8\pi}\left(\frac{2|\mathbf{p}|}{E_{\text{cm}}}\right), \tag{A.58}$$

where $|\mathbf{p}|$ is the magnitude of the 3-momentum of either particle in the center-of-mass frame.

A.6 Physical Constants and Conversion Factors

Precisely known physical constants:

$$\begin{aligned} c &= 2.998 \times 10^{10} \text{ cm/s} \\ \hbar &= 6.582 \times 10^{-22} \text{ MeV s} \\ e &= -1.602 \times 10^{-19} \text{ C} \\ \alpha &= \frac{e^2}{4\pi\hbar c} = \frac{1}{137.04} = 0.00730 \\ \frac{G_F}{(\hbar c)^3} &= 1.166 \times 10^{-5} \text{ GeV}^{-2} \end{aligned}$$

The values of the strong and weak interaction coupling constants depend on the conventions used to define them, as explained in Sections 17.6 and 21.3. For the purpose of estimation, however, one can use the following values:

$$\begin{aligned} \alpha_s(10 \text{ GeV}) &= 0.18 \\ \alpha_s(m_Z) &= 0.12 \\ \sin^2\theta_w &= 0.23 \end{aligned}$$

Particle masses (times c^2):

e :	0.5110 MeV	p :	938.3 MeV
μ :	105.6 MeV	n :	939.6 MeV
τ :	1777 MeV	$\pi^\pm$:	139.6 MeV
$W^\pm$:	80.2 GeV	π^0 :	135.0 MeV
Z^0 :	91.19 GeV		

Useful combinations:

Bohr radius: $$a_0 = \frac{\hbar}{\alpha m_e c} = 5.292 \times 10^{-9} \text{ cm}$$

electron Compton wavelength: $$\lambda\!\!\!^- = \frac{\hbar}{m_e c} = 3.862 \times 10^{-11} \text{ cm}$$

classical electron radius: $$r_e = \frac{\alpha\hbar}{m_e c} = 2.818 \times 10^{-13} \text{ cm}$$

Thomson cross section: $$\sigma_T = \frac{8\pi r_e^2}{3} = 0.6652 \text{ barn}$$

annihilation cross section: $$1 \text{ R} = \frac{4\pi\alpha^2}{3E_{\text{cm}}^2} = \frac{86.8 \text{ nbarn}}{(E_{\text{cm}} \text{ in GeV})^2}$$

Conversion factors:

$$\begin{aligned}
(1\ \text{GeV})/c^2 &= 1.783 \times 10^{-24}\ \text{g} \\
(1\ \text{GeV})^{-1}(\hbar c) &= 0.1973 \times 10^{-13}\ \text{cm} = 0.1973\ \text{fm}; \\
(1\ \text{GeV})^{-2}(\hbar c)^2 &= 0.3894 \times 10^{-27}\ \text{cm}^2 = 0.3894\ \text{mbarn} \\
1\ \text{barn} &= 10^{-24}\ \text{cm}^2 \\
(1\ \text{volt/meter})(e\hbar c) &= 1.973 \times 10^{-25}\ \text{GeV}^2 \\
(1\ \text{tesla})(e\hbar c^2) &= 5.916 \times 10^{-17}\ \text{GeV}^2
\end{aligned}$$

A complete, up-to-date tabulation of the fundamental constants and the properties of elementary particles is given in the *Review of Particle Properties*, which can be found in a recent issue of either *Physical Review* **D** or *Physics Letters* **B**. The most recent *Review* as of this writing is published in *Physical Review* **D50**, 1173 (1994).

Bibliography

Mathematical Background and Reference

Cahn, Robert N., *Semi-Simple Lie Algebras and Their Representations*, Benjamin/Cummings, Menlo Park, California, 1984. Written by a physicist, for physicists.

Carrier, George F., Krook, Max, and Pearson, Carl E., *Functions of a Complex Variable*, McGraw-Hill, New York, 1966. An excellent practical introduction to methods of complex variables and contour integration.

Gradshteyn, I. S. and Ryzhik, I. M., *Table of Integrals, Series, and Products* (trans. and ed. by Alan Jeffrey), Academic Press, Orlando, Florida, 1980.

Physics Background

Baym, Gordon, *Lectures on Quantum Mechanics*, Benjamin/Cummings, Menlo Park, California, 1969. A concise, informal text that is especially rich in nontrivial applications.

Fetter, Alexander L. and Walecka, John Dirk, *Theoretical Mechanics of Particles and Continua*, McGraw-Hill, New York, 1980. Includes several chapters on continuum mechanics and useful appendices of mathematical reference material.

Feynman, Richard P., *QED: The Strange Theory of Light and Matter*, Princeton University Press, Princeton, New Jersey, 1985. A transcription of four lectures given to a general audience, presenting Feynman's approach to quantum mechanics, including Feynman diagrams. Highly recommended.

Feynman, Richard P. and Hibbs, A. R., *Quantum Mechanics and Path Integrals*, McGraw-Hill, New York, 1965. An introduction to the use of path integrals in nonrelativistic quantum mechanics.

Goldstein, Herbert, *Classical Mechanics* (second edition), Addison-Wesley, Reading, Massachusetts, 1980. Chapter 12 introduces classical relativistic field theory.

Jackson, J. D., *Classical Electrodynamics* (second edition), Wiley, New York, 1975.

Landau, L. D. and Lifshitz, E. M., *The Classical Theory of Fields* (fourth revised English edition, trans. Morton Hamermesh), Pergamon, Oxford, 1975. Contains a succinct development of electromagnetic theory from the Lagrangian viewpoint.

Landau, L. D. and Lifshitz, E. M., *Statistical Physics* (third edition, Part 1, trans. J. B. Sykes and M. J. Kearsley), Pergamon Press, 1980. An insightful if concise textbook of statistical mechanics, containing the original pedagogical exposition of Landau's theory of phase transitions.

Reichl, L. E., *A Modern Course in Statistical Physics*, University of Texas Press, Austin, 1980. A complete textbook of statistical mechanics.

Schiff, Leonard I., *Quantum Mechanics* (third edition), McGraw-Hill, New York, 1968.

Shankar, Ramamurti, *Principles of Quantum Mechanics*, Plenum, New York, 1980. A very clear presentation of the basic theory.

Taylor, Edwin F. and Wheeler, John Archibald, *Spacetime Physics* (second edition), Freeman, New York, 1992. An elementary but insightful introduction to special relativity.

Taylor, John R., *Scattering Theory*, Robert E. Krieger, Malabar, Florida, 1983 (reprint of original edition published by Wiley, New York, 1972). A very clear development of scattering theory for nonrelativistic quantum mechanics.

Relativistic Quantum Mechanics and Field Theory

Bailin, D. and Love, A., *Introduction to Gauge Field Theory* (revised edition), Institute of Physics Publishing, Bristol, 1993. Develops the theory entirely from the path integral viewpoint.

Balian, Roger and Zinn-Justin, Jean (eds.), *Methods in Field Theory*, North-Holland, Amsterdam, 1976. Proceedings of the 1975 Les Houches Summer School in Theoretical Physics, including lectures on functional methods, renormalization, and gauge theories.

Berestetskii, V. B., Lifshitz, E. M., and Pitaevskii, L. P., *Quantum Electrodynamics* (second edition, trans. J. B. Sykes and J. S. Bell), Pergamon, Oxford, 1982. An excellent reference for QED applications.

Bjorken, James D. and Drell, Sidney D., *Relativistic Quantum Mechanics*, McGraw-Hill, New York, 1964. Develops Feynman diagrams using intuitive arguments, without using fields.

Bjorken, James D. and Drell, Sidney D., *Relativistic Quantum Fields*, McGraw-Hill, New York, 1965. Redevelops Feynman diagrams from the field viewpoint, using canonical quantization.

Brown, Lowell S., *Quantum Field Theory*, Cambridge University Press, New York, 1992. A careful treatment of the foundations of quantum field theory and its application to scattering processes.

Coleman, Sidney, *Aspects of Symmetry*, Cambridge University Press, Cambridge, 1985. Informal lectures on a number of topics involving gauge theories and symmetry, given between 1966 and 1979.

Collins, John, *Renormalization*, Cambridge University Press, Cambridge, 1984. A careful development of the technical machinery needed for all-orders proofs of renormalizability, operator product expansion, and factorization theorems.

Deser, Stanley, Grisaru, Marc, and Pendleton, Hugh, *Lectures on Elementary Particles and Quantum Field Theory*, MIT Press, Cambridge, 1970, vol. 1. Four extremely useful summer school lectures.

Gross, Franz, *Relativistic Quantum Mechanics and Field Theory*, Wiley, New York, 1993. Includes a number of topics in "advanced quantum mechanics", and an introductory chapter on bound states.

Itzykson, Claude and Zuber, Jean-Bernard, *Quantum Field Theory*, McGraw-Hill, New York, 1980. A comprehensive textbook.

Jauch, J. M. and Rohrlich, F., *The Theory of Photons and Electrons* (second edition), Springer-Verlag, Berlin, 1976. An authoritative monograph on QED.

Kaku, Michio, *Quantum Field Theory: A Modern Introduction*, Oxford University Press, New York, 1993. Contains brief introductory chapters on a number of advanced topics.

Kinoshita, T., ed., *Quantum Electrodynamics*, World Scientific, Singapore, 1990. A collection of review articles on precision tests of QED.

Mandl, F. and Shaw, G., *Quantum Field Theory* (revised edition), Wiley, New York, 1993. The easiest book on field theory; introduces QED and some electroweak theory using canonical quantization.

Ramond, Pierre, *Field Theory: A Modern Primer* (second edition), Addison-Wesley, Redwood City, California, 1989. Contains very nice treatments of the Lorentz group, path integrals, ϕ^4 theory, and quantization of gauge theories.

Ryder, Lewis H., *Quantum Field Theory*, Cambridge University Press, Cambridge, 1985. A concise treatment of the more formal aspects of the subject.

Sakurai, J. J., *Advanced Quantum Mechanics*, Addison-Wesley, Reading, 1967. Develops Feynman diagrams without using fields.

Schweber, Silvan S., *QED and the Men Who Made It: Dyson, Feynman, Schwinger, and Tomonaga*, Princeton University Press, Princeton, 1994. An excellent history of the subject up to about 1950.

Schwinger, Julian (ed.), *Selected Papers on Quantum Electrodynamics*, Dover, New York, 1958. Reprints of important papers written between 1927 and 1953.

Sterman, George, *Introduction to Quantum Field Theory*, Cambridge University Press, Cambridge, 1993. An introductory textbook with special emphasis on the essentials of perturbative QCD.

Elementary Particle Physics

Aitchison, Ian J. R. and Hey, Anthony J. G., *Gauge Theories in Particle Physics* (second edition), Adam Hilger, Bristol, 1989. An elementary introduction to gauge theories, concentrating mostly on tree-level processes.

Barger, Vernon and Phillips, Roger J. N., *Collider Physics*, Addison-Wesley, Menlo Park, California, 1987. Basic discussion of the application of QCD to high-energy collider phenomenology.

Cahn, Robert N. and Goldhaber, Gerson, *The Experimental Foundations of Particle Physics*, Cambridge University Press, Cambridge, 1989. Reprints of many original papers, supplemented by introductory overviews, additional references, and exercises. Highly recommended.

Cheng, Ta-Pei and Li, Ling-Fong, *Gauge Theory of Elementary Particle Physics*, Oxford University Press, New York, 1984. An advanced, authoritative monograph.

Commins, Eugene D. and Bucksbaum, Philip H., *Weak Interactions of Leptons and Quarks*, Cambridge University Press, Cambridge, 1983. A thorough review of both theory and experiment.

Field, Richard D., *Applications of Perturbative QCD*, Benjamin/Cummings, Menlo Park, 1989. A useful description of the techniques needed for QCD calculations beyond the leading order.

Georgi, Howard, *Weak Interactions and Modern Particle Theory*, Benjamin/Cummings, Menlo Park, California, 1984. Advanced, insightful treatment of selected topics.

Griffiths, David, *Introduction to Elementary Particles*, Wiley, New York, 1987. A good undergraduate-level survey.

Halzen, Francis and Martin, Alan D., *Quarks and Leptons: An Introductory Course in Modern Particle Physics*, Wiley, New York, 1984. Uses Feynman diagrams throughout, and concentrates on gauge theories.

Perkins, Donald H., *Introduction to High Energy Physics* (third edition), Addison-Wesley, Menlo Park, California, 1987. A good introduction to phenomena, with relatively little emphasis on Feynman diagrams and gauge theories.

Quigg, Chris, *Gauge Theories of the Strong, Weak, and Electromagnetic Interactions*, Benjamin/Cummings, Menlo Park, California, 1983. A very nice overview of gauge theories and their experimental tests.

Ross, Graham G., *Grand Unified Theories*, Benjamin/Cummings, Menlo Park, California, 1984. A clear introduction to gauge theories that unify the interactions of particle physics.

Taylor, J. C., *Gauge Theories of Weak Interactions*, Cambridge University Press, Cambridge, 1976. A concise treatment of the standard model and related theoretical issues.

Condensed Matter Physics

Abrikosov, A. A., Gorkov, L. P., and Dzyaloshinskii, I. E., *Quantum Field Theoretical Methods in Statistical Physics* (second edition), Pergamon, Oxford, 1965. A classic, but very terse, exposition of the application of Feynman diagrams to condensed matter problems.

Anderson, P. W., *Basic Notions of Condensed Matter Physics*, Benjamin/Cummings, Menlo Park, California, 1984. An informal overview of the concepts of broken symmetry and renormalization as applied to condensed matter systems.

Fetter, Alexander L. and Walecka, John Dirk, *Quantum Theory of Many-Particle Systems*, McGraw-Hill, New York, 1971. A straightfoward introduction to the use of Feynman diagrams in nuclear and condensed matter physics.

Ma, Shang-Keng, *Modern Theory of Critical Phenomena*, Benjamin/Cummings, 1976. An introduction to the use of renormalization group methods in the theory of critical phenomena.

Mattuck, Richard D., *A Guide to Feynman Diagrams in the Many-Body Problem*, McGraw-Hill, New York, 1967. A clear and easy introduction to the use of Feynman diagrams in solid state physics.

Parisi, Giorgio, *Statistical Field Theory*, Benjamin/Cummings, 1988. Far-ranging applications of ideas from quantum field theory to problems in statistical mechanics.

Stanley, H. Eugene, *Introduction to Phase Transitions and Critical Phenomena*, Oxford University Press, Oxford, 1971.

Zinn-Justin, Jean, *Quantum Field Theory and Critical Phenomena* (third edition), Oxford University Press, Oxford, 1996. A treatise on the application of renormalization theory to the study of critical phenomena.

Corrections to This Book

A list of misprints and corrections to this book is posted on the World-Wide Web at the URL 'http://www.slac.stanford.edu/~mpeskin/QFT.html', or can be obtained by writing to the authors. We would be grateful if you would report additional errors in the book, or send other comments, to mpeskin@slac.stanford.edu or to dschroeder@cc.weber.edu.

Index

"This is such a serious competitor to Bjorken and Drell that I fear for our royalties."

—Prof. J. D. Bjorken, Stanford Linear Accelerator Center

"I have used the text of Peskin and Schroeder in teaching several graduate courses. It provides students with nearly all of the tools required of the modern field theorist. It is the only field theory text with a thoroughly modern, Wilsonian treatment of renormalization and the renormalization group. Students are left well equipped to tackle research problems in QCD and the electroweak theory."

—Prof. Michael Dine, University of California, Santa Cruz

"Peskin and Schroeder have written an introductory field theory textbook with the right choice of material at the right level and all presented from a completely modern point of view. It provides a pedagogical introduction to the tools and concepts of field theory that will be of use to students of condensed matter, cosmology, and particle physics alike."

—Prof. Jeffrey Harvey, University of Chicago

An Introduction to Quantum Field Theory is a textbook intended for the graduate physics course covering relativistic quantum mechanics, quantum electrodynamics, and Feynman diagrams. The authors make these subjects accessible through carefully worked examples illustrating the technical aspects of the subject, and intuitive explanations of what is going on behind the mathematics. After presenting the basics of quantum electrodynamics, the authors discuss the theory of renormalization and its relation to statistical mechanics, and introduce the renormalization group. This discussion sets the stage for a discussion of the physical principles that underlie the fundamental interactions of elementary particle physics and their description by gauge field theories.

Michael E. Peskin received his doctorate in physics from Cornell University and has held research appointments in theoretical physics at Harvard, Cornell, and CEN Saclay. In 1982, he joined the staff of the Stanford Linear Accelerator Center, where he is now Professor of Physics.

Daniel V. Schroeder received his doctorate in physics from Stanford University in 1990. He held visiting appointments at Pomona College and Grinnell College before joining the faculty of Weber State University, where he is now Associate Professor of Physics.

ABP ***Advanced Book Program***

Westview Press
5500 Central Avenue
Boulder, Colorado 80301

12 Hid's Copse Road
Cumnor Hill • Oxford OX2 9JJ
www.westviewpress.com

ISBN-10 0-201-50397-2
ISBN-13 978-0-201-50397-5

90000

9 780201 503975